Local chromatin structure of heterochromatin regulates repeated DNA stability, nucleolus structure, and genome integrity

by

Jamy C. Peng

B.S. (University of California, Riverside) 2000
M.S. (University of California, Riverside) 2001

A dissertation submitted in partial satisfaction of the

requirements for the degree of

Doctor of Philosophy

in

Molecular and Cell Biology

in the

Graduate Division

Of the

University of California, Berkeley

Committee in charge:
Professor Gary H. Karpen, Chair
Professor W. Zacheus Cande
Professor Abby Dernburg
Professor Daniel Fletcher

Spring 2007

The dissertation of Jamy C. Peng is approved:

Chair _____ Date _____

_____ Date _____

_____ Date _____

_____ Date _____

University of California, Berkeley

Spring 2007

Abstract

Local chromatin structure in heterochromatin regulates repeated DNA stability, nucleolus structure, and genome integrity

by

Jamy C. Peng

Doctor of Philosophy in Molecular and Cell Biology

University of California, Berkeley

Professor Gary H. Karpen, Chair

Heterochromatin constitutes a significant portion of the genome in higher eukaryotes; approximately 30% in *Drosophila* and human. Heterochromatin contains a high repeat DNA content and a low density of protein-encoding genes. In contrast, euchromatin is composed mostly of unique sequences and contains the majority of single-copy genes. Genetic and cytological studies demonstrated that heterochromatin exhibits regulatory roles in chromosome organization, centromere function and telomere protection.

As an epigenetically regulated structure, heterochromatin formation is not defined by any DNA sequence consensus. Heterochromatin is characterized by its association with nucleosomes containing methylated-lysine 9 of histone H3 (H3K9me), heterochromatin protein 1 (HP1) that binds H3K9me, and Su(var)3-9, which methylates H3K9 and binds HP1. Heterochromatin formation and functions are influenced by HP1, Su(var)3-9, and the RNA interference (RNAi) pathway.

My thesis project investigates how heterochromatin formation and function impact nuclear architecture, repeated DNA organization, and genome stability in *Drosophila melanogaster*. H3K9me-based chromatin reduces extrachromosomal DNA formation; most likely by restricting the access of repair machineries to repeated DNAs. Reducing extrachromosomal ribosomal DNA stabilizes rDNA repeats and the nucleolus structure. H3K9me-based chromatin also inhibits DNA damage in heterochromatin. Cells with compromised heterochromatin structure, due to *Su(var)3-9* or *dcr-2* (a component of the RNAi pathway) mutations, display severe DNA damage in heterochromatin compared to wild type. In these mutant cells, accumulated DNA damage leads to chromosomal defects such as translocations, defective DNA repair response, and activation of the G2-M DNA repair and mitotic checkpoints that ensure cellular and animal viability.

My thesis research suggests that DNA replication, repair, and recombination mechanisms in heterochromatin differ from those in euchromatin. Remarkably, human euchromatin and fly heterochromatin share similar features; such as repeated DNA content, intron lengths and open reading frame sizes. Human cells likely stabilize their DNA content via mechanisms and factors similar to those in *Drosophila* heterochromatin. Furthermore, my thesis work raises implications for H3K9me and chromatin functions in complex-DNA genome stability, repeated DNA homogenization by molecular drive, and in genome reorganization through evolution.

Table of Contents

List of Figures

List of Tables

Acknowledgments

I would like to thank the following people:

My parents

They emigrated to the U.S. for the sole purpose of providing better education and life for my brother and me. My parents always demand their children to have strong morals and work ethnics. At times I found it difficult to meet their expectations, but I am better because of them.

Gary Karpen

As my Ph.D. advisor, Gary fostered a wonderful environment to think about science and work on my projects independently. I was never afraid to ask the 'dumb' questions in his presence. I also learned many life lessons in his lab. I matured, an incredible and fortunate development.

Patrick Heun

I would not have survived the move from San Diego to Berkeley without him. I miss our conversations about science and life in general.

Mike Blower

He is an exemplary scientist for anyone, especially a beginner such as myself.

Abby Dernburg

She set examples for an aspiring woman scientist. I will always remember being her teaching assistant in the FISH section of the imaging course in the Cold Spring Harbor Lab. I learned a lot from her, and I will miss her laughter.

Members of the Karpen lab: David, Samara, Cameron, Sylvia, Weiguo, Barbara, Aki, Sasha

Other than Wallace, I spent the most time with them in the past few years. I very much appreciate these wonderful people for tolerating my intense working style and occasional grumpiness in the lab. They provided many fond memories.

My close friends: Jennie, Jeremy, Shaleah, Ting Ting, Pinky, Diana, Jessie

I very much appreciate the years of their patiently listening to my complaints. Midnight chats, drunken parties, (cliché but true) tears and laughter…

Wallace

A man for whom I invented many endearments, he is my life partner, my best friend, my anchor. During the spring and summer of 2005, he supported me through months of worrying about a possible cancer diagnosis. Through the entire night after my surgery to remove the tumor, Wallace stayed awake sitting by my bed in the hospital so I wouldn't be scared. He held my hand then and continues holding my hand now. For this I am deeply thankful.

Vita

March 9, 1978	Born, Taiwan
2000	B.S. Suma Cum Laude UC Riverside
2001	M.S. UC Riverside
2000 - 2001	Graduate teaching assistant, UC Riverside
2001 - 2002	Research assistant, The Salk Institute
2002	Graduate teaching assistant, UC San Diego
2003 - 2006	Co-Instructor, Cold Spring Harbor Laboratory course Immunocytochemistry, In Situ Hybridization & Live Cell Imaging
2003 - 2006	Graduate research assistant, Lawrence Berkeley National Laboratory
2004	Graduate student instructor, UC Berkeley
2007	Ph.D., UC Berkeley

Publication

Gallie D.R., Fortner D., Peng J., Puthoff D. (2001) ATP-dependent hexameric assembly of the heat shock protein Hsp101 involves multiple interaction domains and a functional C-proximal nucleotide-binding domain. Journal of Biological Chemistry. 277(42): 39617-26

Peng J.C. and Karpen G.H. (2007) H3K9 methylation and RNA interference regulate nucleolar organization and repeated DNA stability. Nat Cell Biol. 9(1):25-35.

Peng J.C. and Karpen G.H. (in preparation) Heterochromatin structure maintains genome stability and organismal survival.

Chapter one: General introduction

Heterochromatin function and formation

The eukaryotic genome contains two types of cytologically and functionally distinct chromatin. Euchromatin predominantly replicates in early to mid S phase, is composed mostly of unique sequences, and contains the majority of single-copy genes. Conversely, heterochromatin frequently replicates late in S phase, is highly enriched in repetitive sequences, and has a relatively low gene density (John, 1988). Emil Heitz initially defined heterochromatin as the part of the genome that remains compacted throughout the cell cycle, thereby postulating that it is consisted of inactive parts of the genome (Heitz, 1928). After gene mapping analyses assigned the vast majority of genes to euchromatin, heterochromatin's reputation as 'junk DNA' was further cemented.

Genetic, genomic, and cytological studies in recent decades have since disputed the notion that heterochromatin is an inert, non-functional part of the genome. The ribosomal RNA (rRNA) genes, the most abundantly transcribed genes, are embedded in the X and Y pericentric heterochromatin of *Drosophila*. Detailed molecular studies showed that heterochromatin, being 30% of the *Drosophila* genome, contains many protein-encoding genes. The Y chromosome, which is entirely heterochromatic by the cytological definition, contains genes essential for male fertility (Yasuhara and Wakimoto, 2006). The *Drosophila* Heterochromatin Genome Project (DHGP) has successfully sequenced and

annotated 35% of *Drosophila* heterochromatin, identifying about 450 heterochromatic genes (Hoskins et al., submitted; Smith et al., submitted).

Further analyses of heterochromatin demonstrated its roles in regulating chromosome organization, centromere function and telomere protection. Cytological and genetic studies showed that heterochromatin is essential for homologous achiasmatic (non-exchange) chromosomes to pair and segregate during meiosis (Dernburg et al., 1996b; Karpen et al., 1996). Heterochromatin also mediates long-range chromatin interactions that regulate gene expression. The bwD allele contains megabases of tandemly repeated simple sequences inserted within the coding region, resulting in epigenetic silencing of the bw locus in cis. Tight association of the bwD locus with the pericentric heterochromatin of the same chromosome (chr. 2) also trans-silences a wild-type *bw* allele on the homolog; the bw+ allele is abnormally associated with 2nd chromosome heterochromatin due to somatic pairing with bwD (Dernburg et al., 1996a). Heterochromatin structure at the mating type locus in *S. pombe* is needed for long-range (~20-kb) interactions of donor loci (*mat2-P* or *mat3-M*) with the expressed *mat1* locus to facilitate mating type switching (Jia et al., 2004). Repositioning lymphoid-lineage genes to heterochromatin effects heritable gene silencing during T cell and B cell development (Brown et al., 1999). This is another example of heterochromatin function in cell differentiation during development.

Heterochromatin also helps maintain proper centromere and telomere functions. Heterochromatin protein 1 (HP1), a structural component of

heterochromatin, helps protect telomeres from the activity of DNA repair machineries that can cause chromosome fusions (de Lange, 2005). The cohesin protein complex maintains sister chromatid cohesion at pericentric heterochromatin and is essential for proper chromosome segregation. HP1 is required for cohesin recruitment to pericentric heterochromatin; HP1 loss causes premature sister chromatid separation, which ultimately leads to chromosome mis-segregation, aneuploidy and genome instability (Bernard et al., 2001). Heterochromatin has also been proposed to present a rigid structure around the centromere that facilitates biorientation of sister chromatid pairs on the mitotic spindle (Allshire, 2004).

Different chromatin states have been correlated with patterns of post-translational histone modifications, including serine phosphorylation, lysine acetylation, and lysine and arginine methylation. For example, actively expressed genes contain H3K4me and hyper-acetylated histones. The H3K9me2 and me3 modifications associated with 'silent' chromatin has become one standard characteristic of heterochromatin in most eukaryotes (Jenuwein and Allis, 2001). Recent studies have shown that RNA interference (RNAi) pathways and dsRNA are required for the initial recruitment of H3 Lys9 methyltransferases, and the establishment and maintenance of heterochromatin (Grewal and Moazed, 2003).

Nuclear architecture

Interphase nuclei exhibit complex and dynamic organization of chromosomes and nuclear structures. Individual chromosomes occupy distinct territories within the nucleus (Cremer and Cremer, 2001; Parada and Misteli,

2002). *Drosophila* and plant interphase chromosomes can display a Rabl arrangement, in which centromeres and telomeres cluster on opposite sides of the nucleus (Abranches et al., 1998; Hochstrasser et al., 1986). Mammalian chromosome positions can be characterized by radial distance (Figure 1-1a) and neighboring chromosomes, i.e. specific chromosomes tend to dwell next to specific chromosomes (Figure 1-1b) (Parada and Misteli, 2002). The relative positions of chromosomes within the nucleus depend upon their intrinsic properties, such as chromosome size and gene density, as well as the cell type, shape, cell cycle stage, and quiescent vs. senescent states. Despite the many variables that can perturb such arrangements, chromosome positions are conserved evolutionarily amongst primate species (Cremer and Cremer, 2001; Mora et al., 2006; Tanabe et al., 2002). Many publications describe the characteristics of chromosome territories, but no study has identified the mechanisms that regulate their formation or maintenance. This has led to the speculation that chromosomes passively arrange themselves according to polymer dynamics, metabolic states and the transcriptional profile of the cell.

Studying the formation of nuclear bodies can be equally perplexing. Examples of nuclear bodies are nucleol, Cajal and PML bodies, speckles, and paraspeckles. Each type of nuclear body contains different molecules (proteins, RNAs, and/or DNA) involved in a common function, and the nuclear bodies are thought to act as 'factories' that facilitate nuclear processes such as replication, splicing, and transcription (Figure 1-1c). For example, ribosomal RNAs are transcribed, processed and assembled into ribosomes in the nucleolus (see

below). Also, the small nuclear ribonucleoprotein particles (snRNPs) that function in RNA splicing are assembled in Cajal bodies (Carmo-Fonseca, 2002).

. Nuclear bodies are not constrained by membranous structures, unlike most cytoplasmic organelles, and their structural components exhibit highly dynamic, diffusion-based mobility to freely exchange with the nucleoplasm (Lamond and Spector, 2003). The diffusive mobility exhibited by these structural components lead to the false interpretation that nuclear body formation occurs anywhere in the nucleus and is passively regulated. In contrary, evidence suggests that nuclear body formation and behavior are function-dependent. Nuclear replication, splicing, and transcription 'factories' dwell in spaces in between chromosome territories, as interchromatin granule clusters (IGC). Speckles and paraspeckles often physically associate, most likely due to the functions, i.e. mRNA splicing and processing, shared by their structural proteins. PML bodies physically associate with telomeres in specific mammalian tissue culture cell types so PML bodies can maintain telomeric DNA lengths using a recombination mechanism termed alterrnative lengthening of telomeres (ALT) (Henson et al., 2002)

The nucleolus and its foundation, rDNA, are the best characterized of all nuclear bodies. The nucleolus is also the most prominent nuclear organelle since it occupies a large proportion of the nuclear volume. Electron microscropy shows that the nucleolus is composed of three structural components: the fibrillar center (the innermost region), the dense fibrillar component, and the granular component. Ribosomal RNAs are transcribed in the fibrillar center, while rRNA

processing starts in the dense fibrillar component and completes in the granular component (Hernandez-Verdun, 2006).

Nucleolus structure is highly dynamic, and its size and morphology depend on cell types and cell cycle stages. The nucleolus also disassembles during mitosis and reassociates at the onset of telophase (Hernandez-Verdun, 2006). How the nucleolar structural proteins coalesce at the site of rDNA is poorly understood. Fluorescent recovery after photobleaching (FRAP) studies showed that individual nucleolar proteins rapidly exchange with the nucleoplasm in diffusive mobility. A subset of these proteins move at slower speeds, suggesting that protein-protein, protein-RNA, or protein-DNA interactions likely delay their mobility (Phair and Misteli, 2000). Single rDNA units inserted within euchromatin are able to seed nucleolus formation (Karpen et al., 1988). Ribosomal RNA transcriptional inhibition by RNA polymerase I inhibitor actinomycin D causes nucleolus structural disruption (Hadjiolova et al., 1995). These studies along with others (Hernandez-Verdun, 2006) suggest that the nucleolus forms by 'self-assembly' at rDNA in response to rRNA transcription and processing and ribosome assembly.

The nucleolus organizer region ribosomal RNA genes (NOR rDNA) are arranged as tandem repeats in most eukaryotes' heterochromatin. The numbers of rDNA units vary from strain to strain and from species to species. The variability of rDNA copies in *D. melanogaster* lies between 120 to 240 per chromosome and about 140 in *S. cerevisiae* (Long and Dawid, 1980). Only some units of the NOR rDNA are actively transcribed. Epigenetic regulation of rDNA

transcription is well documented in yeast, plant, and mammalian systems. For example, a mammalian nucleolar remodeling complex (NoRC) regulates rRNA expression by establishing and maintaining histone H4 deacetylation, H3K9 dimethylation, and *de novo* DNA methylation at silenced rDNA transcription units (Santoro et al., 2002). In contrast, local chromatin structure does not significantly impact *Drosophila* rRNA transcription regulation. In *Drosophila*, selective rRNA units are silenced within the tandem repeats but do not correlate with histone modifications. However, the rRNA units inserted with the R1 and R2 retrotransposable elements are expressed 1/5 to 1/10 the level of those not disrupted (Ye and Eickbush, 2006).

A minimal number of actively transcribed rRNA units are needed for cellular and organismal viability; *D. melanogaster* requires at least 15% of the wild-type rDNA copy number, and *S. cerevisiae* requires 25 copies (Long and Dawid, 1980; Shermoen and Kiefer, 1975). To ensure their viability, both yeast and flies utilize the process of rDNA magnification to make sure individual cells contain enough rDNA content. This process is likely mediated by unequal sister chromatid recombination (Hawley and Marcus, 1989). Ribosomal DNA recombination is also implicated in extrachromosomal (ecc) rDNA formation, especially in *S. cerevisiae,* where heterochromatin proteins such as SIR2 regulate ecc rDNA formation (Blander and Guarente, 2004). Since the DNA repair mechanisms are involved in rDNA magnification and ecc rDNA formation, they function in rDNA and nucleolar structural maintenance, in addition to general DNA repair and maintenance of genome stability.

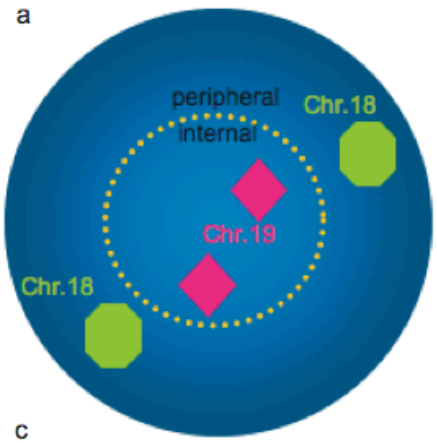

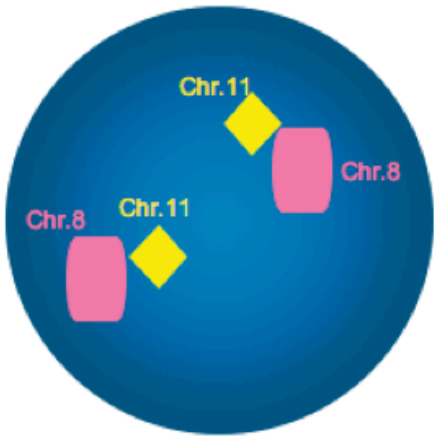

c

Body Name	Marker Protein	Descriptions
Cajal body	Coilin	snRNP and snoRNP biogenesis
Clastosome	20S proteasome	Contains ubiquitin conjugates and parts of 26S proteasome
Cleavage body	CstF	factors involved in 3' cleavage of mRNAs
Nuclear speckle	SC35	pre-mRNA processing; storage, assembly, and modification of pre-mRNA splicing factors
OPT domain	PTF	contains transrcription factors and RNA transcripts; localizes close to nucleolus
Paraspeckle	p54, PSP1	contains RNA-binding proteins; associate with nuclear speckle
PML body	PML	transcriptional regulation, nuclear protein sequestration; telomeric DNA recombination in ALT cells
Polycomb body	Bmi1, Pc2	contains Polycomb repressive complex 1; associates with heterochromatin

Figure 1-1 Interphase eukaryotic cells exhibit dynamic nuclear architecture

a) Chromosomes in interphase cells occupy territories and exhibit spatial relationships. For example, chromosomes 19 tend to occupy the internal regions of the nucleus, while chromosomes 18 locate in the peripheral regions. Adapted from Parada and Misteli, 2002.

b) Certain chromosomes tend to associate with specific chromosomes. One example is illustrated here: chromosomes 8 and 11 tend to dwell next to each other. Adapted from Parada and Misteli, 2002.

c) The chart lists described subnuclear structures and their proposed functions.

Genome stability

One essential goal of the dividing cell is to ensure the faithful transmission of its genetic materials to its daughter cells. This mission is rather difficult to accomplish because DNA damage occurs at frequencies from 1 in 1000 to 1 in a million basepairs everyday. The main causes of DNA damage are environmental factors or normal metabolic processes (Lodish et al., 2004). Conservative estimates of molecular lesions would be 123 per cell per day in *D. melanogaster* (genome size of 122.7 million base pairs) and 3300 for human (3.3×10^9 base-pair genome size). These many DNA lesions present a tremendous challenge for the cell, which must identify DNA damage, signal to halt cell cycle progression to allow sufficient time for repair processes, make sure the damage is indeed repaired, and then resume cell cycle progression.

DNA double-strand breaks (DSBs) are the most dangerous DNA lesions to the cell. DSBs are caused by environmental stress or stalled DNA replication forks. To combat them, the cell utilizes two main repair processes, homologous recombination (HR) and non-homologous end joining (NHEJ). During HR repair, the MRN (MRX in *S. cerevisiae*) complex first recognizes the DSB and creates single-stranded (ss) DNAs around the DSB. The ssDNAs are bound and protected by Rad51 and Rad52, and the protein-DNA complex carries out homologous strand invasion into the unbroken sister chromatid and facilitates homologous sequence-dependent DNA synthesis. Resolution of the resultant four DNA strands and their covalent ligation complete the repair process. In contrast, during NHEJ repair, chromosome ends around the DSBs are

recognized and bound by the Ku70-Ku80 heterodimers without sequence specificity. The Ku proteins hold the two DNA strands in close proximity so ligase 4 and its associated proteins can join the ends together (Figure 1-2) (van Attikum and Gasser, 2005).

In both of these repair processes, the chromatin structure around the DSB is important for the recruitment and retention of DNA repair machineries. Specifically, the phosphorylation of H2A variants—serine 139 of H2Ax in human and yeast (γH2Ax) and serine 137 of H2Av in fly (γH2Av)—is important for recruitment of cohesins (Unal et al., 2004) and ATP-dependent chromatin remodellers (Morrison et al., 2004; van Attikum et al., 2004). Cohesins around the DSBs either help Ku proteins keep the broken ends together for NHEJ repair or hold sister chromatids together for HR repair (Fritsch et al., 2004; van Attikum et al., 2004). The INO80 complex, an ATP-dependent chromatin remodeller, evicts nucleosomes around the DSB to facilitate exonuclease activity so ssDNAs can form to facilitate Rad51-Rad52-ssDNA complex acts during HR repair (van Attikum et al., 2004).

The phosphoinositol kinase ATM (ataxia telangiectasia mutated) and ATR (ATM related) are the main signaling factors responsive to DSBs. They phosphorylate various repair proteins and the H2A variants in *S. cerevisiae* and mammalian cells to facilitate recruitment to the DSB site. The ATM and ATR proteins also activate G1-S or G2-M cell cycle arrest if the repair machineries need more time to accomplish their task. The action of ATM/ATR leads to the downstream activation of checkpoint kinase 1 (Chk1) or checkpoint kinase 2

(Chk2) or both, which then delay cell cycle progression (Brodsky et al., 2004; Jaklevic and Su, 2004; Xu et al., 2001). Recent studies demonstrated that dephosphorylation of γH2Ax in regions distal to the DSB site are required to resume cell cycle progression after DNA repair completion (Keogh et al., 2006; Tsukuda et al., 2005).

The signaling mechanisms for DNA damage in *Drosophila* differ significantly from the yeast and mammalian cells. *mei-41* is the *Drosophila* homolog of ATR, and is the main factor responsive to DSBs (Brodsky et al., 2000; Hari et al., 1995; Jaklevic and Su, 2004). ATM in *Drosophila* (*tefu*), functions in telomere protection and apoptotic signaling by activating p53 in response to persistent, unrepaired DNA damage (Larocque et al., 2006). Surprisingly, p53 in *Drosophila* does not directly participate in DNA damage checkpoint response; it is the effector of apoptosis pathway (Song, 2005). These and other significant mechanistic divergences in *Drosophila* DNA repair can make it difficult to make use of knowledge from other model systems. Despite such a risk, protein conservation exists in *Drosophila* and ultimately facilitates mechanistic study to benefit the field of DNA repair study.

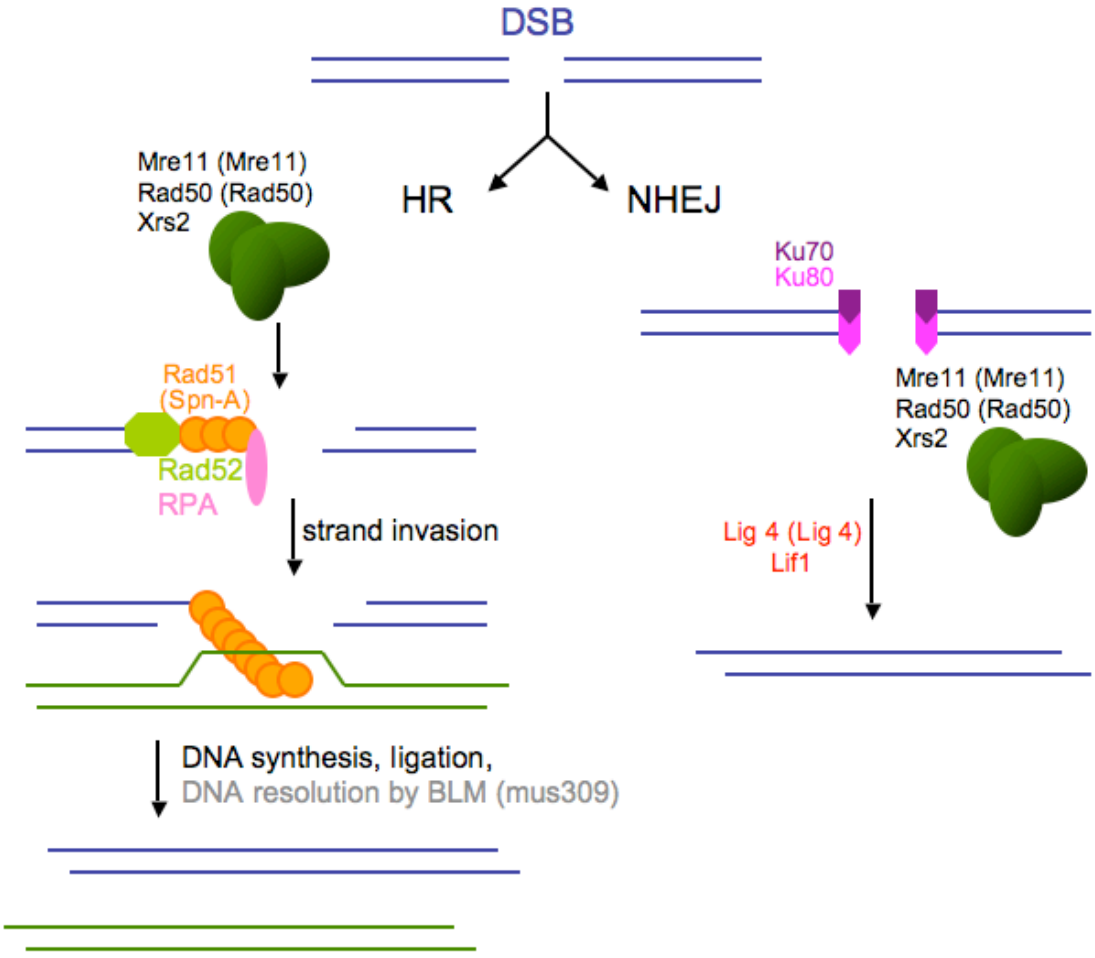

Figure 1-2 Eukaryotic cells utilize two main pathways for DNA repair. The diagram outlines the mechanistic actions of the two main DNA repair pathways. Names in parenthesis are known *Drosophila* homologs. Adapted from (van Attikum and Gasser, 2005).

Thesis Overview

My thesis project investigates how heterochromatin function and formation impact nuclear architecture, repeated DNA organization, and genome stability in *Drosophila melanogaster*. The fly is a multicellular organism with complex developmental timing and processes. Experimentalists have studied this

organism for a hundred years and accumulated highly sophisticated genetic techniques that greatly benefit current and future scientific investigations. Knowledge about this organism has consistently contributed to our understanding of human cell functions and diseases (Bier, 2005; Bilen and Bonini, 2005).

Remarkably, human euchromatin shares more similarities with the fly heterochromatin than the fly euchromatin. Repeat DNA content and gene structures, such as intron length and overall open reading frame sizes, in fly heterochromatin more closely resemble those in human euchromatin. The human euchromatin is also repeat-rich, making it difficult to completely sequence and annotate. The DHGP have made great efforts to sequence and annotate the *Drosophila* heterochromatin, thus making *D. melanogaster*'s heterochromatin the best understood heterochromatin in multicellular organisms. Knowledge gained from these studies will apply to investigations of other complex, repeat-rich genomes.

Drosophila genetic screens over the years accumulated a library of more than 100 mutations that perturb heterochromatin-mediated silencing; some of these mutations regulate heterochromatin function and formation (Donaldson et al., 2002; Grigliatti, 1991; Reuter and Spierer, 1992; Reuter et al., 1982). Knowledge about the molecular functions of these genes will increase understanding about heterochromatin (Reuter and Spierer, 1992). For example, Su(var)3-9 H3 K9 methyltransferase regulates H3K9 methylation in heterochromatin. *Su(var)3-9*^{null} mutant flies exhibit very few developmental

defects, suggesting that H3K9 methylation by Su(var)3-9 minimally regulates gene expression, unlike its counterparts in mouse (Peters et al., 2001). This mutation allowed me to conduct functional studies of heterochromatin without worries about indirect effects from transcriptional deregulation.

My thesis work focuses on heterochromatin function in genome stability. In the next chapaters I will discuss my demonstration that heterochromatin impacts nucleolar structure, repeated DNA organization, and genome stability. I showed that local chromatin structure inhibits extrachromosomal DNA formation from repeated DNAs by the repair machineries. This regulation maintains structural integrity of rDNA, thereby stabilizing nucleolus formation. Local chromatin structure inhibits DNA breaks in heterochromatin; cells with compromised heterochromatin structure—due to *Su(var)3-9*^{null} or dcr-2 mutation—display severe DNA damage compared to wild type. Accumulated DNA damage is likely responsible for the shortened lifespan of the *Su(var)3-9*^{null} animals. Increased DNA damage also leads to chromosomal defects such as translocations and aneuploidy, defective DNA repair response, and activation of the G2-M DNA repair and mitotic checkpoints that ensure cellular and organismal viability. Altogether I demonstrated how local chromatin structure in heterochromatin, beyond roles in transcriptional regulation, benefits the health and survival of a multicellular organism. The similarities shared by the *Drosophila* heterochromatin and mammalian euchromatin raises the intriguing probability that mammalian cells utilize chromatin structure to help stabilize their DNA contents. Further mechanistic investigations of how heterochromatin structure helps stabilize

Drosophila genome will contribute to our understanding of how human cells stabilize their genome.

Chapter Two:

The histone H3K9 methylation and RNAi pathways regulate nucleolar and repeated DNA organization by inhibiting formation of extrachromosomal DNAs

Introduction

Nuclei and chromosomes maintain specific and dynamic architectures, which are required for many essential functions (Francastel et al., 2000). Nuclear bodies are involved in diverse biological processes and exhibit dynamic mobility, and individual chromosomes occupy distinct domains within interphase nuclei (Cremer and Cremer, 2001). Chromosomes in the metazoan interphase nucleus are comprised of two types of cytologically and functionally distinct chromatin, euchromatin and heterochromatin (John, 1988). Patterns of post-translational histone modifications associated with these domains are strongly correlated with functions such as gene regulation, chromosome inheritance, and replication timing (Martin and Zhang, 2005). For example, regions that display heterochromatin-mediated gene silencing are rich in histone H3K9 methylation and lack many histone acetylations, whereas histones in transcriptionally-active euchromatic regions are highly acetylated and methylated at H3K4 (Jenuwein and Allis, 2001).

The first indication that chromosome organization can affect gene expression stems from the discovery of position effect variegation (PEV) in *Drosophila* by H.J. Muller (Muller, 1930). PEV describes the epigenetic

inactivation or silencing of a euchromatic gene that has been positioned close to or within heterochromatin, or a heterochromatic gene moved to distal chromosome locations. PEV is exquisitely sensitive to the dosage of genetic modifiers, known as suppressors and enhancers of variegation (*Su(var*)s and *E(var)*s) (Schotta et al., 2003). PEV modifiers regulate heterochromatin formation and functions. The *Su(var)3-9* family encodes a histone methyltransferase (HMTase) that catalyzes H3K9 methylation, and *Su(var)2-5* encodes the structural component Heterochromatin Protein1 (HP1). Methylated H3 K9 and Su(var)3-9 both bind to HP1, providing a molecular mechanism for maintaining the silenced epigenetic state(Jenuwein and Allis, 2001).

Recent studies have shown that the RNA interference (RNAi) pathway and double-stranded (ds) RNAs are required for the initial recruitment of H3K9 methyltransferase, and the establishment and maintenance of heterochromatin (Grewal and Moazed, 2003). In *S. pombe*, RNA-dependent RNA polymerase amplifies dsRNAs from repeated DNA elements that are initially transcribed by RNA polymerase II . Dicer 1 then processes dsRNAs into small interfering (si) RNAs. The siRNAs are bound by the RITS (RNA-induced initiation of transcriptional gene silencing) complex, which contains Tas3, Ago1, and Chp1. The siRNA-RITS complex then interacts and directs the localization of clr4, the Su(var)3-9 homolog, to the repeated DNAs. Once recruited there, clr4/Su(var)3-9 methylates K9 residue of histone H3, thereby initiating heterochromatin formation (Cam and Grewal 2004 review). Genetic analysis showed that some *Drosophila* RNAi mutants, *piwi*, *aubergine*, and *spindle-E*, act as *Su(var)s* that

influence silencing of tandem repeats (Pal-Bhadra et al., 2004). These proteins were later found to regulate dsRNA cleavage during repeat-associated siRNA (rasiRNA) production (Aravin et al., 2004; Tomari et al., 2004). Other RNAi genes, such as argonaute-2 and dicer-2, seem to regulate siRNA but not rasiRNA production.

The nucleolus, the site of ribosome assembly, is an example of an essential nuclear organelle. The structural foundation of the nucleolus is the organizer region ribosomal DNAs (NOR rDNAs). The rDNAs are tandemly repeated sequences embedded in heterochromatin in most eukaryotes, and single rDNA genes can form mini-nucleoli via a self-assembly process (Karpen et al., 1988). The rRNA transcription is epigenetically in yeast, plant, and mammalian systems. A mammalian nucleolar remodeling complex (NoRC) regulates rRNA expression by by histone H4 deacetylation, H3K9 dimethylation, and *de novo* DNA methylation at rDNA (Santoro et al., 2002). In contrast, rRNA expression regulation in *D. melanogaster* does not correlate with its chromatin structure; the R1 and R2 retrotransposable elements inserted within the rDNA spacers influence rRNA expression (Ye and Eickbush, 2006). rDNA magnification occurs in yeast and flies with low rDNA content, and this process is likely mediated by unequal sister chromatid recombination(Hawley and Marcus, 1989). Finally, mutations in a protein that regulates silencing in *S. cerevisiae* (SIR2) result in extrachromosomal (ecc) rDNA formation, which is thought to impact cell senescence and aging (Blander and Guarente, 2004).

It is surprising that rDNA produces the overwhelming majority of RNAs in the cell, despite its association with ‘silenced’ heterochromatin. This paradox suggests that the evolutionarily conserved positioning of NORs in heterochromatin may regulate important, unknown features of nucleolus formation. Here, I test the hypothesis that heterochromatin and associated proteins regulate the organization of nucleoli and repeated DNAs in *Drosophila*. Our results demonstrate that a subset of *Su(var)* proteins, including the *Su(var)*3-9 HMTase, HP1, and the RNAi pathway, are required for the normal organization of nucleoli and satellite DNAs in the nucleus. Furthermore, these regulators of heterochromatin suppress eccDNA formation from repeated DNAs, which is mediated by non-homologous end-joining (NHEJ) or other recombination/repair pathways.

Results

Multiple nucleoli are present in *Su(var)* mutant cells

I used indirect immunofluorescence (IF) to examine nucleolar organization in whole-mount (three dimensional) imaginal disc tissues and polytene larval salivary glands from wild type and *Su(var)* mutant larvae (see Materials and Methods). Staining for fibrillarin, a component of the rRNA processing machinery (Tollervey et al., 1993), confirmed that wild type polytene and diploid cells contain single nucleoli (Figure 2-1). In contrast, salivary gland cells from animals homozygous for mutations in the Su(var)3-9 histone H3K9 methyltransferase or HP1/*Su(var)2-5* genes contained between 1 and 12 nucleoli (Figure 2-1a, Table 2-1). The average numbers of nucleoli in mutant cells (*Su(var)3-9*^{null} = 2.7, *Su(var)3-9*^{1699} = 5.0, *HP1*^{null} = 2.8) were significantly higher than in wild type (avg=1, Table 2-1). Increases in nucleolar numbers was accompanied by a proportional increase in both nuclear and nucleolar volume, even though the ratio remained constant (data not shown). Irregularly-shaped, multi-lobed nucleoli were observed in 44% of *Su(var)3-9*^{null} mutant diploid imaginal disc cells, versus only 10% in wild type cells (Figure 2-1b). For all experiments we chose to analyze *Su(var)3-9*^{null} mutant flies whose parents are null mutants because maternal effects may exist in *Su(var)3-9*^{null} mutant flies from heterozygous mothers carrying one wild type copy of *Su(var)3-9*.

Fibrillarin staining in salivary glands of *Su(TDA-PEV)1650* (Figure 2-1a) and *Su(var)2-10/dPIAS* mutant cells also displayed the multiple nucleoli phenotype, whereas mutations in seven other *Su(var)* loci and two Polycomb-

Group (PcG) genes had no effect on nucleolar organization (Table 2-1). I conclude that many but not all regulators of gene silencing (4/13) are required for the formation of a normal, single nucleolus.

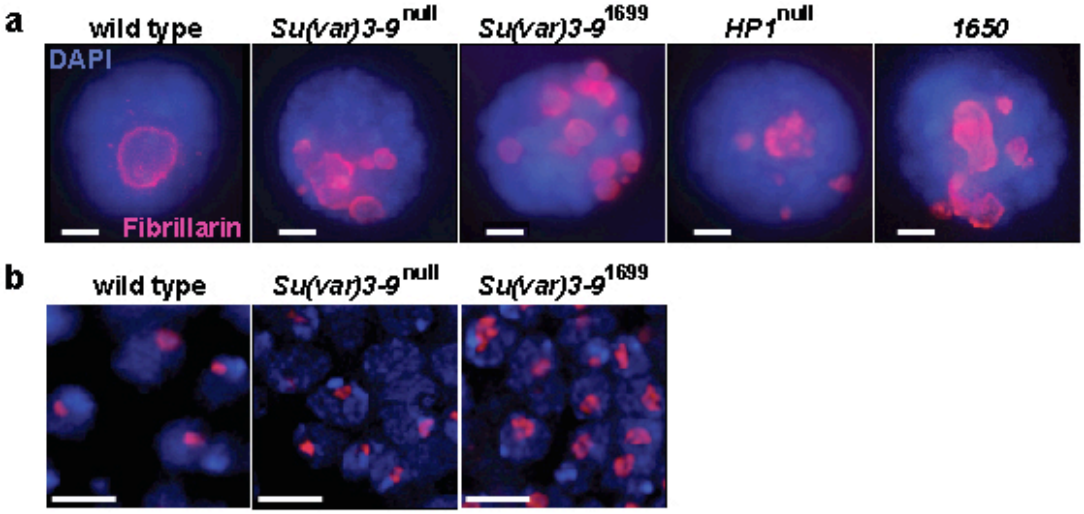

Figure 2-1 *Su(var)* mutants contain multiple nucleoli.

a) IF with antibodies against the nucleolus marker fibrillarin (red) in whole-mount salivary gland nuclei from wild type, *Su(var)3-9*^{null}, *Su(var)3-9*^{1699}, *HP1*^{null} and *Su(TDA-PEV)1650* homozygous mutants. Wild type cells have one nucleolus, whereas the mutants display multiple nucleoli. Blue = DAPI. Scale bars are 10μm.

b) Fibrillarin IF in whole-mount imaginal disc and brain tissues from wild type and *Su(var)3-9* mutants are shown. The single, wild type nucleolus (N=51) tended to be round, whereas nucleoli in the mutants were irregular (lobed) and larger. Quantitative analysis showed that 44% of *Su(var)3-9*^{null} mutant nuclei contained lobed nucleoli (N=55), versus 10% for wild type ($p<0.001$). The scale bars are 5μm.

Table 2-1: Effects of mutations on salivary gland nucleoli.

Locus / Molecular Function	Alleles Tested	Refs.	# Nucleoli		
			Mean ± SD	Range	[c] P values
Wild type [a]			1±0	1	NA
Su(var)3-9 H3K9 methyltransferase	*1699* (missense), *6* and *17* (nulls)	(Donaldson et al., 2002; Schotta et al., 2002)	2.7± 1.4 N = 54	1 to 9 (null); 1 to 12 (1699)	<0.001
Su(var)2-5 / HP1 chromodomain/ binds H3K9me	transheterozygous 1009/1209 (nulls)	(Donaldson et al., 2002)	2.8± 0.83 N = 21	1 to 4	<0.001
Su(var)2-10 / dPIAS Protein Inhibitor of Activated STAT / SUMOylation	transheterozygous 02/Pex14A (nulls)	(Hari et al., 2001b)	multiple [b]	N.D[b].	
Su(TDA-PEV) 1650 ? function	*1650*	(Donaldson et al., 2002)	3.6± 1.6 N = 35	1 to 8	<0.001
*Su(var)*3-7 zinc Finger/ DNA binding	*234*	(Donaldson et al., 2002)	1 [b]		
l(3)73Ah ubiquitin ligase	*1044*	(Donaldson et al., 2002)	1 [b]		
Su(TDA-PEV) 1025 ? function	*1025*	(Donaldson et al., 2002)	1 [b]		
Su(TDA-PEV) 1260 ? function	*1260*	(Donaldson et al., 2002)	1 [b]		
Su(TDA-PEV) 1128 ? function	*1128*	(Donaldson et al., 2002)	1 [b]		
Su(var)4-20 H4K20 methyltransferase	BG00814 and EY07422 P insertions (hypomorphic)	(Schotta et al., 2004)	1 [b]		
dSIR2 NAD-dependent histone deacetylase	*17* (null)	(Astrom et al., 2003)	1 [b]		
Pc PcG complex	*1* and *7* (nulls)	(Gindhart-Jr and Kaufman, 1995; Tearle and Nusslein-	1 [b]		

		Volhard, 1987)			
Ph PcG complex	*410* (null)	(Hodgson et al., 1997)	1 [b]		
Lig4 DNA ligase	29 and 57 (nulls)	(Romeijn and Ferro, 2004)	1 [b]		
Lig4; Su(var)3-9 N.A.	double transheterozygous mutant		1.7± 0.8 N = 83	1 to 4	<0.001 [d]

[a] heterozygous for *Su(var)*

[b] evaluated qualitatively from multiple images

[c] p values reflect comparisons of the mean # nucleoli in wild type versus mutant

[d] p values reflect comparisons of the mean # nucleoli in the double mutant versus wild type, and separately versus *Su(var)3-9*^{null} mutant

Ectopic nucleoli in *Su(var)* mutants contain rDNA

Multiple, ectopic nucleoli associated with *Su(var)* mutations could result from dispersion or fission of nucleolar material initially formed around a single rDNA cluster, or from mislocalization of rDNA. These hypotheses were tested by evaluating the association of rDNA with ectopic nucleoli, using combined fibrillarin IF and rDNA FISH. Wild type polytene nuclei displayed single rDNA sites within each nucleolus, whereas nuclei from *Su(var)3-9*, *HP1*, and *Su*(*TDA-PEV)1650* mutants contained multiple, dispersed rDNA foci associated with ectopic nucleoli (Figure 2-2a). Similarly, 33% of *Su(var)3-9*^{null} diploid disc cells contained multiple rDNA sites (average=1.44±0.72), compared to only 2% of wild type (average=1±0.1, Figures 2-2b and c). These results demonstrate that

ectopic nucleoli in *Su(var)* mutants are nucleated independently by mislocalized rDNA, including the multi-lobed nucleoli observed in mutant diploid cells.

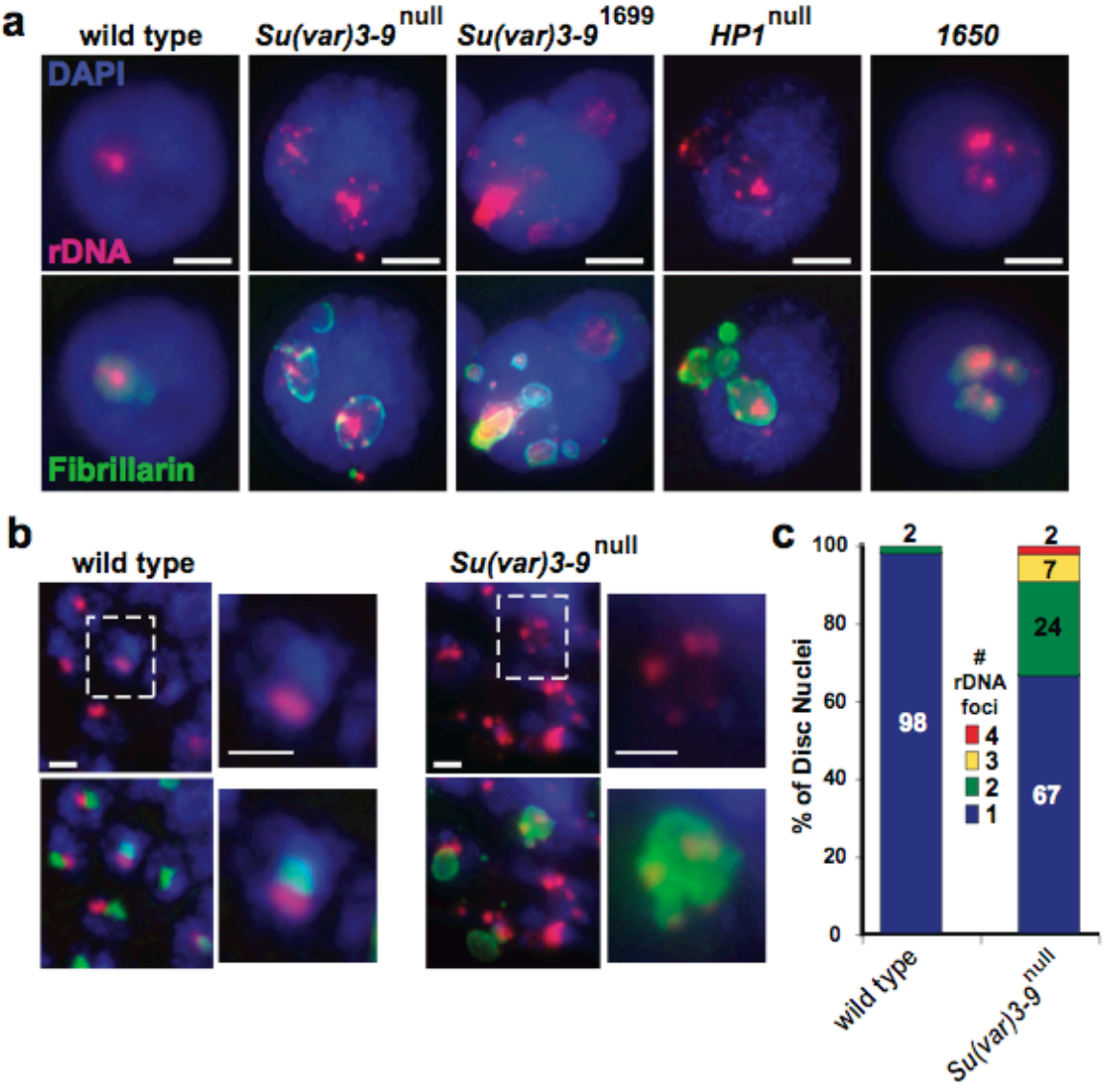

Figure 2-2 *Su(var)* mutants have dispersed rDNA foci, each of which forms an ectopic nucleolus.

a) Fluorescence in situ hybridization (FISH) for rDNA (red) and IF for fibrillarin (green) were performed on whole-mount salivary glands from wild type, *Su(var)3-*

9^{null}, *Su(var)3-9*^{1699}, *HP1*^{null}, and *Su(TDA-PEV)1650* homozygous mutants. Blue = DAPI. There is a single site of rDNA in >98% of wild type nuclei, whereas the *Su(var)* mutant nuclei contain multiple rDNA foci, which are all surrounded by fibrillarin. Scale bars are 15μm.

b) Combined rDNA FISH (red) and fibrillarin IF (green) analysis of whole-mount imaginal disc and brain tissues from wild type and *Su(var)3-9*^{null} mutant larvae. Wild type nucleoli contain a single, compact rDNA focus, whereas *Su(var)3-9*^{null} mutants frequently display multiple rDNA foci. Scale bars are 3μm.

c) Quantitative analysis of the number of rDNA foci in wild type and *Su(var)3-9*^{null} diploid nuclei. 98% of wild type cells (N=96) contain one rDNA signal, compared to 67% of *Su(var)3-9* null nuclei, and the percent with 2, 3, and 4 rDNA signals was 24%, 7%, and 2%, respectively (average =1.44 ± 0.73 rDNA foci per mutant nucleus, N=53, $p<0.001$).

***Su(var)3-9* mutants disrupt the organization of other repeated DNAs**

The severe disruption of rDNA and nucleolar organization raised the possibility that the 3-dimensional spatial relationships of other heterochromatic DNAs are also affected by *Su(var)* mutations. FISH analysis on polytene nuclei was performed using probes to tandemly-repeated satellite DNAs (Figure 2-3a), which localize to the heterochromatic chromocenter (Spradling and Orr-Weaver, 1987). An average of two sites were observed in wild type nuclei for satellites 1.688 and 1.686, compared to 3 sites in *Su(var)3-9*^{null} mutants (Figure 2-3b and c; $p<0.001$). Similar observations were made with satellites AACAC and AATAT (data not shown). Distances between signals for each satellite increased

significantly in *Su(var)3-9*^{null} mutants (1.688 = 9-fold, 1.686 = 3-fold; Figure 2-3b and d; $p<0.001$). Notably, mislocalized satellite DNA and rDNA were not restricted to a specific nuclear compartment. I conclude that heterochromatic repeated DNAs become dispersed and disorganized in *Su(var)3-9* mutants, as observed for rDNA and nucleoli.

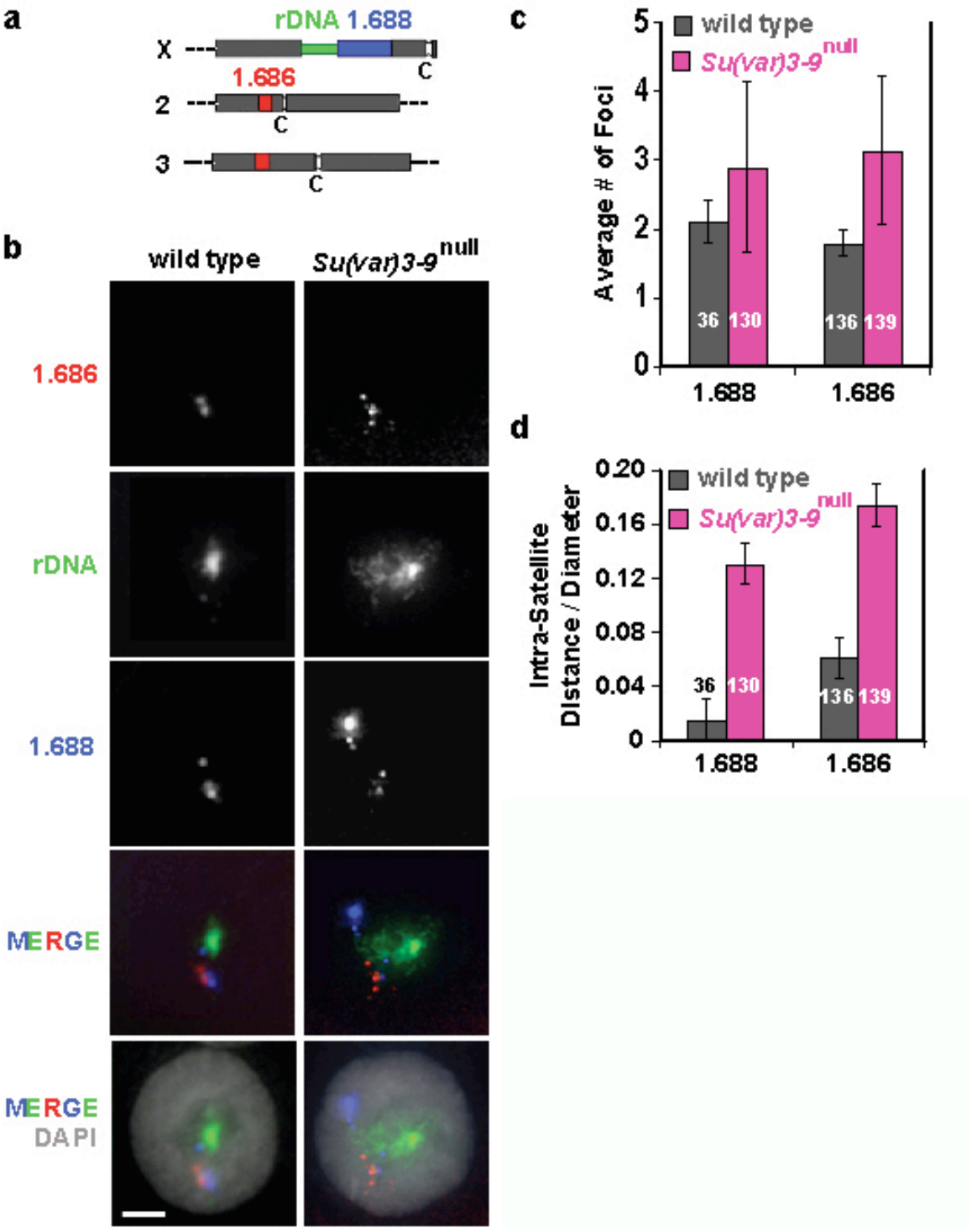

Figure 2-3 Satellite DNA organization is disrupted in *Su(var)3-9*^{null} mutant nuclei. a) Locations of rDNA and satellite DNAs in the *Drosophila melanogaster* genome (not to scale). The rDNA is located in the heterochromatin of the X and Y sex

chromosomes, the 1.688 satellite (359-bp repeats) is next to the X rDNA, and the 1.686 satellite is in the heterochromatin of chromosomes 2 and 3.

b) FISH was performed on whole-mount polytene salivary glands isolated from wild type and *Su(var)3-9*^{null} mutants. In wild type nuclei, specific satellite DNAs are localized at single sites, and the different satellite signals are close to each other. In *Su(var)3-9*^{null} mutant nuclei, individual satellite DNAs are dispersed to multiple sites and are not clustered with other satellites. Gray is DAPI, FISH probe colors correspond to the diagram in a. Scale bars are 15μm.

c) The number of 1.688 and 1.686 foci were significantly higher in mutant nuclei compared to wild type ($p<0.001$). d) Distances between satellite signals were quantitated in 3-dimensional reconstructions. The intra-satellite distances in *Su(var)3-9*^{null} mutant nuclei were significantly higher than in wild type ($p<0.001$).

The RNAi pathway is also required for normal nucleolar organization

The targeting of H3K9me2 by the RNAi pathway (Grewal and Moazed, 2003) and the presence of small RNAs homologous to the 1.688 satellite and other repeats (Aravin et al., 2003) led us to examine RNAi mutants for disorganized nucleoli. At least one mutant allele at all five RNAi loci examined displayed significantly increased nucleolus numbers, in comparison to wild type ($p<0.01$ for all except for *hls*$^{\Delta 215}$, $p<0.08$; Table 2-2, Figure 2-4a). Combined fibrillarin IF and rDNA FISH in *dcr-2*$^{L811\ fsx}$ mutant demonstrated that the mutant nuclei also contain dispersed rDNA loci (Figure 2-4b).

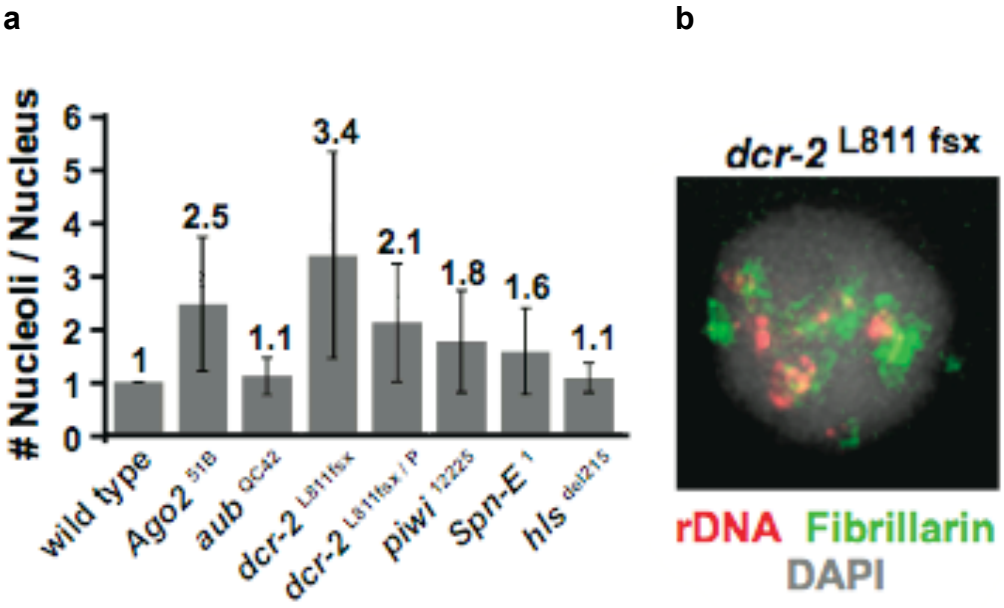

Figure 2-4 The RNAi pathway is also required to maintain the structural integrity of repeated DNAs and the nucleolus.

a) The histogram shows the average numbers of nucleoli in different RNAi mutants examined. At least one allele at all loci contained significantly more nucleoli than wild type ($p<0.01$). The *hls*^{del215} allele of *SpnE* had a mild phenotype ($p = 0.083$).

b) Combined rDNA FISH (red) and fibrillarin IF (green) shows that *dcr-2*^{L811fsx} polytene nuclei contain multiple rDNA foci and ectopic nucleoli. The nucleus is 22um.

Table 2-2: Effects of mutations of RNAi genes on salivary gland nucleoli.

Locus / Molecular Function	Alleles Tested	Refs.	# Nucleoli		
			Mean ± SD	Range	[b]P values
Wild type [a]			1±0	1	NA
Ago2 siRNA loading	*51B* (null)	(Xu et al., 2004)	2.5± 1.3 N = 79	1 to 5	0.001
Aub RNAi complex	*QC42* (?)	(Wilson et al., 1996)	1.1± 0.4 N = 85	1 to 3	0.004
hls / Spn-E RNA helicase (of RNAi complex)	*Δ215* (null) and *1* (hypomorph)	(Gillespie and Berg, 1995; Gonzalez-Reyes et al., 1997)	1.1± 0.3 N = 40 and 1.6± 0.8 N = 78	1 to 4	0.083 and <0.001
piwi mRNA binding (of RNAi complex)	*06843* (null)	(Lin and Spradling, 1997)	1.8± 1.0 N = 102	1 to 5	<0.001
dcr-2 RNA helicase (of RNAi complex)	*L811fsx* (hypomorph) and P insertion (null)	(Lee et al., 2004)	3.4± 1.9 N = 60	1 to 6	<0.001

[a] heterozygous for *Su(var)*

[b] p values reflect comparisons of the mean # nucleoli in wild type versus mutant

H3K9me2 levels at rDNA and satellite DNAs decrease significantly in *Su(var)3-9* and *dcr-2* mutants

Heterochromatic nucleosomes in a variety of organisms, including *Drosophila*, are enriched for the H3K9me2 modification. Thus, HP1 and Su(var)3-9 could control rDNA and nucleolar organization indirectly by regulating the flanking heterochromatin, or could act directly on rDNA chromatin. To address this question, we aimed to determine whether rDNA and satellite DNAs contained methylated H3K9, and if this modification was disrupted in *Su(var)3-9* mutants. Combined IF and FISH studies indicated that H3K9me2 partially

overlapped with rDNA in wild type diploid cells, and was significantly reduced in *Su(var)3-9*^{null} mutants (Figure 2-5a). H3K9me2 IF showed that H3K9me2 is mislocalized in *dcr-2*$^{L811\ fsx}$ diploid nuclei when compared to wild type (Figure 2-5a). While H3K9me2 signals mostly localize to DAPI-bright regions (heterochromatin) in the wild type, their staining patterns in *dcr-2* mutant nuclei are more broadly distributed.

Quantitative Chromatin ImmunoPrecipitation (ChIP) showed that rDNA, 5S rDNA, and satellite DNAs were enriched for H3K9me2 in wild type diploid cells, and that this modification was not well represented at single copy gene controls (actin and HDAC3; Figure 2-5b). Moreover, the levels of H3K9me2 on all repeated DNAs decreased substantially in chromatin isolated from *Su(var)3-9*^{null} mutant discs. The reductions in H3K9me2 levels varied among the different repeats and within the rDNA (6- to 226-fold, Figure 2-5b, top), most likely reflecting known redundancy in the HMTases responsible for this modification in flies (Schotta et al., 2002). ChIP analysis of *dcr-2* mutant (*dcr-2*^{L811fsx}) revealed significant H3K9me2 reduction in the rDNA; unlike *Su(var)3-9* mutants, reductions were not observed for 5S rDNA and satellite 1.688 ($p<0.05$, Figure 2-5c). In sum, the ChIP and combined IF-FISH results suggest that the effects of Su(var)3-9 and the RNAi pathway on rDNA and nucleolar organization are mediated through the chromatin structure of the rDNA itself, rather than solely through the flanking heterochromatin.

H3K4me2 and H3K9ac have been characterized as modifications associated with active or open chromatin. ChIP analysis showed that chromatin

associated with repeated DNAs contained low levels of H3K9ac (Figure 2-5d) and H3K4me2 (Figure 2-5e), which remained mostly unchanged in *Su(var)3-9*^{null} mutants. Exceptions were significant increases in 5S rDNA H3K9ac levels in the mutants ($p<0.03$), and H3K4me2 decreases for the 1.688 satellite ($p<0.04$).

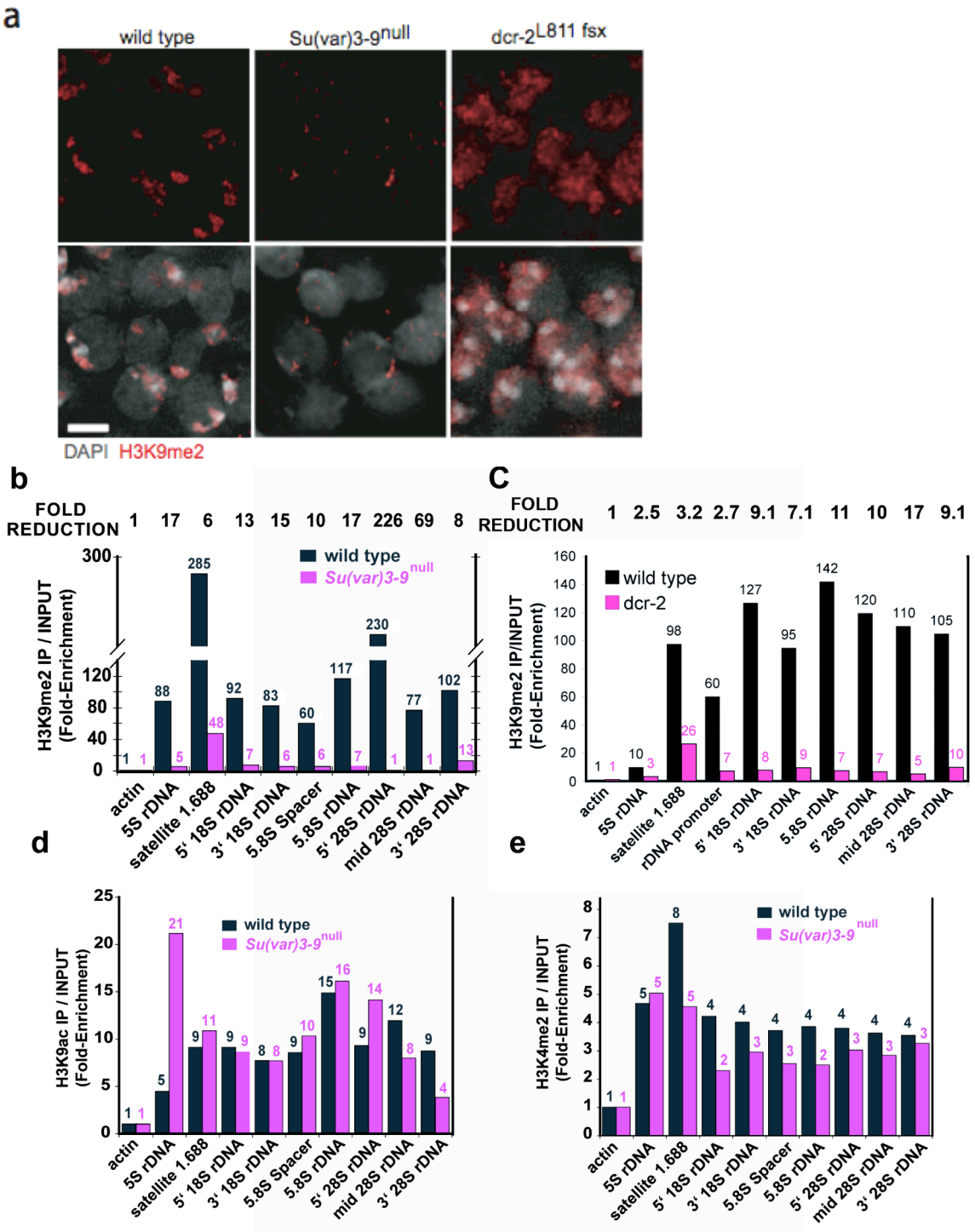

Figure 2-5 Analysis of histone modifications in chromatin containing repeated DNA in wild type, *Su(var)3-9*^{null}, and *dcr-2*$^{L811\ fsx}$ cells.

a) IF using antibodies that specifically bind H3K9me2 (red) in squashed diploid nuclei from wild type, *Su(var)3-9*^{null}, and *dcr-2*$^{L811\ fsx}$ animals. H3K9me2 localizes predominantly in DAPI-bright heterochromatin regions in wild type, but is mostly missing in *Su(var)3-9*^{null} nuclei and becomes more broadly distributed in *dcr-2*^{L811fsx} nuclei. Scale bar is 3μm.

b) Chromatin immunoprecipitation (ChIP) analysis of H3K9me2 levels in wild type and *Su(var)3-9*^{null} mutant imaginal disc tissues. The graph shows H3K9me2 levels for the repeated DNAs examined by PCR, standardized to actin and HDAC single copy controls (see Materials and Methods); values were averages of 5 ChIP experiments. In wild type cells, the 1.688 satellite (359-bp repeats), 5S rDNA (in chromosome 2 euchromatin), and the rDNA on the sex chromosomes contain significant enrichment for H3K9me2, compared to input chromatin and controls. H3K9me2 levels in chromatin derived from *Su(var)3-9*^{null} mutant tissues were significantly reduced (6- to 226-fold) compared to wild type.

c) ChIP analysis reveals reduced H3K9me2 levels in *dcr-2*^{L811fsx} chromatin compared to wild type ($p<0.05$), more so for rDNA than the 5S rDNA and satellite 1.688. Values are averages of 4 PCR reactions from 2 ChIP experiments.

d) and e) ChIP analysis of two modifications associated with 'active' or 'open' chromatin (H3K9ac and H3K4me2). Small enrichment for these modifications was observed on repeated DNAs in wild type chromatin, compared to input and single copy controls. For most of the repeated DNAs, levels were not significantly altered in *Su(var)3-9*^{null} mutant chromatin ($p>0.5$ for all regions). H3K9ac levels were significantly increased in 5S rDNA in the mutants ($p<0.05$), and H3K4me2

was significantly decreased for the 1.688 satellite ($p<0.05$). Values are averages of 2 experiments.

Su(var)3-9 and *dcr-2*$^{L811\ fsx}$ mutations cause significant increases in the amount of extrachromosomal repeated DNA

How do chromatin changes affect the organization of repeated DNAs and nucleoli? Loss of H3K9me2 could generate extrachromosomal (ecc) DNA through intra-chromatid recombination, or chromatin decondensation could cause dispersal of repeated DNAs in the nucleoplasm. To test these hypotheses, eccDNA was quantitated in mutant and wild type cells using 'Hirt' supernatants, which separates ecc from genomic DNAs (Hirt, 1967) (Materials and Methods). Wild type polytene tissues contained ecc 5S rDNA and satellite 1.688 DNA, as observed previously (Pont et al., 1987), but very low levels of ecc 18S/5.8S/28S rDNA (Figure 2-6a). The amounts of eccDNA increased dramatically in *Su(var)3-9*^{null} mutant tissues versus wild type for rDNA (46- to 78-fold) and satellite 1.688 (20-fold) (Figure 2-6b; $p<0.05$ for all regions), which was not observed for the single copy genes actin and HDAC. Similarly, the ecc rDNA increased in *dcr-2*^{L811fsx} mutants (13- to 29-fold, Figure 2-6c), consistent with ectopic nucleolus formation. For diploid cells, ecc repeated DNAs were ~2-fold higher in *Su(var)3-9* mutant tissues than in wild type (Figure 2-6d; $p<0.05$ for all regions). Lower levels of eccDNA in mutant diploid cells likely results from the absence of endoreplication and loss during mitosis (see Discussion). We conclude that loss of H3K9me2 from chromatin containing repeated DNAs results in eccDNA

formation, and that the increased ecc rDNA leads to the formation of ectopic nucleoli.

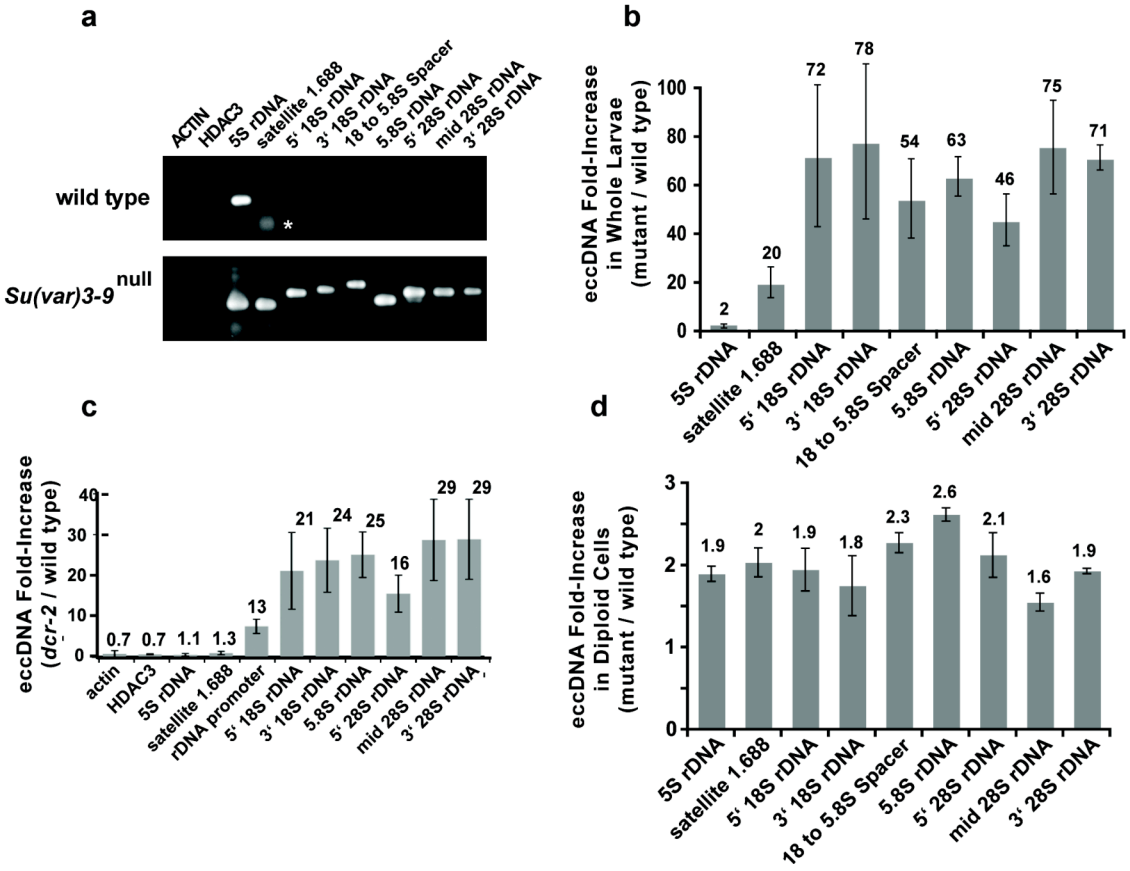

Figure 2-6 Levels of extrachromosomal repeated DNAs are significantly increased in *Su(var)3-9*^{null} and *dcr-2*$^{L811\ fsx}$ mutant tissues compared to wild type. a) Extrachromosomal DNA was isolated from wild type and *Su(var)3-9*^{null} mutant larvae, and PCR reactions, terminated at logarithmic phase of amplification, were performed to evaluate the amounts of eccDNA corresponding to specific sequences (see Materials and Methods). The gel shows an example of the PCR reactions for the specific regions examined. EccDNAs from the single-copy genes (actin and HDAC3) were not detected in either wild type or mutant larvae.

The asterisk indicates that the band in the 1.688 satellite lane corresponds to the primers, not the PCR products.

b) Quantitation demonstrates that the amount of eccDNA for the 1.688 satellite and different regions of the rDNA are significantly higher in *Su(var)3-9*^{null} mutants compared to wild type (20- to 78-fold enrichment); the increase for 5S rDNA was only 2-fold, because wild type larvae contain high levels of ecc 5S rDNA. The values were averages of 3 sample extractions.

c) Ecc rDNA levels in *dcr-2*^{L811fsx} mutant larvae are significantly higher than in wild type (13- to 29-fold increases), but eccDNA levels for 5S rDNA and satellite 1.688 did not increase.

d) Quantitation of PCR products indicates that the amount of eccDNA in *Su(var)3-9*^{null} mutant diploid cells is about two-fold higher than in wild type. The values were averages of 3 sample extractions, and p values were <0.05 for the regions examined.

The level of repeat-associated cohesins is reduced in *Su(var)3-9*^{null} mutants, but a cohesin mutation does not increase extrachromosomal DNA formation

Sister chromatid cohesion (maintained by the protein complex cohesin) inhibits ecc rDNA formation in *S. cerevisiae* (Kobayashi and Ganley, 2005), and H3K9me2 and the HP1 homolog SWI6 are required for cohesin recruitment in *S. pombe (Nonaka et al., 2002)*. Thus, recruitment of cohesin to pericentric heterochromatin by the H3K9me pathway could also regulate repeated DNA structural integrity in *Drosophila*. ChIP analysis showed that levels of the SMC1

cohesin subunit (Losada et al., 1998) were significantly reduced in chromatin containing repeated DNA in *Su(var)3-9*^{null} mutants (16 to 29 % of wild type levels, Figure 2-7a). However, the amount of eccDNA isolated from animals homozygous for the *smc1*^{exc461} mutation did not differ significantly from wild type (Figure 2-7b). Therefore, I conclude that Su(var)3-9 and H3K9 methylation are required for cohesin recruitment at repeated DNAs in *Drosophila*, but cohesin is not essential for repressing eccDNA formation.

The reduction of cohesins at the repeated DNAs suggests that sister chromatid cohesion defects during mitosis may occur. Cell cycle analysis of the *Su(var)3-9*^{null} cells showed mitosis delay (Chapter 3) that reinforces this idea. I therefore hypothesize that the reduced amount of cohesins in the *Su(var)3-9*^{null} cells may cause cell viability defects. Progeny analysis of the cross of *smc1*^{exc46}, *Su(var)3-9*^{17} / TM3 flies with the *Su(var)3-9*^{6} / TM3 flies showed that *smc1*^{exc46}, *Su(var)3-9*^{17} / *Su(var)3-9*^{6} progeny are 75% viable compared to the *smc1*^{exc46} / *Su(var)3-9*^{6} flies from the control cross (p value <0.01 by chi-square test). This result indicates that cohesins are haplo-insufficient in the *Su(var)3-9*^{null} background.

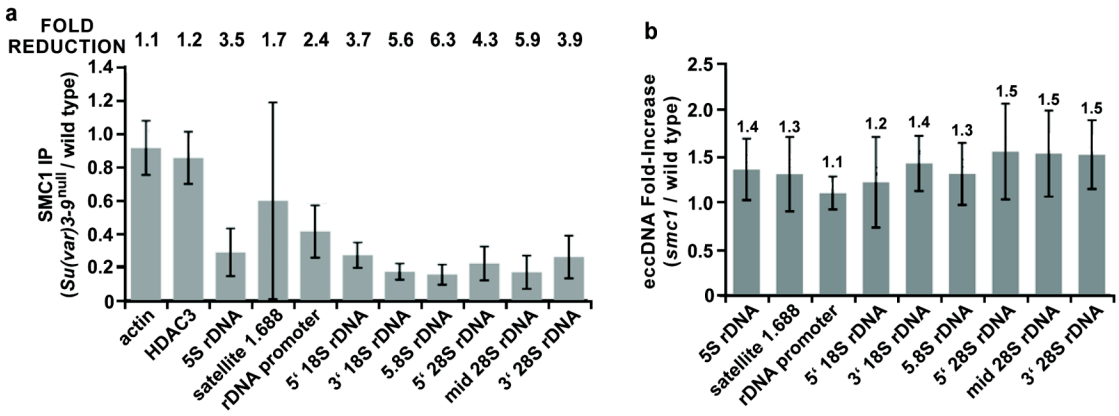

c

virgins	Su(var)3-9^{6} / TM3, Sb, Ser males crossed with			
	smc1^{exc46} / TM3, Sb		smc1^{exc46}, Su(var)3-9^{17} / TM3, Sb	
progeny genotypes	smc1^{exc46} / Su(var)3-9^{6}	TM3 flies	smc1^{exc46}, Su(var)3-9^{17} / Su(var)3-9^{6}	TM3 flies
progeny numbers / %	198 / 41.6 %	278 / 58.4 %	148 / 31.8 %	318 / 68.2 %

Figure 2-7 Cohesin protein, SMC1, does not regulate eccDNA formation. Its mutant genetically interacts with *Su(var)3-9*^{null} mutations.

a) ChIP analysis shows reduced SMC1 levels at repeated DNAs in *Su(var)3-9*^{null} chromatin, relative to wild type; fold reductions are shown above ($p<0.05$ for all repeated DNA except 5S rDNA). Values were averages of 4 PCR reactions from 2 ChIP experiments.

b) The amount of eccDNA from satellite 1.688 and rDNA in *smc1*^{exc46l} mutant tissues do not differ significantly from wild type.

c) *Su(var)3-9*^{6} / TM3, Sb, Ser males were crossed with either *smc1*^{exc46} / TM3, *Sb* (control cross) or *smc1*^{exc46}, *Su(var)3-9*^{17} / TM3, *Sb* virgins. The progeny were scored by the presence and absence of the *Sb* phenotype. The *smc1*^{exc46} / *Su(var)3-9*^{6} flies from the *smc1*^{exc46} / TM3, *Sb* mothers were 42% of total progeny, while the *smc1*^{exc46} , *Su(var)3-9*^{17} / *Su(var)3-9*^{6} flies from the *smc1*^{exc46}, *Su(var)3-9*^{17} / TM3, *Sb* mothers were 32 % of the total progeny. Compared to

the control, the *smc1*^{exc46} , *Su(var)3-9*^{17} / *Su(var)3-9*^{6} flies have a 76 % viability (p value <0.01 by chi-square test).

Ligase 4 and *Spn-A/Rad51* mutations partially suppress the disorganized nucleolus phenotype observed in *Su(var)3-9* mutants

Extrachromosomal DNA formation likely arises from somatic recombination, as suggested by the observation that *sir2*-dependent ecc rDNA formation in *S. cerevisiae* requires the RAD52 complex (Blander and Guarente, 2004; Lin and Keil, 1991). Efforts to identify recombination proteins required for eccDNA formation in *Drosophila* have been unsuccessful (Cohen et al., 2003), and *Drosophila RAD52* homologs have not been identified. A recent study identified Ligase IV, an essential regulator of non-homologous end joining (NHEJ), as necessary for eccDNA formation in mammals (Cohen et al., 2006). Cells from the *Lig4*^{null}; *Su(var)3-9*^{null} double mutant displayed an average of 1.7 nucleoli (± 0.8; N = 83), which is significantly lower than the 2.7 nucleoli observed in *Su(var)3-9*^{null} single mutants (Figure 2-8a, p<0.001). Thus, loss of Lig4 partially suppresses the formation of multiple nucleoli in *Su(var)3-9* mutants. Homozygous mutations in the homologous recombination (HR) protein, Spn-A (*Drosophila* homolog of Rad51, a single-strand binding protein that facilitates homologous strand invasion during homologous recombination process), also partially suppresses ectopic nucleolus formation. The average nucleolus number in *dcr-2*$^{L811\ fsx}$ *; Spn-A*$^{095/02}$ polytene nuclei is 1.77 (N=58) and significantly lower (Figure 2-8b, p<0.001) than the average 3.38 (N=60) nucleoli observed in *dcr-2*$^{L811\ fsx}$ mutant nuclei. Surprisingly, mus309 (the *Drosophila* homolog of Bloom

DNA helicase *RecQ*) in the HR pathway does not suppress ectopic nucleolus formation (Figure 2-8b). mus309 in *Drosophila* participates in synthesis-dependent strand annealing (SDSS), part of the HR pathway (Adams et al., 2003); therefore, eccDNA formation likely does not utilize the SDSS mechanism. In sum, I conclude that the NHEJ pathway and the HR pathway both participate in eccDNA formation in *Drosophila* (see Discussion).

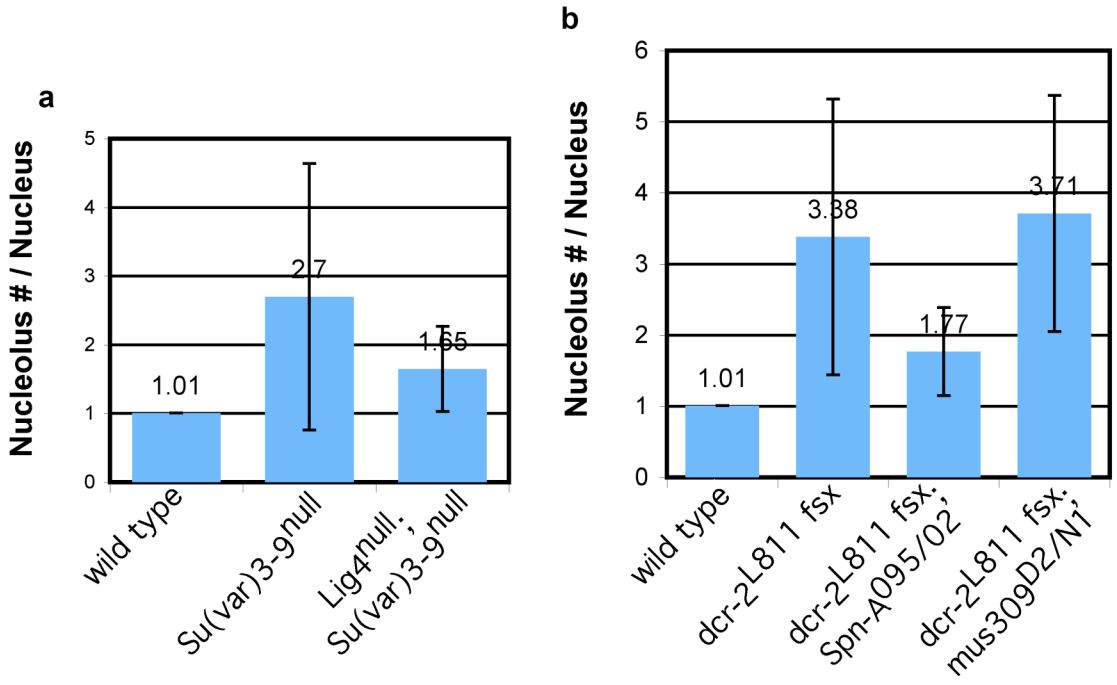

Figure 2-8 Ligase 4 and Rad51 (Spn-A) partially suppress ectopic nucleolus formation.

a) Ligase 4 mutations partially suppress ectopic nucleolus formation in *Su(var)3-9* mutants. Average nucleolus number of *Lig4*^{null}*; Su(var)3-9*^{null} polytene nuclei is 1.7 (N=83), which is significantly lower ($p<0.001$) than the average 2.7 (N=54) nucleoli observed in *Su(var)3-9*^{null} mutant nuclei.

b) Spn-A (homolog of Rad51) mutations partially suppress ectopic nucleolus

formation in *dcr-2*$^{L811\ fsx}$ mutants. Average nucleolus number of *dcr-2*$^{L811\ fsx}$ *; Spn-A*$^{095/02}$ polytene nuclei is 1.77 (N=58), which is significantly lower ($p<0.001$) than the average 3.38 (N=60) nucleoli observed in *dcr-2*$^{L811\ fsx}$ mutant nuclei. The average nucleolus number of 3.71 (N=45) in *dcr-2*$^{L811\ fsx}$ *; mus309*$^{D2/N1}$ polytene nuclei does not significantly differ from that in *dcr-2*$^{L811\ fsx}$ mutant nuclei ($p=0.35$).

Discussion

The H3K9 methylation and RNAi pathways regulate the organization of repeated DNAs and the nucleolus

Post-translational histone modifications have been correlated with regulation of gene expression (Martin and Zhang, 2005). However, recent discoveries of distinct patterns of centromeric histone modifications and the requirement of H3K9me2 in transcriptional elongation indicate that some combinations of modifications defy simple global interpretations (Sullivan and Karpen, 2004; Vakoc et al., 2005). In addition, limited knowledge exists about the impact of chromatin structures on other nuclear functions, such as genome stability, and the 3-dimensional organization of sequences, chromosomes, and nuclear organelles. Here I have shown that the Su(var)3-9 H3K9 methyltransferase, its binding partner HP1, and five components of the RNAi pathway are required for the normal organization of rDNA, satellite DNAs, and nucleoli in *Drosophila*. When animals lack these components, repeated DNAs and nucleoli become dispersed to multiple nuclear locations. ChIP and IF-FISH showed that H3K9me2 levels in chromatin associated with repeated DNAs are strongly reduced in *Su(var)3-9* and *dcr-2* mutant animals. Finally, I observed significantly increased amounts of extrachromosomal repeated DNAs in these mutants. I conclude that the H3K9 methylation and RNAi pathways directly regulate nuclear architecture, by affecting chromatin structure and repressing eccDNA formation of rDNA and satellites.

I observed that other genes involved in heterochromatin structure and function are also required to maintain the structural integrity of repeated DNA and nucleoli, specifically the dPIAS SUMO E3 ligase (Hari et al., 2001a; Jackson, 2001) and *Su(TDA-PEV)1650* (function unknown). Further studies are required to determine if these proteins impact the integrity of repeated DNA and nucleoli via H3K9 methylation or other pathways. Mutations in 9 out of 18 loci associated with gene silencing had no effect on nucleolar organization, including dSIR2 and two Polycomb group genes (Supplemental Table 1). Interestingly, loss of the SUV4-20 H4K20 methyltransferase did not produce multiple nucleoli; this result demonstrates that H3K9 methylation is the primary histone modification responsible for maintaining repeated DNA integrity, and not H4K20 trimethylation by SUV4-20, which requires H3K9me2 (Schotta et al., 2004). In addition, *Drosophila sir2* mutants did not contain multiple nucleoli, despite SIR2 repression of ecc rDNA formation in *S. cerevisiae* (Blander and Guarente, 2004). In sum, rDNA organization and nucleolar architecture are regulated by some but not all proteins involved in heterochromatin structure and function.

Differential effects of components of the H3K9 methylation and RNAi pathways

Dicer-2 regulates H3K9me2 levels and eccDNA formation at some but not all repeated DNAs, in contrast to the broad impact of Su(var)3-9. For example, *Su(var)3-9* mutants displayed increased levels of ecc rDNA, 5S rDNA, and 1.688 satellite, whereas only ecc rDNA levels increased significantly in *dcr-2* mutants The *Drosophila* dcr-2 locus has been shown to regulate siRNA production but not

an influential factor in miRNA production (Lee et al., 2004). In *S. pombe*, siRNAs recruit the RITS complex to repeated DNAs to establish heterochromatin structure (Moazed et al., 2006; Noma et al., 2004), and siRNAs are produced from rDNA repeats (Cam et al., 2005). These demonstrations point to the intriguing probability that dcr-2 and the siRNA mechanism preferentially direct Su(var)3-9 to methylate H3K9 at rDNA, leaving the rasiRNA mechanism to regulate Su(var)3-9 methyltransferase activity in other repeated DNAs, e.g., 5S rDNA and 1.688 satellite.

The overall distributions of H3K9me2 observed with IF analysis differ between *Su(var)3-9* and *dcr-2* mutants. H3K9me2 levels were significantly reduced in *Su(var)3-9* mutant nuclei, though visible amounts were retained in the heterochromatin (Figure 5a). In contrast, overall H3K9me2 levels were not reduced in *dcr-2* mutant diploid cells, and instead were reduced at some repeats and mislocalized to a larger portion of the nucleus (Figure 5b). This observation is surprising, since H3K9me is not detectable in RNAi mutants in *S. pombe* (Cam et al., 2005). I conclude that the absence of dicer-2 alters the specificity of siRNA-mediated targeting of H3K9me2 in *Drosophila*.

Impact of Su(var)3-9 and H3 K9 methylation on cells and animals

Mice deleted for both *Suv3-9* genes exhibit genome instability and early embryonic lethality (Peters et al., 2001). In contrast, *Drosophila Su(var)3-9*^{null} flies are viable and fertile, despite very low levels of H3K9me2. Residual amounts of this modification in the absence of *Su(var)3-9* is likely due to the presence of a redundant H3K9-methyltransferase which has recently been identified (Mis et al.,

2006; Schotta et al., 2002). Our studies show that the absence of Su(var)3-9 has dramatic effects on nuclear organization. The presence of fibrillarin around ectopic rDNAs suggests that transcription and processing of ribosomal RNA occur in ectopic nucleoli. Similarly, ectopically-integrated rDNA forms functional 'mini-nucleoli' (Karpen et al., 1988) and rescues defects in X-Y pairing in male meiosis caused by endogenous rDNA deletion (McKee and Karpen, 1990). These observations suggest that increased nucleolar volumes and ecc rDNA do not cause significant growth abnormalities. However, more developmental or physiological phenotypes may yet be discovered. For example, we have observed that non-recombinant chromosomes display significantly increased levels of meiotic non-disjunction in *Su(var)3-9*^{null} females (GHK, unpublished), consistent with previous studies demonstrating heterochromatin's participation in achiasmate segregation (Dernburg et al., 1996b; Karpen et al., 1996).

Another explanation for the absence of dramatic phenotypic abnormalities in *Su(var)3-9*^{null} animals arises from our observation that diploid tissues display lower levels of ectopic nucleoli and eccDNA compared to polytene cells. EccDNAs lack functional centromeres and should be poorly transmitted in rapidly dividing diploid cells, but would be retained in the non-mitotic polytene cells. I propose that the levels of eccDNA and ectopic nucleoli in mitotic larval cells that give rise to most adult tissues are not high enough to affect viability and fecundity. Chapter 3 will discuss the role of the DNA damage repair checkpoint in the viability of *Su(var)*3-9 mutants.

A model for the regulation of nuclear architecture by the Su(var)3-9/H3K9 methylation pathway

Our findings demonstrate that chromatin structures regulated by Su(var)3-9, HP1, the RNAi pathway, and H3K9 methylation are required to maintain the structural integrity of tandemly repeated, heterochromatic sequences (Figure 8). *HP1* mutant cells display increased restriction enzyme accessibility in heterochromatin, consistent with chromatin decondensation and loss of gene silencing (Cartwright et al., 1999). H3K9 methylation, and perhaps other heterochromatic properties and components, generate a chromatin structure that normally restricts access of DNA repair proteins to repeated DNA substrates, or locally inhibits their activity (Figure 9). Mutations affecting the NHEJ (Lig4) and HR (Rad51) pathways both partially suppress ectopic nucleolus formation in *Su(var)3-9*^{null} mutants supporting a role for DNA repair in eccDNA formation. Finally, cohesins are significantly reduced at repeated DNA chromatin in *Su(var)3-9*^{null} nuclei. However, complete loss of the SMC1 cohesin component did not lead to increases in eccDNA. This suggests that cohesins do not suppress eccDNA formation in Drosophila, contrary to observations in *S. cerevisiae* (Kobayashi and Ganley, 2005).

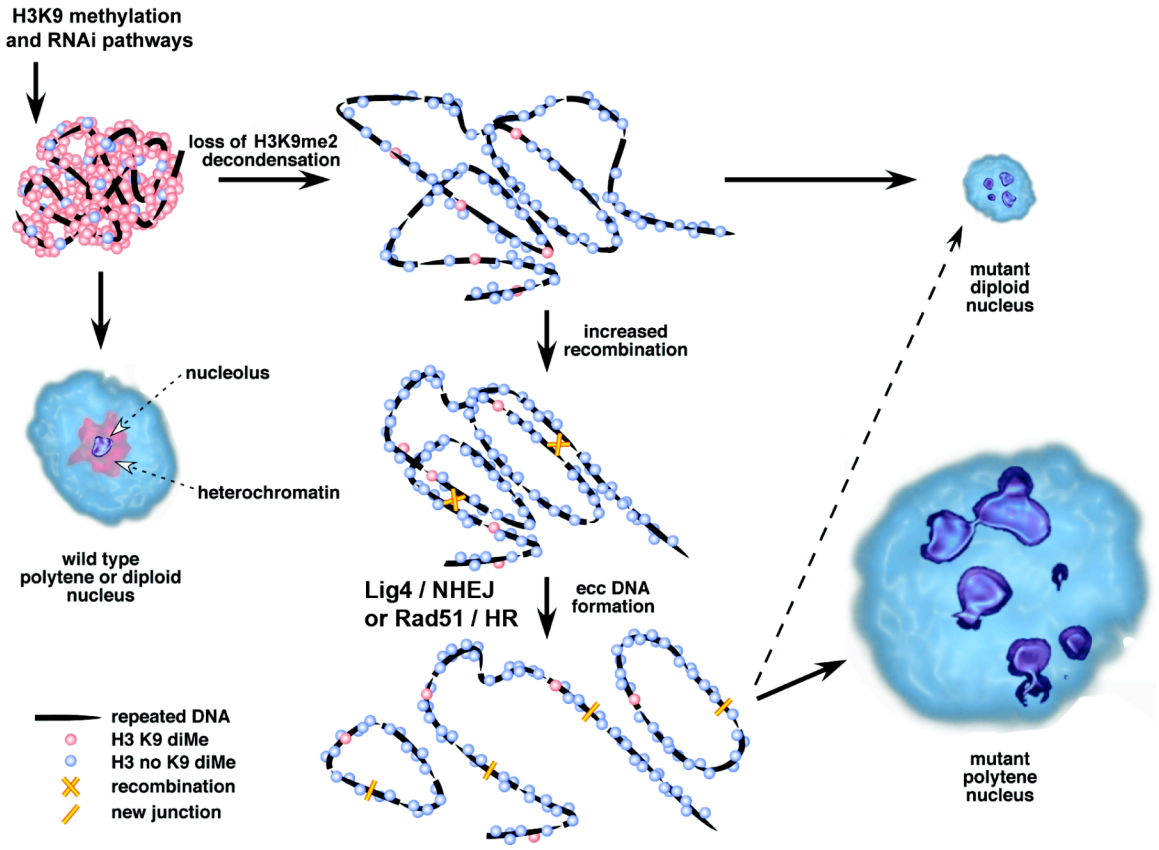

Figure 2-9 A model for regulation of nuclear architecture by the H3K9 methylation and RNAi pathways. In wild type diploid and polytene nuclei, the majority of the heterochromatin contains H3K9me2, and a single nucleolus forms around the rDNA. Loss of H3K9me2 from repeated DNA, due to *Su(var)3-9*, *HP1* or RNAi mutations, causes chromatin decondensation and elevated recombination between repeated DNA copies. The recombination process, catalyzed by the NHEJ or HR DNA repair pathways, results in formation of extrachromosomal DNAs that localize throughout the nucleoplasm, causing dispersal of satellite DNAs (not shown) and, in the case of rDNA, the formation of ectopic nucleoli. Decondensation is proposed to be primarily responsible for the 'lobed' structure of rDNA and nucleoli in diploid cells, with a minor contribution

from low levels of ecc rDNA formation (dotted line). In polytene cells, decondensation is likely to be a prerequisite for increased recombination, but the much higher levels of ecc rDNA is proposed to generate the majority of the ectopic nucleoli.

Chromatin decondensation (e.g. 'looping') and increased recombination likely occur in both diploid and polytene cells in response to loss of H3K9 methylation (Figure 2-9). The much larger increases in eccDNAs and ectopic nucleoli in polytene tissues probably reflect a stronger requirement for repressing DNA recombination or NHEJ. In highly endoreplicated nuclei, euchromatic sequences are present in thousands of copies, satellite sequences are replicated at most twice, and rDNA is replicated to intermediate levels (~250 copies) (Spradling and Orr-Weaver, 1987). This differential endoreplication results in stalled forks at euchromatin-heterochromatin junctions (Glaser et al., 1992), and presumably between the rDNA and adjacent sequences. Stalled forks and associated single-stranded DNA in *S. cerevisiae* have been shown to provide substrates for repeated eccDNA formation (Ivessa et al., 2000), and could play similar roles in polytene cells that lack *Su(var)3-9* and H3K9 methylation. Diploid cells would not be expected to generate as much eccDNA and ectopic nucleoli as endoreplicating cells, because DNA copy numbers are much lower, and they would not contain as many stalled replication forks. Furthermore, diploid nuclei would not retain eccDNAs, since they are likely to be lost during cell division; maintenance of eccDNAs in polytene nuclei would be higher, since they are non-mitotic.

Other examples of heterochromatic silencing mechanisms affecting recombination have been reported. Some combinations of *Su(var)* mutations increase meiotic recombination in *Drosophila* heterochromatin (Westphal and Reuter, 2002), and loss of gene silencing components in budding and fission yeasts increases both meiotic and somatic recombination in the rDNA (Cam et al., 2005; Kaeberlein et al., 1999). Similarly, the G9a H3K9 methyltransferase regulates accessibility of the V(D)J recombination machinery during mouse lymphocyte development (Osipovich et al., 2004). In Chapter 2, I expanded on previous studies by demonstrating the impact of these mechanisms on nucleolar organization and the spatial arrangement of repeated sequences in the nucleus of a developing animal. In addition, these findings may have broader significance to genome stability; the extensive sequence homology inherent to repeated DNAs would presumably generate translocations and other chromosome aberrations in somatic and/or germ cells if exchange was not repressed by heterochromatic structures. In Chapter 3, I will report my efforts to follow up on the question whether H3K9 methylation in *Drosophila* heterochromatin impacts genome stability in general.

Materials and Methods

Fly stocks

All fly stocks were raised at 22 ^{o}C. Information regarding the fly strains are described in Table 1. We received the *suv4-20*, *Pc*, *Ph*, *Lig4*, *aub*, *Spn-E*^{1}, and *piwi* flies from the Bloomington stock center, and the *dcr-2* P element insertion from the Harvard fly center. The *hls*$^{\Delta 215}$ flies are from James Birchler, *DCR2*^{L811fsx} from Richard Carthew, *smc1*^{exc461} from Scott Hawley, *Ago2*^{51B} from Fenbiao Gao, *Su(var)3-9* null alleles 6 and 17 from Gunter Reuter, and *dSir2*^{17} from Jasper Rine.

Antibodies

The human anti-fibrillarin antibody (dilution 1:500 in IF) was a gift from Mike Pollard, and the rabbit anti-H3K9me2 antibody (dilution 1:100 in IF and 1:1000 in ChIP) was provided by Thomas Jenuwein (Peters et al., 2003). Rabbit antibodies against H3K9-acetyl and H3K4me2 were purchased from Upstate. Rabbit antibodies against smc1 (1:1000 in ChIP) were a gift from Dale Dorsett (Dorsett et al., 2005).

IF, FISH, and IF-FISH of whole-mount tissues and squashed tissues.

IF was performed as previously described (Hari et al., 2001a). FISH was performed as previously described (Dernburg et al., 1996b) using 100 ng of each probe. In combined IF-FISH experiments, IF was performed before the FISH treatment. FISH probes were made with nick translation and terminal labeling, using materials previously published (Karpen et al., 1988).

Volumetric, distance, and colocalization analysis

All images were captured using an Applied Precision Deltavision Workstation and deconvolved using the conservative algorithm with 8 iterations. SoftWorx software was used to measure colocalization and distances, which were normalized to nuclear diameter. The deconvolved, stacked images were converted to TIFF files and 3-dimensionally reconstructed, and volumes of nuclei (DAPI signals) and nucleoli (fibrillarin signals) were measured using Metamorph software. All statistical comparisons and p values were calculated using the two-sample t test, assuming unequal variance.

Chromatin Immunoprecipitation (ChIP)

Protocols were modified from Austin et al.(Austin et al., 1999) Brain and disc tissues were dissected from fifty 3rd instar larvae, then fixed in 1.8% paraformaldehyde/PBST for 10 minutes at room temperature. The tissues were washed twice in cold PBST, then one time in cold TE and RIPA lysis buffer. Sonication in a 1 ml volume was performed with a Branson Sonifier 450 (6 times with a 90 % duty cycle and a 5.5 power output; each cycle included a 2-minute rest interval) or the Bioruptor (Diagenode; 30 second on-off cycles for 12 minutes at high intensity). 300 µl of the sheared chromatin was used for IP. The input and IP'd DNAs were resuspended in 100µl, 1µl of which was used in 25-µl PCR reactions that were terminated at the logarithmic phase of amplification. Signals from the PCR products were captured using a BioRad Gel Doc workstation and analyzed with Quantity One software. Values were calculated as a percentage of

input. Real-time PCR was also performed to confirm our results. Primer sequences are available upon request.

All the individual H3K9me2 ChIP experiments showed the same trends of H3K9me2 level reduction in *Su(var)3-9*^{null} chromatin (statistical analysis always showed significant reduction), although the absolute values differed. Both the cytology and ChIP results agreed that H3K9me2 levels are significantly lower in *Su(var)3-9*^{null} chromatin.

Hirt extrachromosomal DNA isolation and detection

Approximately 200 larvae were frozen in liquid nitrogen, ground with a mortar and pestle, resuspended in 500 µl Hirt lysis buffer (0.6% SDS; 10mM EDTA, pH 8)(Hirt, 1967), then incubated at room temperature for 10 to 20 minutes. 125µl of 5M NaCl was added to the extract, which was incubated at 4^{o}C overnight (8 to 20 hours). The larval extract was centrifuged at 14,000g and 4^{o}C for 40 minutes. The supernatant was phenol-chloroform extracted 3 times and the Hirt DNA was ethanol-precipitated. To check for any genomic DNA contamination, the Hirt supernatant before pheno-chloroform extraction was methanol-acetic acid fixed on slides and examined by DAPI staining (Kuschak et al., 2001). The precipitated Hirt DNA was also examined by standard electrophoresis agarose gel and ethidium bromide staining. 200ng of Hirt DNA was used for each PCR reaction to probe for specific DNAs. Signals from the PCR products were captured and analyzed using a BioRad Gel Doc workstation and Quantity One software, as described above. For diploid tissues, 50 sets of brains and discs were dissected and lysed with 100µl Hirt lysis buffer. The Hirt

DNA isolated from diploid cells contains some genomic DNA, so the relative amount of eccDNAs in mutant and wild type tissues were quantitated by comparing the results from separate PCR reactions for Hirt DNA and genomic DNA preparations.

Chapter Three:

Chromatin structure of heterochromatin maintains heterochromatin and genome stability

Introduction

To ensure the faithful transmission of its genetic materials to the next generation, the cell must constantly repair high incidence of DNA damage that arises as a consequence of normal DNA metabolism. Double-strand DNA breaks (DSBs) are caused by environmental stress or stalled DNA replication forks, and they are the most dangerous DNA lesions. The cell utilizes two major processes to repair DSBs, homologous recombination (HR) and non-homologous end joining (NHEJ). Numerous human disorders, including ataxia telangiectasia, Bloom syndrome, and Cockayne syndrome, are caused by mutations of factors involved in DNA repair mechanisms. Patients suffering from these genetic disorders also exhibit much higher susceptibility to cancer and neurological defects (Subba Rao, 2007).

When the cell cannot rapidly repair DNA breaks, it activates the DNA damage checkpoint to delay cell cycle progression. The phosphoinositide 3-kinases (PI(3)Ks) ATM (ataxia telengiectasia mutated) and ATR (ATM-related) are the key factors that trigger checkpoint responses to DNA damage. They activate checkpoint kinase 1 (Chk1, *grp* in *Drosophila melanogaster*) and/or checkpoint kinase 2 (Chk2, *lok* in *D. melanogaster*) to signal G1-S or G2-M cell cycle arrest (Brodsky et al., 2004; Jaklevic and Su, 2004; Xu et al., 2001).

Signaling for DNA repair in *Drosophila* is different than in yeast and mammalian cells. While ATM is considered more critical than ATR in DNA damage checkpoint signaling in yeast and mammals, ATR/*mei-41* is the primary factor responsive to DNA breaks in *Drosophila* (Brodsky et al., 2000; Hari et al., 1995; Jaklevic and Su, 2004). ATM in *Drosophila* (*tefu*) functions in telomere protection and apoptotic signaling, where it activates p53 (Larocque et al., 2006). Surprisingly, p53 in *Drosophila* does not directly participate in the DNA damage checkpoint response as in yeast and mammalian cells; instead, it activates the apoptosis pathway in response to persistent DNA damage (Song, 2005).

The chromatin structure in the vicinity of DSBs is important for the recruitment and retention of DNA repair complexes. A number of covalent histone modifications stabilize repair factor loadings onto damage sites during DNA repair processes (Karagiannis and El-Osta, 2006). The best characterized histone modification in this context is phosphorylation of the histone H2A variants H2Ax in humans and yeast (S139 phosphorylation = γH2Ax) and H2Av in flies (S137 phosphorylation = γH2Av). This phosphorylation is important to recruit and retain cohesins (Unal et al., 2004) and ATP-dependent chromatin remodellers (Morrison et al., 2004; van Attikum et al., 2004). Cohesins contribute to NHEJ by by keeping broken ends together during NHEJ repair, and they also contribute to homologous recombination by holding sister chromatids together (Fritsch et al., 2004; van Attikum et al., 2004). The INO80 complex, an ATP-dependent chromatin remodeller, evicts nucleosomes around DSBs to facilitate the activities of the Rad51-Rad52-ssDNA complex during HR repair (van Attikum et al., 2004).

H3K9 methylation is a characteristic mark of heterochromatin in most eukaryotes (Jenuwein and Allis, 2001). Several H3K9 methyltransferases have been identified in mammals: Suv39h 1 and 2 (Peters et al., 2001), G9a (Tachibana et al., 2002), SETB1 (Schultz et al., 2002), and RIZ1 (Kim et al., 2003). G9a, SETB1, and RIZ1 mainly function in transcriptional silencing of euchromatic genes via H3K9 methylation, while the two Suv3-9 isoforms are responsible for euchromatic gene regulation in addition to H3K9 methylation in pericentric heterochromatin. *Suv39h1/2* double knockout mice are born in sub-Mendelian ratios due to prenatal inviability. Postnatal *Suv39h1/2* double knockout mice develop systemic developmental defects—hypogonadism, B cell lymphomas, spermatogenesis failure, and meiotic chromosome segregation defects—that are indicative of global transcriptional mis-regulation (Peters et al., 2001). Suv39H1 associates with the Rb protein to silence genes such as Cyclin E during cell cycle progression; this further confirms Suv3-9's essential role in gene regulation in the mouse (Nielsen et al., 2001).

The Suv39h homologs are essential for the establishment and maintenance of heterochromatin in organisms from *S. pombe* to human. *Drosophila* Su(var)3-9 mutations are known suppressors of position effect variegation (PEV) (Schotta et al., 2002), which results from silencing of euchromatic genes positioned near or within heterochromatin (Muller, 1930). In contrast to *Suv39h1/2* double knockout mice, *Su(var)3-9*^{null} (*Drosophila* homolog of Suv39) flies do not exhibit dramatic developmental defects (Schotta et al.,

2002). *Su(var)3-9*^{null} mutations allow functional studies of heterochromatin with minimal indirect effects from general transcriptional mis-regulation.

Heterochromatin structure involves H3K9me2, Su(var)3-9 and heterochromatin protein 1 (HP1) and is regulated by the RNAi pathway. In Chapter 2, I demonstrated that chromatin structure in heterochromatin inhibits the formation of extrachromosomal DNA, a process mediated by DNA repair mechanisms. This regulation maintains structural integrity of repeated DNAs and ribosomal DNA, thereby stabilizing nucleolus formation (Peng and Karpen, 2007). Here I present additional evidence that H3K9me contributes in additional ways to heterochromatin stability and cellular survival. *Su(var)3-9*^{null} mutant cells exhibit increased DNA damage in heterochromatin in the absence of induced damage, as well as a defective DNA repair response after radiation. *Su(var)3-9*^{null} adult animals live half the lifespan of wild type flies, likely due to accumulated DNA damage. The G2-M DNA repair and mitotic checkpoints are required to ensure the cellular and organismal viability of *Su(var)*3-9 mutants. Repeated DNAs constitute nearly half of the vertebrate genomes, similar to *Drosophila* heterochromatin. My works suggest that vertebrate genomes may protect their genomes by similar mechanisms.

Results

Su(var)3-9^{null} embryos exhibit mild developmental defects and shorter lifespan

Previous analysis showed that *Drosophila Su(var)3-9*^{null} flies are viable and fertile despite containing very low levels of H3K9me2 (Schotta et al., 2002). In contrast, mice deleted for both *Suv3-9* genes exhibit genome instability and prenatal lethality (Peters et al., 2001). These results suggest that there is greater redundancy among K9 HMTases in flies, or that mice are more sensitive to reductions in K9 methylation. To investigate the roles of the H3 K9 and RNAi pathways in cell and organismal viability and fertility, I first performed more detailed developmental analysis of *Su(var)3-9*^{null} and dcr2 mutants.

Quantitative analysis of survival at various developmental stages showed significant differences between wild type, *Su(var)3-9*^{null} and *dcr-2*$^{L811\ fsx}$ animals (Figure 3-1a). *dcr-2*$^{L811\ fsx}$ mutant parents produced only 79% fertilized eggs, compared to 93.4% for *Su(var)*3-9 mutants and 98.5% for wild type. Once fertilized, homozygous *Su(var)3-9*^{null} and *dcr-2*$^{L811\ fsx}$ mutants displayed moderate lethality (72 and 70% hatching, respectively), compared to wild type (94% hatching). Once they hatched into larvae, *Su(var)3-9*^{null} and *dcr-2*$^{L811\ fsx}$ mutants developed with timing comparable to wild type, and they eclosed into adults at similar rates.

Despite normal rates of eclosion into adults, lifespan analysis showed that *Su(var)3-9*^{null} adult flies live half as long as wild type (Figure 3-1b, $p < 0.001$). Adult *Drosophila* animals contain predominantly non-replicative cells, other than

germline and intestinal stem cells. We propose that elevated levels of DNA breaks (see below) compromise the mutant cells' viability, leading to cellular degeneration and shortened lifespan of the organism (more in discussion).

In conclusion, careful developmental analysis showed that *Su(var)3-9*^{null} eggs derived from homozygous mutant mothers display mild infertility, moderate defects in embryogenesis . Eggs laid by *dcr2* homozygous mutant mothers have high levels of infertility and moderately defective embryogenesis. For both mutants, larvae develop normally into adults, though *Su(var)3-9*^{null} adults have half the lifespan of wild type.

a

	wild type	Su(var)3-9^{null}	dcr-2$^{L811\ fsx}$
% fertilized (# fertilized / total)	99 (3/196)	93 (13/189)	79 (40/188)
% hatched (# hatched / total)	94 (482/513)	73 (475/653)	73 (228/314)
% eclosed (# eclosed / total)	96 (210/220)	95 (198/209)	96 (189/198)

b

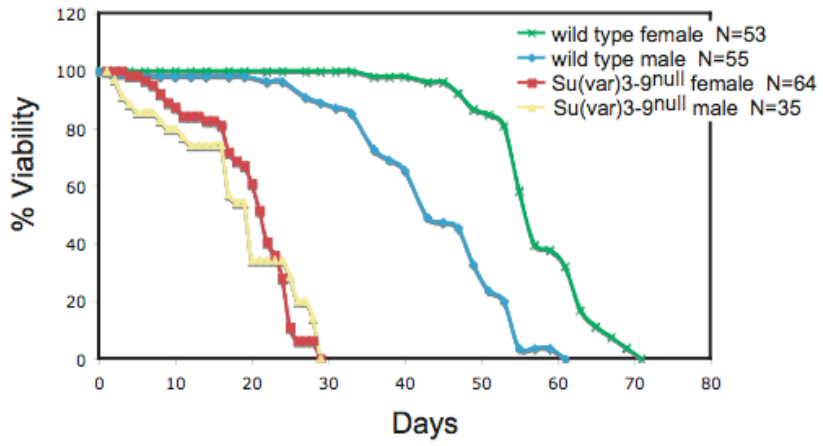

Figure 3-1 Survival analysis of wild type, *Su(var)3-9*^{null} animals and *dcr-2*$^{L811\ fsx}$ animals.

a) Analysis of developmental stages of wild type, *Su(var)3-9*^{null} and

dcr-2$^{L811\ fsx}$ animals. The three genotypes laid comparable numbers of eggs. In all three assays, the p values comparing *Su(var)3-9*^{null} to wild type are <0.001, and the p values comparing *dcr-2*$^{L811\ fsx}$ to wild type are <0.01 by Student's t test. All sample sizes are > 150.

b) The graph shows lifespan analysis of wild type and *Su(var)3-9*^{null} adult flies. The *Su(var)3-9*^{null} flies live half the lifespan of wild type flies (p value is <0.001 by Student's t test).

***Su(var)3-9*^{null} mutants display increased sensitivity to irradiation**

The observation that *Su(var)*3-9 and *dcr2* animals contain elevated levels of extrachromosomal circular repeated DNAs (Chapter 2) raised the possibility that loss of the H3K9 methylation or RNAi pathways results in increases in DNA damage and resultant recombination. To investigate whether the *Su(var)3-9*^{null} cells can repair exogenous DNA damage as efficiently as wild type cells, diploid tissues were treated with 5 Gy of x-ray irradiation, allowed to recover for variable time periods, and mitotic indices were measured as a readout for recovery from DNA damage (Materials and Methods). Wild type cells subjected to 5 Gy of X-ray irradiation displayed similar mitotic indices up to 160 minutess post treatment, and a slight increase in mitotic index after 4 hours (Figure 3-2a), relative to unirradiated cells. Control, non-irradiated *Su(var)3-9*^{null} cells exhibited a 3-fold increase in mitotic index at 160 minutes (Figure 3-2a) relative to wild-type and also showed a further 2-fold increase in the mitotic index after 5 Gy of irradiation and 4 hours of recovery time ($p < 0.001$; Figure 3-2a). This suggests that *Su(var)3-9*^{null} mutant cells are more sensitive to radiation; mutant cells either

contain more damage after irradiation, or they cannot repair exogenous DSBs as efficiently as the wild type.

The impact of the increased radiation sensitivity on organismal health was evaluated by monitoring survival to adulthood after one X-ray irradiation treatment at doses of 0, 3, 6, and 12 Gy (Materials and Methods). *Su(var)3-9*^{null} survival was significantly lower than wild type ($p < 0.001$, Figure 3-2b) at all doses tested. The X-ray dose corresponding to 50 % survival (LD_{50}) is 3.75 Gy for wild type and 2.75 Gy for *Su(var)3-9*^{null} mutants. These data show that the increased sensitivity to radiation displayed by *Su(var)3-9*^{null} mutant cells lead to lower survival in response to exogenous DNA damage.

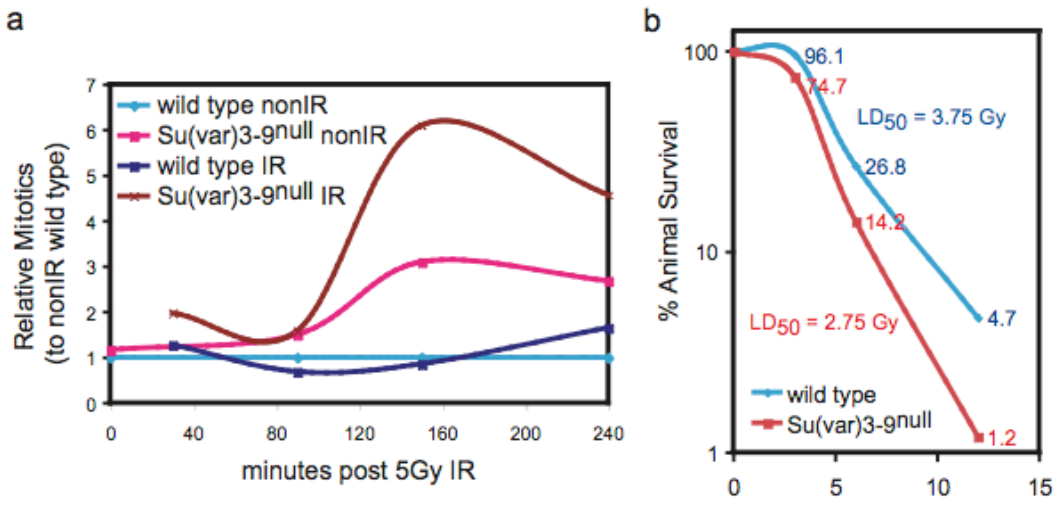

Figure 3-2 Analysis of DSB repair response in wild type and *Su(var)3-9*^{null} cells. a) The graph shows the mitotic indices of wild type and *Su(var)3-9*^{null} cells in response to irradiation. All mitotic indices were normalized relative to non-irradiated wild-type cells at each time point. After 5 Gy of X-ray treatment, the mitotic index of irradiated *Su(var)3-9*^{null} cells was 2-fold higher than in non-irradiated *Su(var)3-9*^{null} cells (p value is <0.001 by Student's t test). The mitotic

index of irradiated wild-type cells does not significantly differ from that of non-irradiated wild-type cells.

b) The semi-logarithmic graph shows the survival to adulthood of wild type and the *Su(var)3-9*^{null} animals after embryos were treated with variable doses of IR. Survival of *Su(var)3-9*^{null} animals was significantly less than for wild type (p value is <0.001 by chi-square test). The survival rates (# adult / # eggs laid) were normalized to the survival rates in the absence of irradiation.

Uninduced DNA breaks are more prevalent in *Su(var)3-9*^{null} mutants

Phosphorylation of the histone variant H2Av (γH2Av) is often used as a reporter for DNA damage in fixed samples. Indirect immunofluorescence (IF) with antibodies that specifically recognize this histone modification was used to evaluate DNA damage levels in whole-mount (three dimensional) brain and imaginal disc tissues from wild type, *Su(var)3-9*^{null} , and *dcr-2*$^{L811\ fsx}$ mutant larvae (Materials and Methods). An average of 0.43 ± 0.48 % of wild type cells contained γH2Av signals. In contrast, 8.9 ± 2.9 % of the *Su(var)3-9*^{null} mutant cells contained γH2Av signals, a 21-fold increase compared to wild type (Figure 3-3a).

Mutations in components of the RNA interference (RNAi) pathway caused loss of H3K9me2 mislocalization from repeated DNA and heterochromatin, correlating with eccDNA formation from ribosomal DNA but not other repeated DNAs (Chapter 2). We wanted to know whether RNAi mutants also contain elevated frequencies of DNA damage. Quantiative analysis of whole-mount diploid tissues showed a 4.7-fold increase in γH2Av-positive *dcr-2*$^{L811\ fsx}$ cells

compared to wild type ($p < 0.05$ by Student's t test, Figure 3-3a). This demonstrated that loss of the H3K9 methylation and RNAi pathways results in increased levels of DNA damage in the absence of irradiation; however frequencies are higher in *Su(var)3-9*^{null} mutant compared to the hypomorphic *dcr-2* mutants.

The Rad51 protein facilitates DNA repair of DSBs via homologous recombination. Analysis of Rad51 foci by IF showed an 11-fold increase in Rad51-positive *Su(var)3-9*^{null} cells and a 3.5-fold increase in Rad51-positive *dcr-2*$^{L811\ fsx}$ cells compared to the wild type (Figure 3-3b). IF using anti-γH2Av and anti-Rad51 antibody showed that nearly 76% of cells with γH2Av signals displayed colocalization of γH2Av and Rad51 (Figure 3-3c). This suggests that most of the increased DNA damage in mutants is due to double-stranded DNA breaks. The 24% of cells with only γH2Av signals may indicate the presence of other kinds of damage, which would not recruit Rad51, DSBS being repaired by NHEJ, or DSBs that have already been repaired.

Given my previous demonstration that loss of the H3K9 methylation or RNAi pathways resulted in ecc repeated DNAs, I was interested to learn whether most of the DNA damage in the *Su(var)3-9*^{null} cells occurs in heterochromatin. Assessment of damage frequencies in heterochromatin versus euchromatin is challenging, particularly in these mutants due to the reduction or mislocalization of the standard heterochromatin markers H3K9me2 and HP1. However, the AT-rich components of heterochromatin in *Drosophila* interphase cells coalesce into regions characterized by intense DAPI staining. Analysis via this criterion

underestimates the actual % of DNA breaks occurring in heterochromatin, which is also present in the DAPI-weak region. Nevertheless, in the absence of HP1 or H3K9me2 staining, this criterion is the simplest and the broadest cytological visualization of heterochromatin.

Quantitation of DSBs by immunofluorescence can be challenging due to both the sensitivity and specificity of the signals. To minimize these problems, I performed double labeling with antibodies to γH2Av and Rad51, and counted only foci staining with both antibodies as *bona fide* DSBs. Analysis showed 70 ± 7.9 % of foci containing both γH2Av and Rad51 colocalized with DAPI-bright regions (Figure 3-3c) (Materials and Methods).

I also used the TUNEL (TUNEL-mediated dUTP nick end labeling) assay to visualize and quantify the locations of damage in *Su(var)3-9*^{null} diploid tissues. This assay uses TUNEL (terminal deoxynucleotidyl transferase), an enzyme that processively adds dNTPs to unprotected DNA ends, to mark sites of DNA damage. TUNEL-positive cells, 12.8% (S.D. 2%) of *Su(var)3-9*^{null} cells (no signals were observed in wild-type cells), were divided into 3 categories (Figure 3-3d): 57 ± 15 % contained signals located in DAPI-bright/heterochromatin, 25 ± 14 % contained signals in the DAPI-weak regions, and 18 ± 18% contained signals in both DAPI- bright and weak regions (p value comparing DAPI-bright vs. DAPI-weak is <0.008 by Student's t test). Thus, at least 75% of TUNEL positive cells contain breaks in the heterochromatin (Figure 3-3e), comparable to frequencies observed with γH2Av-Rad51 staining.

Reduced H3K9me due to *Su(var)3-9*^{null} mutations led to ribosomal DNA (rDNA) instability, resulting in extrachromosomal rDNA that can seed ectopic nucleolus formation (Chapter 2). We hypothesized that the increased DNA breaks may preferentially occur in rDNA. To test this, I performed combined rDNA FISH and γH2Av IF on whole-mount diploid tissues from wild type and *Su(var)3-9*^{null} mutants. Surprisingly, there was no significant colocalization between the rDNA and γH2Av signals in the *Su(var)3-9*^{null} diploid cells (data not shown), indicating that the increased DNA breaks do not occur in rDNA, or that DNA breaks within rDNA do not recruit γH2Av. An alternative explanation is that DNA repair occurs very efficiently in rDNA, in contrast to those in the flanking heterochromatin.

In conclusion, these data show that at least 70% of the elevated frequencies of endogenous DNA breaks in *Su(var)3-9*^{null} mutant cells are in the heterochromatin. More direct molecular assessment, such as ChIP-array analysis, is required to determine whether all breaks occur in heterochromatin in *Su(var)*3-9 mutants, and to assess the frequencies of damage in different classes of repeated sequences.

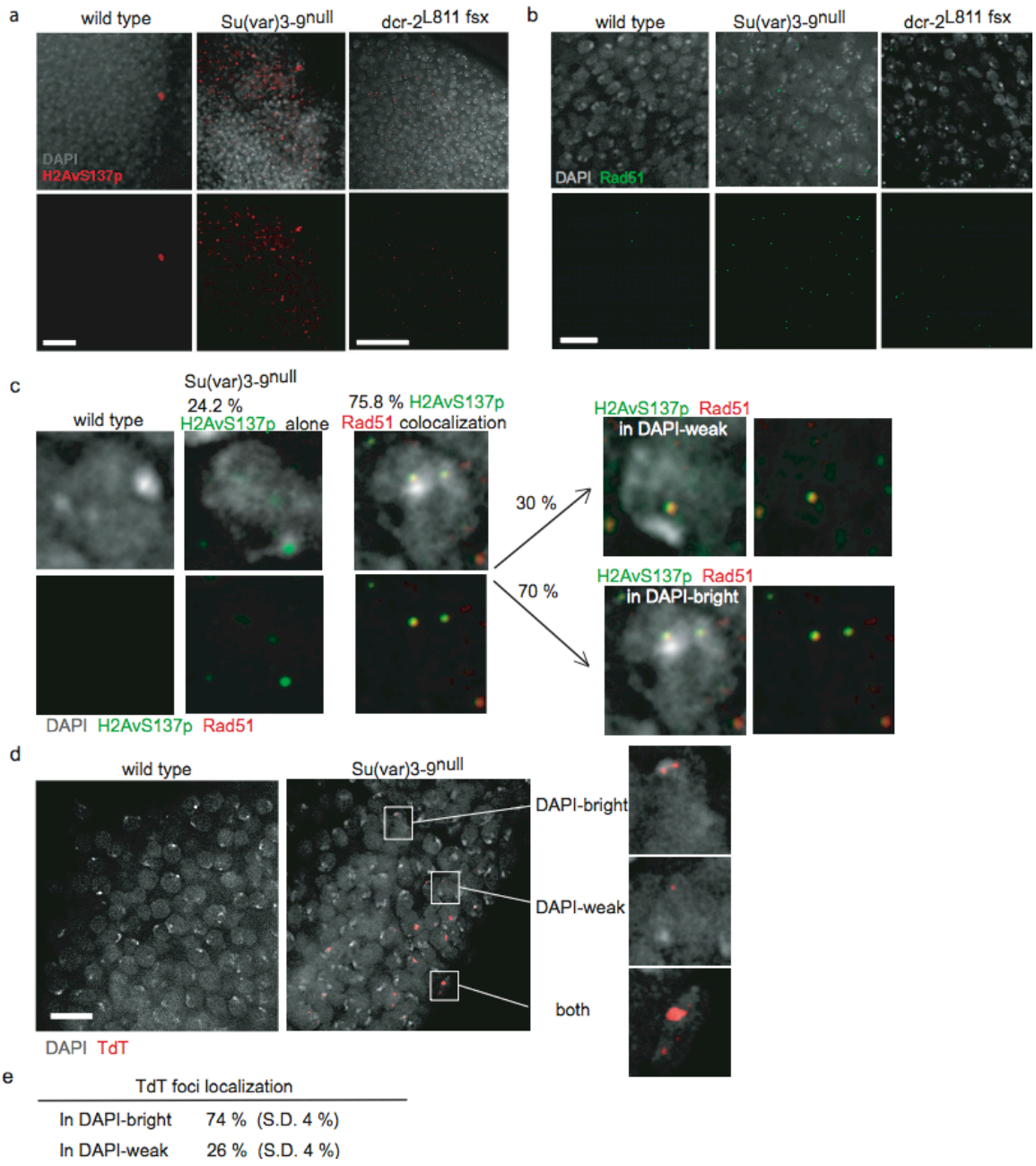

Figure 3-3 DNA damage in heterochromatin increases in *Su(var)3-9*^{null} diploid tissues in the absence of radiation.

a) γH2Av (red) IF in whole-mount brain tissues from wild type, *Su(var)3-9*^{null}, and *dcr-2*$^{L811\ fsx}$ mutants are shown. The number of cells containing γH2Av is 21-fold ($p < 0.01$ by Student's t test) higher in *Su(var)3-9*^{null} nuclei and 4.7-fold higher in

dcr-2$^{L811\ fsx}$ nuclei ($p < 0.05$ by Student's t test) compared to wild type. Each image is an optical section. The scale bar is 15 um.

b) Rad51 (green) IF in whole-mount diploid tissues from wild type and *Su(var)3-9*^{null} mutants are shown. The number of cells containing Rad51 is 11-fold higher in *Su(var)3-9*^{null} nuclei ($p < 0.01$ by Student's t test) and 3.5-fold higher in *dcr-2*$^{L811\ fsx}$ nuclei ($p<0.01$ by Student's t test) compared to wild type. Each image is an optical section. The scale bar is 8 um.

c) γH2Av (green) and Rad51 (red) IF in wild-type and *Su(var)3-9*^{null} diploid nuclei are shown. An average of 76 % (S.D. 3.1 %) of the γH2Av foci inside *Su(var)3-9*^{null} nuclei colocalize with Rad51 foci. Within this group, an average of 70 % (S.D. 7.9 %) of the γH2Av /Rad51-positive *Su(var)3-9*^{null} cells contain foci in DAPI-bright regions, while 30% (S.D. 7.9 %) of foci locate within DAPI-weak regions (N=167; p value comparing DAPI-bright vs. DAPI-weak is <0.001 by Student's t test). Each image is an optical section. Cells are 3um wide.

d) TUNEL signals (red) in diploid tissues from wild type and *Su(var)3-9*^{null} mutants are shown. The TUNEL signals were detected in 12.8% (S.D. 2%) of *Su(var)3-9*^{null} cells but not detected in wild type cells. TUNEL signals in *Su(var)3-9*^{null} cells were assessed for colocalization with the DAPI-bright or DAPI-weak regions Each image is an optical section. The scale bar is 8 um.

e) Analysis showed that 75 % of TUNEL foci colocalize with the DAPI-bright regions.

γH2Av signals, signifying DNA breaks, increase in *Su(var)3-9*^{null} oocytes and nurse cells, especially in heterochromatin

Classical genetic studies have shown that reciprocal meiotic recombination (crossing-over) occurs an average of once per euchromatic arm per nucleus, and does not occur in heterochromatin (Mehrotra and McKim, 2006; Stern, 1936). The significant increase in DNA damage and DSBs in the heterochromatin in *Su(var)*3-9 mutant somatic cells suggests that similar changes may occur in mutant meiotic cells. The germarium is the part of the *Drosophila* ovary that contains developing oocytes and nurse cells, which share the same cytoplasm and expression of Spo11 (the *Drosophila* homolog is mei-W68 (McKim and Hayashi-Hagihara, 1998)), which actively produce DSBs. Some DSBs in the oocytes will undergo meiotic recombination during prophase I.

IF analysis showed a dramatic increase in γH2Av signals in *Su(var)3-9*^{null} mutant germaria compared to wild type (Figure 3-4a). Compared to wild-type nurse cells, wild-type oocytes have 2-fold increase in γH2Av signal volumes (p value < 0.05 by Student's t test). *Su(var)3-9*^{null} nurse cells display a 3-fold increase in the volume of γH2Av signals compared to wild type nurse cells (p value < 0.001 by Student's t test), and *Su(var)3-9*^{null} oocytes exhibit a 4-fold increase compared to wild-type oocytes (p value <0.001 by Student's t test) and a 6-fold increase compared to *Su(var)3-9*^{null} nurse cells (p value < 0.001 by Student's t test).

Does the increased DNA damage in *Su(var)3-9*^{null} mutant oocytes and nurse cells occur in heterochromatin, as observed for diploid cells? The heterochromatic regions in oocytes and nurse cells do not coalesce into clearly-definable regions, and HP1 is mislocalized in *Su(var)3-9*^{null} cells due to severely reduced H3K9me. Therefore, to test this hypothesis, I performed combined γH2Av IF and FISH with satellite DNA probes in whole-mount wild type and *Su(var)3-9*^{null} mutant germaria. The probes included the 1.688, AACAC, AATAT, dodeca, AATAG, 1.686, and AAGAG satellites, which correspond to approximately 34 megabases of the heterochromatin (Materials and Methods), less than half of the total amount of heterochromatic DNA. γH2Av IF and satellite FISH signals overlapped in 21 % (S.D. 9.6 %, n=151) of *Su(var)3-9*^{null} oocytes and nurse cells, and was never observed in wild type cells (Figure 3-4c; p value <0.001 by Student's t test). These data show that a significant proportion of the elevated levels of DNA breaks in *Su(var)3-9*^{null} mutant oocytes and nurse cells occur in heterochromatin. We conclude that H3K9 methylation by Su(var)3-9 is important for maintaining the structural integrity of heterochromatin in mitotic and meiotic cells.

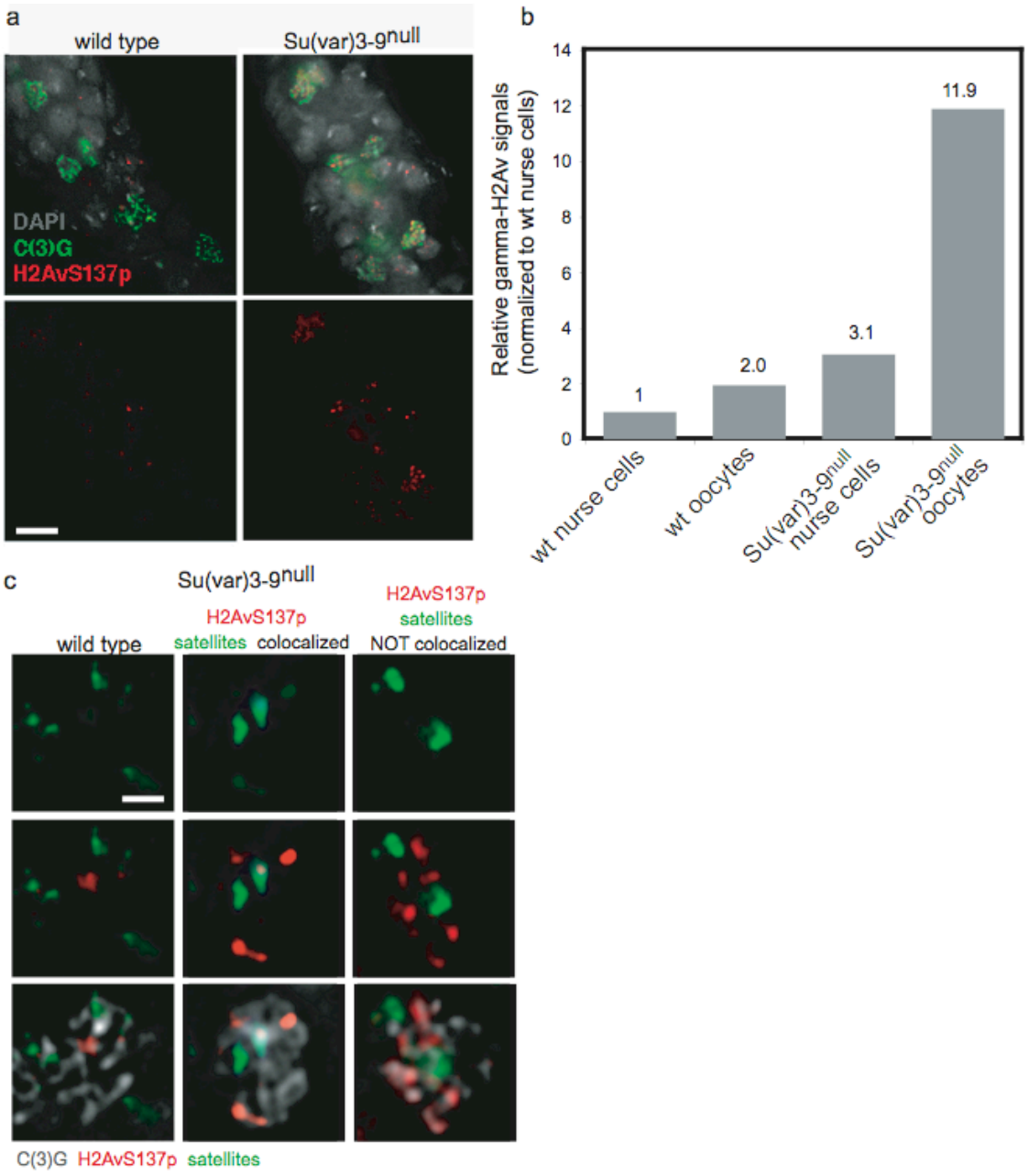

Figure 3-4 Heterochromatic DNA damage increases in *Su(var)3-9*^{null} mutant oocytes and nurse cells.

a) γH2Av (red) and C(3)G (green) IF in whole-mount germaria from wild type and *Su(var)3-9*^{null} mutants. C(3)G is part of the synaptonemal complex and is used to

distinguish oocytes from nurse cells, both of which contain DSBs. Each image is an optical section. The scale bar is 7 um.

b) The graph shows the relative γH2Av signals/nuclear volume in nurse cells and oocytes from wild type and *Su(var)3-9*^{null} mutants. Compared to wild-type nurse cells, wild-type oocytes have 2-fold increase in γH2Av signal volumes (p value < 0.05 by Student's t test). *Su(var)3-9*^{null} nurse cells display a 3-fold increase in the volume of γH2Av signals compared to wild type nurse cells (p value < 0.001 by Student's t test), and *Su(var)3-9*^{null} oocytes exhibit a 4-fold increase compared to wild-type oocytes (p value <0.001 by Student's t test) and a 6-fold increase compared to *Su(var)3-9*^{null} nurse cells (p value < 0.001 by Student's t test).

c) Combined γH2Av IF (red) and satellite FISH(green) in wild-type and *Su(var)3-9*^{null} oocytes are shown. C(3)G (grey) IF is used to mark oocytes. An average 21.3 % (S.D. 9.6 %, n=151) of *Su(var)3-9*^{null} oocytes and nurse cells contain overlap between γH2Av and satellite signals (p value <0.001 by Student's t test). Each image is an optical section. Cells are 5um wide.

Su(var)3-9^{null} cells contain elevated frequencies of aberrant mitotic chromosome morphologies and chromosome rearrangements

Persistent DNA damage could lead to structural defects such as chromosomal rearrangements and aneuploidy. To test this hypothesis, I visualized wild type and *Su(var)3-9*^{null} mitotic chromosomes by DAPI-staining. All wild-type mitotic chromosomes exhibited banding patterns characteristic of heterochromatin. In contrast, a subset of the *Su(var)3-9*^{null} mitotic chromosomes

exhibit defects such as hypo-condensation (Figure 3-5a, 2nd panel) and extra DAPI-bright bands (Figure 3-5a, 3rd panel).

I used FISH paints that hybridize to the euchromatic regions of three *Drosophila* chromosomes (X, 2 and 3) to determine if *Su(var)3-9*^{null} cells contain increased frequencies of rearranged chromosomes compared to wild type cells (Materials and Methods). The first panel of Figure 3-5b shows an example of the chromosome paints on wild-type mitotic chromosomes. The third chromosomes are pseudocolored in red, the 2nd chromosomes in green, and the X chromosomes in blue. I could not make paints specific for the Y and fourth chromosomes due to their high repeat content.

Quantitative analysis of the painted chromosomes showed that 1.1% of *Su(var)3-9*^{null} mitotic chromosomes exhibit structural defects such as deletions, duplications, and translocations (Figure 3-5c). The 2nd panel in Figure 5B shows a deletion of one third chromosome arm, and the 3rd panel shows a translocation between the X and third chromosomes.

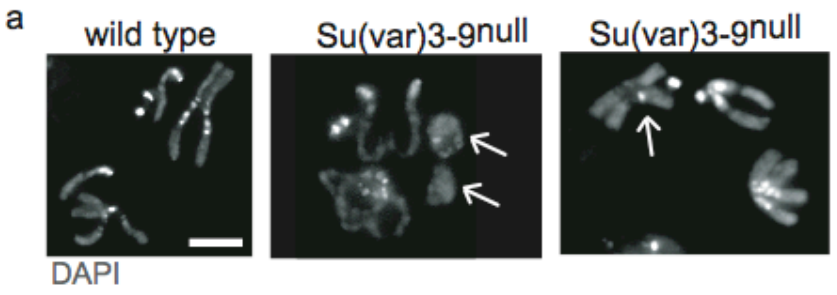

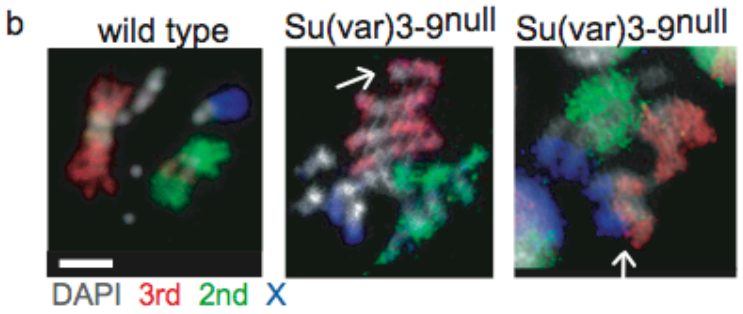

c

Genotypes	Wild type	Su(var)3-9null
# mitotics scored	239	524
# (%) defects	0 / 0 %	6 / 1.1 %

Figure 3-5 *Su(var)3-9*^{null} chromosomes exhibit morphology defects and rearrangements.

a) DAPI staining of mitotic chromosomes from wild type and the *Su(var)3-9*^{null} mutant are shown. Structural defects in *Su(var)3-9*^{null} mitotic chromosomes are indicated by white arrows. Each image is an optical section. The scale bar is 2um.

b) Chromosome painting of mitotic chromosomes from wild type and *Su(var)3-9*^{null} mutants. The third chromosomes are in red, the second chromosomes are green, and the X chromosomes are blue. The fourth chromosomes and the Y chromosome are only stained by DAPI. Structural defects in *Su(var)3-9*^{null} mitotic chromosomes, such as deletions and translocations, are indicated by white arrows. Each image is an optical section. The scale bar is 2um.

c) Quantitation showed that 1.1 % of the *Su(var)3-9*^{null} mitotic chromosomes exhibited structural defects, compared to 0% for wild type. The p value is 0.025 by chi square test.

G2 and mitotic checkpoints are activated in *Su(var)3-9*^{null} cells

*Su(var)*3-9 mutants are mostly viable and fertile (Figure 3-1) despite significantly elevated levels of DNA breaks (Figure 3-3), . I hypothesized that repair checkpoints are activated in mutant cells that delay cell cycle progression until the damage is repaired. To test this hypothesis, I compared the distributions of cell cycle stages in wild type and *Su(var)3-9*^{null} cells. Diploid tissues were squashed into single-cell layers on slides, and IF was performed with antibodies to the cell cycle markers PCNA (S phase), Cyclin A (Cyc A, S phase, G2 and mitosis), and PH3 (H3 phosphorylated at serine 10, mitosis), and TUNEL staining was used to identify apoptotic cells (Materials and Methods). The percent of PCNA-positive cells were the same in wild type and mutant animals, indicating that there was no delay or arrest in S phase (Figure 3-6a). Therefore, although CycA expression begins in S phase and ends in mitosis, G2 cells could be identified as Cyc A-positive but PH3-negative,

The cell cycle analysis showed that a larger proportion of *Su(var)3-9*^{null} mutant cells are in G2 and mitosis, and undergo apoptosis, in comparison to wild type cells (Figure 3-6a). Compared to the 7.2 % of wild-type cells that are in G2, 47.3 % of the *Su(var)3-9*^{null} cells are in G2, representing a 6.6-fold increase. 1.2% of the *Su(var)3-9*^{null} cells are in mitosis, a 4-fold increase compared to wild type (0.3%). The apoptotic cells increase from 0.09 % in wild type to 0.96 % in

the *Su(var)3-9*^{null} cells, a 10.7-fold increase. I conclude that loss of *Su(var)*3-9 results in significant increases in G2 and mitotic arrest or delay, as well as elevated apoptosis. It is important to note that although the fold increases for mitotic and apoptotic cells are large, the actual % of cells is low (~1% each). Nearly half the mutant cells are in G2, suggesting that the major response is activation of the G2 DNA repair checkpoint.

PCNA staining identifies cells in S phase, G2 cells are Cyc A-positive but PH3-negative, and mitotic cells are PH3-positive but CycA negative. Apoptotic cells were identified by TUNEL staining (Materials and Methods). CycA expression begins in S phase and ends in mitosis, so it is not exclusive to G2. However, since cells in S phase are proportionally the same in wild type and the *Su(var)3-9*^{null} mutant (Figure 3-6a), we can effectively compare the relative amount of CycA-positive but PH3-negative cells between wild type and mutant.

To investigate whether activation of cell cycle checkpoints and apoptosis are required for the viability of *Su(var)3-9*^{null} mutants, I analyzed double mutant combinations between *Su(var)3-9*^{null} and mutations that compromise DNA damage checkpoint activation. *Drosophila* homologs of ATR, checkpoint kinase 1 (chk1), and checkpoint kinase 2 (chk2) are *mei-41*, *grp*, and *lok*. They activate G1-S and G2-M arrest in response to DNA damage. Double mutants of *Su(var)3-9*^{null} with cell cycle checkpoint mutations showed sub-viability (synthetic lethality) ranging from 50% to 64.6% (Figure 3-6b). Overall, mutations in *mei-41, grp,* or *lok* cause ~50% lethality of *Su(var)3-9*^{null} double mutants.

The *p53*$^{11\text{-}1B\text{-}1}$, *Su(var)3-9*^{null} double mutant exhibited 100 % viability (Figure 3-6b and c), suggesting that the apoptosis pathway, governed by p53, does not impact the viability of *Su(var)3-9*^{null} animals. Even though apoptotic cells increase by 10-fold in the *Su(var)3-9*^{null} mutant, their actual number amounts to 0.86 % (S.D. 0.29 %), suggesting that the G2 and mitotic checkpoints enable repair of the majority of DNA breaks. The apoptotic pathway is only activated upon persistent damage, which likely results in the observed mitotic chromosomal defects (Figure 4).

The relative amount of CycA-positive and PH3-negative cells in the *grp*^{06034}*; Su(var)3-9*^{null} and the *lok*^{p6}*; Su(var)3-9*^{null} mutants showed that their G2 contents are comparable to the wild type ($p < 0.05$ by students' t test). These data showed that the DNA damage checkpoint is responsible for the G2 delay or arrest observed in the *Su(var)3-9*^{null} mutant, and that the checkpoint is important for the mutant's viability.

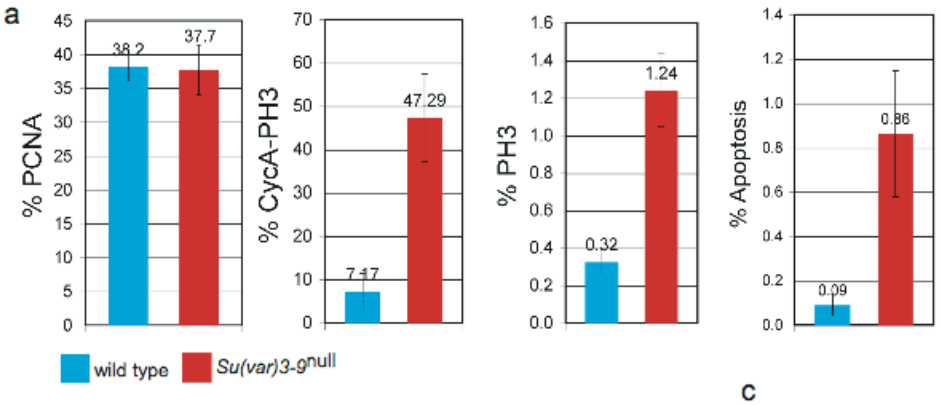

b

homologs tested	double mutant genotypes	% viability compared to controls	p values
ATR	*mei41*^{29D} ; *Su(var)3-9*^{null}	64.6	0.025
chk2	*lok*^{P6} ; *Su(var)3-9*^{null}	50.6	<0.001
chk1	*grp*^{06034}; *Su(var)3-9*^{null}	45.4	<0.001
p53	*p53*$^{11-1B-1}$, *Su(var)3-9*^{null}	100	N.A.

c

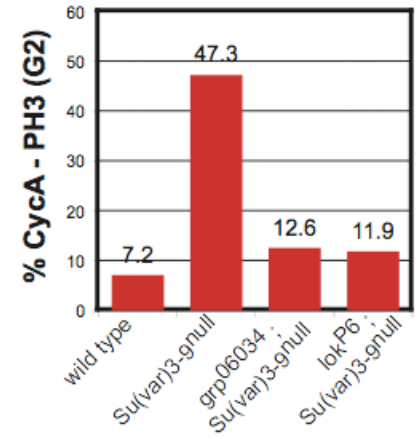

d

Genotypes	G2 (%)	S.D.	p values compared to wild type	p values compared to Su(var)3-9^{null}
wild type	7.2	4.2	N.A.	0.011
Su(var)3-9^{null}	47.3	10.2	0.009	N.A.
grp^{06034}; Su(var)3-9^{null}	12.6	4.0	0.146	0.020
lok^{P6}; Su(var)3-9^{null}	11.9	1.9	0.184	0.025

Figure 3-6 The G2, mitotic, and apoptotic checkpoints are activated in the *Su(var)3-9*^{null} cells. Mutations in the DNA damage checkpoint genetically interact with the *Su(var)3-9*^{null} mutations.

a) The histograms show cell cycle stage analysis of wild type and *Su(var)3-9*^{null} cells; the number above each bar is the actual % of cells. Compared to wild type, the increase in G2 (CycA-PH3), mitotic (PH3), and apoptotic %'s in the *Su(var)3-9*^{null} cells is 6.6-fold (47.3%/7.2% = 6.6), 4-fold (1.2%/0.3% = 4), and 10.7-fold (0.96%/0.09% = 10.7) (p values are <0.001 by Student's t test).

b) The chart lists the viability of the double mutants of the *Su(var)3-9*^{null} mutation with mutations in the DNA damage checkpoint pathways. Compared to control

crosses, all double mutants are sub-viable, except *p53*; *Su(var)3-9* double null mutant. The p values are calculated by the chi-square test.

c) and d) are the graph and chart showing the %'s of G2 cells in wild type, *Su(var)3-9*^{null} mutants, the *grp*^{06034}*; Su(var)3-9*^{null} double mutants, and the *lok*^{p6}*; Su(var)3-9*^{null} double mutants. The percentage of cells in G2 in the *grp*^{06034}*; Su(var)3-9*^{null} and *lok*^{p6}*; Su(var)3-9*^{null} mutants are comparable to wild type ($p < 0.05$ by students' t test).

Both the DNA damage pathway and cohesin defects in the *Su(var)3-9*^{null} mutant cells activate the mitotic checkpoint, which is critical for the mutant animal's viability

To investigate whether the mitotic checkpoint and apoptosis activation impact organismal survival of the *Su(var)3-9*^{null} mutant, I analyzed the viability of the *Su(var)3-9*^{null} animals containing mutations in *rod, ZW10* (*Drosophila* homolog is *mit(1)15*), and *p53*. As part of the outer kinetochore, the rod-ZW10 complex activates the mitotic checkpoint, which monitors kinetochore to microtubule attachment and regulates the metaphase to anaphase transition. *grp* and *lok* have also been shown to regulate the metaphase-anaphase transition during mitosis (Royou et al., 2005; Xu and Du, 2003).

Difference in the viability of *rod*^{EY04576}; *Su(var)3-9*^{null} and *mit(1)15*^{5}; *Su(var)3-9*^{null} mutants (51.7 % vs 0 %, Figure 3-7a) is most likely caused by the nature of these mitotic checkpoint mutations. The available *rod*^{EY04576} mutation is hypomorphic, and the *mit(1)15*^{5} mutation is amorphic. Regardless, 0% viability of the *mit(1)15*^{5}; *Su(var)3-9*^{null} mutant reflects the essential function of the mitotic

checkpoint for *Su(var)3-9*^{null} survival. Previously demonstrated cohesin reduction from heterochromatin of the *Su(var)3-9*^{null} mutant cells (Peng and Karpen, 2007) and the sub-viability (76.4 %) of the *smc1*$^{exc46/+}$; *Su(var)3-9*^{null} animals (Figure 3-7a, $p<0.0013$) further confirms that cohesin defects do occur in the *Su(var)3-9*^{null} organism. Therefore, the mitotic checkpoint is activated in the *Su(var)3-9*^{null} cells by sister chromatid cohesion defects and the DNA damage checkpoint to inactivation of the repair checkpoint that feeds into the mitotic checkpoint (via chk1 and chk2, Figure 3-7b and c).

The *grp* and the *lok* mutations almost entirely suppress the mitotic index increase in *Su(var)3-9*^{null} mutants (Figure 3-7b and c), confirming that chk1 and chk2 regulate the mitotic checkpoint (Royou et al., 2005; Xu and Du, 2003). This result also suggests that increased DNA breaks in addition to sister cohesin defects in the *Su(var)3-9*^{null} cells activate mitotic arrests via chk1 and chk2, which are epistatic to rod-ZW10. In all, the G2 and mitotic checkpoints are essential for the viability of the *Su(var)3-9*^{null} mutant animals.

a

homologs tested	double mutant genotypes	% viability compared to controls	p value
rod	*rod*^{EY04576}, *Su(var)3-9*^{null}	51.7	<0.001
ZW10	*y, mit*^{1}, *15*^{5}*/Y ; Su(var)3-9*^{null}	0	<0.001
SMC1	*smc1*^{exc46}, *3-9*^{17} */ 3-9*^{6}	76.4	<0.01

c

Genotypes	mitotic index (%)	S.D.	p values compared to wild type	p values compared to Su(var)3-9^{null}
wild type	0.3	0.1	N.A.	0.009
Su(var)3-9^{null}	1.2	0.2	0.009	N.A.
grp^{06034}; Su(var)3-9^{null}	0.5	0.4	0.264	0.010
lok^{P6}; Su(var)3-9^{null}	0.6	0.3	0.065	0.012

b

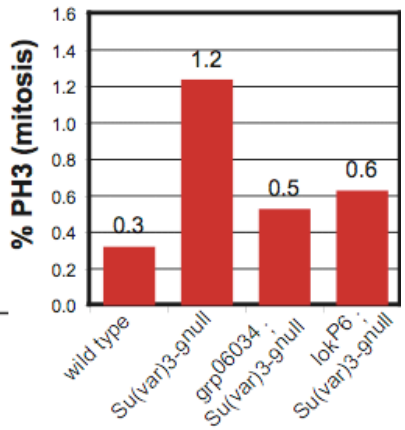

Figure 3-7 Mutations in the mitotic checkpoint genetically interact with *Su(var)3-9*^{null} mutations, while p53^{null} mutation does not.

a) The chart lists the viability of the double mutants of *Su(var)3-9*^{null} mutation with mutations in the mitotic checkpoint. Compared to control crosses, all double mutants are sub-viable. The p values are calculated by the chi-square test.

b) and c) are the graph and chart showing the mitotic indices in wild type, *Su(var)3-9*^{null} mutants, *grp*^{06034}*; Su(var)3-9*^{null} mutants, and *lok*^{p6}*; Su(var)3-9*^{null} mutant. Mitotic indices in *grp*^{06034}*; lok*^{p6}*; Su(var)3-9*^{null} and *Su(var)3-9*^{null} double mutants are comparable to wild type ($p < 0.05$ by students' t test).

Discussion

The H3K9 methylation and RNAi pathways stabilize heterochromatin

Here I have demonstrated that *Su(var)*3-9 mutants are more sensitive to exogenous DNA damage induced by radiation, in terms of both elevated levels of mitotic arrest and organismal viability (Figure 3-2). This observation suggests that the H3K9 methylation pathway serves to 'protect' heterochromatin from exogenous damage, either by reducing the frequencies of induced breaks, or by facilitating DNA repair. However, even in the absence of radiation, the frequency of DNA damage increases ~ 20-fold, with majority of the DNA breaks in heterochromatin, in somatic cells from *Su(var)3-9*^{null} and *dcr-2*$^{L811\ fsx}$ mutants (Figure 3-3). In addition, *Su(var)*3-9 mutants display elevated γH2Av signals, indicative of DNA breaks, in oocytes and nurse cells (Figure 3-4), demonstrating a role for the Su(var)3-9 and RNAi pathway in meiosis and the germ line. These observations suggest that the H3K9 methylation and RNAi pathways are required for other aspects of DNA repair in heterochromatin, in addition to protection from exogenous damage.

Two non-mutually exclusive scenarios may contribute to the observed phenotypes in this chapter. Specifically, altered heterochromatin structure, due to *Su(var)3-9*^{null} or RNAi mutations, could lead to increased endogenous DNA breaks or a defective DNA damage response. The main causes of DSBs and other types of DNA damage are environmental stresses and defective DNA replication, which can lead to stalled and/or collapsed replication forks. The latter is more likely to contribute to the increased 'endogenous' DNA damage

frequency in *Su(var)3-9*^{null} mutant cells. This leads to the question how altered heterochromatin structure would impact replication to cause DSBs. Heterochromatin replication occurs in late S phase, and SuUR (suppressor of underreplication) is the only factor identified to directly regulate late replication timing of heterochromatin (Belyaeva et al., 1998). The *SuUR* and *orc2* (origin recognition complex 2, which also interacts with HP1) mutants have been shown to function as *Su(var)*'s (Belyaeva et al., 1998; Pak et al., 1997), suggesting that replication components and heterochromatin replication timing are involved in heterochromatin establishment and maintenance (Wallace and Orr-Weaver, 2005). This conclusion leads me to propose that H3K9me2 reduction in heterochromatin likely causes mis-coordination of replisomes and/or replication origin firing in heterochromatin, leading to timing deregulation, collapsed replication forks, and DSB formation.

An alternative explanation is that H3K9 methylation by Su(var)3-9 is required for DNA damage recognition and/or repair in heterochromatin . In this model, reduced H3K9 methylation in heterochromatin causes inefficient damage recognition and impairs subsequent DNA repair processes, resulting in the retention of damage. Chromatin conformational changes play a central role in damage recognition, repair machinery recruitment and retention, and cell cycle checkpoint responses (Karagiannis and El-Osta, 2006; Keogh et al., 2006; van Attikum and Gasser, 2005). For example, chromatin surrounding individual DSBs expands immediately after DNA breaks; this process is independent of H2AX and ATM and occurs in both euchromatin and heterochromatin. These data and

others suggest a rapid energy-dependent chromatin decondensation, an event that allows subsequent access of repair machineries to DSB sites for efficient repair (Kruhlak et al., 2006). It is possible that chromatin structural changes in response to DNA damage in heterochromatin require H3K9me.

H3K9me may also function in the DNA damage response in heterochromatin via recruitment of cohesins. Our previous study demonstrated that reduced H3K9me decreases the levels of cohesins in heterochromatin (Peng and Karpen, 2007). Cohesins are essential for both HR and NHEJ repair processes, thus reduced cohesins in heterochromatin may contribute to an ineffective DNA damage response.

These proposed functions for H3K9me in DNA repair differ from other histone modifications, which mainly help the loading and activation of DNA repair factors and cell cycle checkpoint regulators. γH2Ax has been shown to help recruit and retain DNA repair factors, cohesins and chromatin remodeling complexes at DSBs (Karagiannis and El-Osta, 2006; van Attikum and Gasser, 2005). Other histone modifications implicated in assisting cell cycle regulators and DNA repair factors loading are phosphorylation, acetylation, and methylation of histone H4 residues, H3K79 methylation, H2BK123 ubiquitination, and H2AS129 phosphorylation (Karagiannis and El-Osta, 2006).

H3K9 methylation does not appear to be directly involved in repair factor loading and cell cycle regulator activation. Cytological assays using TUNEL and γH2Av / Rad51 IF yielded similar quantitative results (Figure 3-3), demonstrating efficient γH2Av foci formation and recruitment of repair machineries in *Su(var)3-*

9^{null} mutant cells. In addition, cell cycle checkpoints are activated in the *Su(var)3-9*^{null} mutant cells and are essential for organismal viability (Figures 3-6 and 3-7). Genomes with complex DNA organization and high repeat contents, such as *Drosophila* heterochromatin and vertebrate genomes, present challenges for the cell especially during DNA replication, repair, and recombination. Repeated DNA sequences can form secondary structures, such as hairpins, that are difficult for the replisomes to physically overcome while maintaining faithful DNA replication. Replication across repeated seqeuences can result in sequence expansion, or duplications, as well as replication fork stalling that can produce DSBs. Recombination between allelic repeats may cause unequal exchange to alter repeat lengths and exchange between non-homologus chromosomes to form dicentric chromosomes and aneuploidy (Pearson et al., 2005). Simple repeat expansions cause two dozen hereditary disorders in humans, including fragile X syndrome, myotonic dystrophy, Huntington's disease, various spinocerebellar ataxias, and others (Mirkin, 2006). The cell must devise some mechanisms to prevent or repair DNA repeat-associated damages, such as single-strand annealing repair (SSAR). In SSAR of tandemly repeated DNA sequences, two single-strand homologues, generated from opposite sides of a DSB, can anneal in a Rad51-independent fashion to facilitate recombination repair (Lambert et al., 1999; Weinstock et al., 2006). However, SSAR inevitably results in deletions of sequencers between the two single-strand homologues. Our data strongly suggest that DNA repair mechanisms, and/or the response to damage, differ between heterochromatin and euchromatin. For example, cells may preferentially

repair breaks in heterochromatin by SSAR instead of NHEJ or HR, and H3K9 methylation may be involved in repair pathway choices.

Cell cycle checkpoint responses to DNA damage ensures the viability of *Su(var)3-9*^{null} flies

In response to DNA damage, the cell delays cell cycle progression to allow sufficient time for repair. Here we showed that *Su(var)3-9*^{null} mutants activate cell cycle arrests in G2 and mitosis in response to increased frequencies of DNA damage in heterochromatin. The analysis of Rad51 foci suggests that the majority of the damage in somatic cells is DSBs (Figure 3-3). In support of this conclusion, other types of DNA lesions, such as single-stranded DNA breaks, should activate the S phase checkpoint. However, there was no difference in the percent of cells in S phase in *Su(var)*3-9 mutants versus wild type (Figure 6A), suggesting that the S phase checkpoint is not activated and that most if not all of the damage is in the form of DSBs.

Mutations in the DNA damage checkpoint (*mei-41*^{29D}, *grp*^{06034}, and *lok*^{P6}) suppress the G2 arrest in the *Su(var)3-9*^{null} mutant cells (Figure 3-6c), confirming that the DNA damage checkpoint pathway is responsible for the G2 arrest. These mutations exhibit synthetic lethality with the *Su(var)3-9*^{null} mutation, further cementing the essential role of the DNA damage checkpoint for the viability of the *Su(var)3-9*^{null} mutant animals. Thus, I conclude that the viability *Su(var)*3-9 mutants, despite significant increases in DNA damage, is ensured by a G2 cell cycle arrest, which allows the damage to be repaired efficiently. The incomplete

synthetic lethality of the double mutants (~ 50 %, Figure 3-6b) reflects the redundant nature of the checkpoint proteins.

Cohesin reduction in heterochromatin in *Su(var)3-9*^{null} mutants (Peng and Karpen, 2007) is likely to cause sister chromatid cohesin defects that trigger the mitotic checkpoint. Subsequent analysis revealed that *smc1*^{exc46}, *Su(var)3-9*^{17}/*Su(var)3-9*^{6} (one wild-type copy of *smc1* in the *Su(var)3-9*^{null} mutant) double mutant animals exhibit 25% lethality (Figure 7A), demonstrating that cohesin reduction impacts *Su(var)3-9*^{null} viability. Mitotic checkpoint activation in the *Su(var)3-9*^{null} cells (Figure 3-6a) is reduced by mutations in chk1 (*grp*) or chk2 (*lok*) (Figure 3-7b and c), thus confirming past studies that grp and lok regulate the metaphase-anaphase transition during mitosis, in addition to their roles in the DNA repair checkpoint (Royou et al., 2005; Xu and Du, 2003). This is a conserved function at least for chk1, whose mammalian homolog participates in mitotic checkpoint signaling (Zachos et al., 2007).

A significant percentage of damaged cells, when stuck in a prolonged G2-M arrest, can escape the G2 arrest and progress into mitosis without DNA repair (Deckbar et al., 2007). Such an escape occurs within some of the *Su(var)3-9*^{null} cells, activating the mitotic checkpoint or creating chromosomal morphological defects shown in Figure 3-5. If still left unrepaired, these cells then activate the apoptosis pathway, leading to the 10-fold increase (to 0.86% of total cells) in apoptotic cells observed in the *Su(var)3-9*^{null} mutants (Figure 3-6a). The 0% viability of the *mit(1)*15^{5}; *Su(var)3-9*^{null} (*mit(1)15* is ZW10 homolog in *Drosophila*) double mutant signifies the critical role of the mitotic checkpoint in *Su(var)3-9*^{null}

survival (Figure 3-7b and c), that the mitotic checkpoint is likely more important than the G2 repair checkpoint. It is important to note that the mitotic checkpoint is likely activated by both cohesin defects and persistent DNA damage into mitosis.

A wealth of evidence, however mostly indirect, supports the proposal that accumulated DNA damage compromises the transcription of non-mitotic cells, leading to cellular degeneration and age-related deterioration of animals, especially in the nervous system (Abner and McKinnon, 2004; Ahel et al., 2006). Adult fruitflies consist of almost all non-mitotic cells, except the germline and intestinal stem cells. Ectopic expression of human superoxide dismutase 1 (SOD1, neutralizing reactive oxygen species that creates DSBs) in the motorneurons of adult flies can increase lifespan by 40% (Parkes et al., 1998). Therefore, the ability to combat DNA damaging agents is a major determinant of adult fruitfly lifespan. We hypothesize that increased DNA damage exhibited by the *Su(var)3-9*^{null} mutant cells ultimately contribute to shortened lifespan (Figure 3-1b).

Instability of repeated DNA contributes to cancer progression

'Fragile' sites exist in human chromosomes, which are vulnerable to breakage and can produce chromosomal rearrangements found in malignant cancers (Le Beau et al., 1984; Yunis and Soreng, 1984). Fragile sites can also cause replication timing deregulation, eventually leading to gene amplification and aneuploidy (Debatisse et al., 1998). How these fragile sites arise is not entirely clear, but indirect evidence suggests one contributing factor is the high

repetitive content of mammalian chromosomes. (Flores-Rozas and Kolodner, 2000).

Mammalian genomes are composed of highly complex DNA structures. More than 40% of the human euchromatic genome consists of repeated DNAs, and about 1% of the genome contains protein-encoding genes (Lander et al., 2001). Unregulated recombination of repeated sequences lend ample opportunities for chromosomal rearrangements, which participates in uncontrolled cell growth and tumorigenesis. Supporting this hypothesis is the findings that recurrent chromosomal rearrangements are observed in virtually all tumor types (Mitelman et al., 2007).

The Alu repeats, consisting of 11 % of the human genome, and heterochromatin on human chromosome 1 (band 1q12) are well-studied examples of repeated DNAs implicated in human diseases and cancer formation. Alu repeats can recombine to cause recurrent gene mutations that result in human diseases such as breast cancer (*BRCA1* deletion), glioma brain tumors (*RB1* deletion), and familial hypercholesterolemia (LDL receptor deletion) (Kolomietz et al., 2002). Like many repeated sequences in *Drosophila* and humans, the chromatin associated with Alu repeats are enriched with H3K9me (Kondo and Issa, 2003), whose function is not entirely clear. As part of constitutive heterochromatin in human cells, band 1q12 contains a fragile site that causes chromosome translocations which have been implicated in cancers of breast tissue, lymphoid, skin, reproductive organs, and endothelial tract (Rupa et al., 1995). Results from comparative genome hybridization (CGH) of cancer

samples suggests that satellite 2 DNA demethylation within 1q12 leads to high incidence of chromosomal translocations (Wong et al., 2001).

Our study here shows that chromatin alterations contribute to consequences beyond deregulation of gene expression. Reduced H3K9 methylation in *Drosophila* results in eleveated levels of DNA damage, chromosomal rearrangements and cell cycle checkpoint activation. Therefore, the structure of heterochromatin, regulated by H3K9 methylation, helps maintain genome stability and organismal survival. Intriguingly, *Drosophila*'s heterochromatin, not euchromatin, resembles the mammalian genomes in their complex DNA organization. Mammalian systems may employ similar mechanisms to regulate the stability of repeated DNAs, which consist of almost half of the genome.

Materials and Methods

Fly stocks

All fly stocks were raised at 22 ^{o}C. We received the *grp*^{06034}, *rod*^{EY04576}, *mit*(1)15^{5}, and *p53*$^{11\text{-}1B\text{-}1}$ flies form the Bloomington stock center. The *lok*^{P6} flies are from Michael Brodsky, *dcr2*^{L811fsx} from Richard Carthew, *smc1*^{exc461} from Scott Hawley, *Su(var)3-9* null alleles 6 and 17 from Gunter Reuter, and *mei-41*^{29D} flies from Tin Tin Su,. Fly crosses were performed using standard genetic techniques. Some double mutants were made by meiotic recombination: one, *rod*^{EY04576}, *Su(var)3-9*^{null}; two, *p53*$^{11\text{-}1B\text{-}1}$, *Su(var)3-9*^{null}; three, *smc1*^{exc46}, *Su(var)3-9*^{17} flies. These flies were scored by PCR reactions, using template DNA from single flies that primers that distinguish wild type from mutated DNA sequences.

Fly developmental stage analysis

% fertilization

Flies were allowed to lay eggs on soft agars containing yeast paste for 4 hours at 25 ^{o}C. After eggs were incubated for 6 hours at 25 ^{o}C, all the eggs were fixed using the standard method. Nuclei in the fixed eggs were visualized by DAPI staining. The %'s of unfertilized eggs were calculated by the formula: (total number of eggs – the number of eggs containing one- or two- nuclei)/total number of eggs X 100%.

% hatched eggs

Flies were allowed to lay eggs on soft agars containing yeast paste overnight at 25 ^{o}C, and the numbers of eggs laid were counted afterwards. The eggs were allowed to incubate at 25 ^{o}C for more than 30 hours, and the numbers

of unhatched eggs were counted afterwards. The %'s of hatched eggs were calculated by the formula: (number of eggs laid – number of unhatched eggs)/number of eggs laid X 100 %.

% eclosion

Flies were allowed to lay eggs overnight in a bottle containing fly food at 25 ^{o}C. The bottles were incubated at 25 ^{o}C for 2 weeks. The %'s of eclosion were calculated by the formula: number of hatched pupa cases/total number of pupae X 100 %.

Fly lifespan analysis

More than 120 flies from each genotype, after one day of eclosion, were incubated at 25 ^{o}C and passed onto new vials every other day. Each vial contains approximately 20 flies. Dead flies were counted every other day. When all flies died, the total number of flies was summed from the numbers of dead flies. The %'s of viability were calculated by dividing the number of flies alive at specific time periods by the total number of flies.

Antibodies

Rabbit antibody against γH2Av (1:250 dilution) was purchased from Rockland. The rabbit anti-Rad51 antibody (1:100 dilution after direct labeling) was a generous gift from Jim Kadonaga. The anti-Rad51 antibody was directly labeled as previously described (Oegema et al., 2001). The mouse anti-C(3)G antibody (1:500 dilution) was a generous gift from Scott Hawley. The rabbit anti-PCNA antibody (1:100 dilution) was a generous gift from Daryl Henderson. The rabbit anti-PH3 (1:1000 dilution) was purchased from Upstate. The anti-CycA

mouse monoclonal antibody (1:20 dilution) was purchased from the Developmental Studies Hybridoma Bank. Alexa dye-conjugated secondary antibodies were purchased from Invitrogen and used at 1:500 dilution.

IF, FISH, and IF-FISH of whole-mount tissues and squashed tissues.

IF was performed as previously described (Hari et al., 2001a). Germarium was fixed as previously described (D. Gilliland et al., 2005), except ovaries were dissected within 24 hours of mating. FISH was performed as previously described (Dernburg et al., 1996b) using 100 ng of each probe. In combined IF-FISH experiments, IF was performed before the FISH treatment. FISH probes targeting *Drosophila* satellite DNAs were made from aminoallyl-dUTP end-labeling of oligonucleotides using TUNEL with, followed by dye conjugation.

TUNEL assay

Whole-mount tissues were fixed with 4 % paraformaldehyde in PBS and 0.2 % of TritonX-100, washed and permeabilized overnight with PBS and 0.2 % of Triton-X-100. Tissues were incubated with TUNEL buffer (1x TUNEL buffer from Roche, 2.5mM CoCl2, 0.2% TritonX-100) for 10 min, then in TUNEL buffer plus dNTPs (final concentrations of 10 uM of dATP, dCTP, and dGTP, 3.3uM dTTP, and 6.6uM DIG-dUTP) and enzyme (20U/ml final concentration) for 3 hours at 37 ^{o}C. Afterwards, DIG signals were detected via standard IF procedure using rhodamine-labeled anti-DIG antibody. To analyze % cells in apoptosis, brain and imaginal disc tissues were squashed onto slides into single cell layer using standard technique. The slides were washed extensively with PBS and 0.2 % of Triton-X-100, incubated with TUNEL buffer plus dNTPs (final concentrations

of 10 uM of dATP, dCTP, and dGTP, 3.3uM dTTP, and 6.6uM DIG-dUTP) and enzyme (20U/ml final concentration) for 2 hours at 37 ^{o}C. Afterwards, DIG signals were detected via standard IF procedure using rhodamine-labeled anti-DIG antibody.

Microscopy, volumetric and colocalization analysis

All images were captured using an Applied Precision Deltavision Workstation and deconvolved by the SoftWorx software, using the conservative algorithm with 5 to 8 iterations. The SoftWorx-deconvolved images were converted to TIFF files and then into stack images for volumetric analysis with the Metamorph 7.0 software.

For foci localization and colocalization studies, optical sections of deconvolved images were enhanced contrast and counted in relation to its localization to DAPI-bright vs. DAPI-weak regions. DAPI signals were not enhanced contrast. DAPI-bright regions were regions that contain contiguous (>5 pixels) bright DAPI signals; representative DAPI images are shown in Figure 3-3.

Statistical comparisons and p values were calculated by the chi-squre test or the two-sample t test, assuming unequal variance.

Chromosome paints

FISH paints were made by degenerate PCR using templates described below. The PCR products were digested with 4-base restriction enzymes, AluI, HaeIII, MseI, MspI, RsaI, and Sau3AI. From that, the DNA's were end-labeled with TUNEL using aminoallyl-dUTPs followed by dye conjugation. Templates for

chromosomes 2 and 3 were bacterial artificial chromosomes (BACs) containing *Drosophila* sequences. The BACS were placed by the Berkeley Drosophila Genome Project to lie in the genomic tiling path, spaced in 500kb intervals, and of low repeat content. Templates for chromosome X were provided by Abby Dernburg, who micro-dissected polytene chromosome X and amplified them via degenerate PCR as a PhD student.

FISH using chromosome paints were done as the following. Acid-squashed slides were treated in ethanol series, incubated in 0.005 % pepsin in 10mM HCl for 1 minute, rinsed in PBS, and treated in ethanol series to dry. The slides were treated with 2X SSCT (0.1 % Tween-20) for 5 minutes, 50 % formamide in 2X SSCT for 5 minutes, and 70 % formamide in 2X SSCT for 5 minutes. Slides were incubated in fresh 70 % formamide in 2X SSCT at 37 ^{o}C for more than 1.5 hours; solutions need be changed at least 3 times during this period. Chromosomes on the slides, incubated in 70 % formamide and 2X SSCT, were denatured on the hot plate of a PCR machine that increases temperature from 22 to 74 ^{o}C within 1.5 minutes, stays at 74 ^{o}C for 1.5 minutes, and decreases temperature from 74 to 22 ^{o}C within 1.5 minutes. The slides were then treated with ethanol series to dry, and the denatured probes (in probe mix 50% formamide, 10% dextran sulfate, 2X SSCT, 1ug Cot-1 DNA) were added onto chromosomes to allow hybridization overnight. After the incubation, the coverslips were removed, and the slides were washed with 50% formamide, 2X SSCT at 37 ^{o}C for 4 times, at 30 minutes each time.

DSB repair response assay

Dissected brain and imaginal disc tissues incubated in PBS were irradiated with 5 Gy of x-ray, allowed to incubate at room temperature at various lengths of time, then acid squashed onto slides. Mitotic chromosomes were scored by PH3-positive signals.

For survival assay, flies were allowed to lay eggs in vials containing fly food overnight at 25 ^{o}C. For each genotype and each x-ray dose, 5 to 7 vials were prepared. The numbers of eggs laid within each vial was counted, and then the embryos were treated with 0, 3, 6, 12 Gy of x-ray. Afterwards, the embryos were incubated at 25 ^{o}C for 2 weeks, and the number of eclosed adults in each vial was counted. The %'s of eclosion were calculated by the formula: (number of eclosed adults/number eggs laid) X 100 %. The %'s of survival were calculated by the formula: (% eclosion at each dose/% eclosion at 0 Gy) X 100 %.

Cell Cycle analysis

Brain and imaginal discs were fixed in 4 % paraformaldehyde and PBS for 5 minutes, washed with PBS 4 times for 5 minutes each. The fixed tissues were incubated in Collagenase solution (0.04 % Collagenase type IV, Sigma, in PBS) for 10 minutes, squashed onto slides using RainX-treated coverslips, and frozen in liquid nitrogen. After coverslips are removed, the slides were allowed to warm for less than 30 seconds, fixed in 4 % paraformaldehyde and PBS for 5 minutes, washed with PBS 4 times for 5 minutes each. IF of cell cycle markers were performed using methods described, except no TritonX100 was used for CycA IF. Images were captured by an Applied Precision Deltavision

Workstation and converted to TIFF images. The Metamorph 7.0 software was used to score cells positive for cell cycle markers or TUNEL signals. For each genotype and each marker, >3000 cells from at least 3 animals were analyzed.

Chapter Four: General discussion and future directions

General summary

Like many PhD students, I began my projects with a goal that differed from the ultimate subject of my thesis. I wanted to identify regulators of nuclear architecture, using the attractive genetic system in *Drosophila melanogaster* and unique tools, such as the minichromosome γ878, available in the lab of my advisor Gary Karpen. While I was conducting a genetic screen to isolate the identity of mutations that perturb the reporter *yellow*$^{+}$ expression on γ878, I was also using immunofluorescence (IF) to examine subnuclear structures in known Su(var) mutants. This assay revealed that some Su(var) mutants, such as those of *Su(var)3-9* and *Heterochromoatin Protein 1* (*HP1*), exhibited nucleolus structural instability.

This serendipitous discovery directed my efforts to an otherwise little studied function of histone modifications and chromatin structure, especially in heterochromatin. I decided to pursue the thesis that heterochromatin structure—which forms around histone H3 K9 methylation (H3K9me), Su(var)3-9, and heterochromatin protein 1 (HP1), and is regulated by the RNA interference (RNAi) process—is essential for the maintenance of heterochromatin sequences and genome stability. I have discovered that compromised heterochromatin structure leads to the following: elevated DNA damage in heterochromatin and activation of repair and mitotic checkpoints, extrachromosomal DNA (eccDNA)

formation from repeated DNAs, ectopic nucleolus formation from ecc ribosomal DNA (rDNA) and nuclear organization disruption.

Findings from my thesis project suggest the idea that the repeated DNAs in heterochromatin require special mechanisms and components to maintain their integrity. There are still many questions that need to be addressed in the future to provide a mechanistic understanding of the roles of the RNAi and H3K9 methylation pathways in maintaining the stability of heterochromatic DNAs. Why does the cell need to safeguard heterochromatin stability? How does the cell accomplish this task? Does DNA damage recognition and repair differ between euchromatin and heterochromatin? Since mammalian euchromatin is interspersed with many repeated DNAs like *Drosophila* heterochromatin, does it utilize similar mechanisms and components to stabilize their repeated DNAs? In this chapter I will summarize our current understanding about these issues and outline future directions.

Functional significance: why does the cell contain heterochromatin?

High repeat content in nearly 30 % of the *Drosophila* genome begs the question about whether the presence of heterochromatin is under evolutionary selection. Functional analyses in higher eukaryotes revealed that heterochromatin regulates centromere function, telomere protection, meiotic chromosome pairing, and gene regulation during development (detailed in Chapter 1). From the functional standpoint, heterochromatin behaves like a subnuclear organelle. Like the nucleolus, heterochromatin formation is based on

DNA and is epigenetically regulated, but its persistence through evolution likely depends on its many functions.

The cell has evolved mechanisms to stabilize heterochromatin for reasons that remain unclear. One example is the recent discoveries of repeat-associated small interfering RNA (rasiRNA) molecules, a demonstration that the cell uses the RNA interference (RNAi) pathway to safeguard repeated DNAs (Theurkauf et al., 2006). Specifically, rasiRNAs in the germline help regulate expression of retrotransposons and the Stellate focus, which is composed of repeated Stellate transcription units (Aravin et al., 2004; Tomari et al., 2004; Vagin et al., 2006). Further analyses of mutations in the rasiRNA pathway (*armitage* (*armi*), *aubergine* (*aub*), and *spindle-E* (*spn-E*)) showed that embryonic axis specification is disrupted (Cook et al., 2004), and germline-specific accumulation of γH2Av foci, indicative of increased DNA damage (Klattenhoff et al., 2007). Mutations in the DNA damage checkpoint (*mei-41*/ATR and *lok*/chk2) are able to suppress γH2Av foci accumulation, but not retrotransposon and *Stellate* deregulation in the rasiRNA mutants (Klattenhoff et al., 2007). These data suggest that the rasiRNA pathway influences multiple processes within the germline, and one is to maintain genome integrity.

My thesis extends beyond the work from Theurkauf's group, demonstrating that the cell utilizes the RNAi and H3K9 methylation pathways to maintain heterochromatin stability. H3K9me reduction from heterochromatin, due to mutations in the H3K9 methyltransferase *Su(var)3-9* or the RNAi pathway, caused a significant increase the the frequency of DNA damage in

heterochromatin. This defect strongly correlates with the following observations: DNA breaks occur in heterochromatin of the *Su(var)3-9*^{null} meiotic cells, the mutant cells are sensitivity to exogenous DNA damage, the mutant mitotic chromosomes exhibit morphological defects and rearrangements, and the DNA damage checkpoint and mitotic checkpoints are essential for *Su(var)3-9*^{null} survival (Chapter 3). These results demonstrate the importance of heterochromatin in cellular functions and survival. However, they do not address the reason(s) why heterochromatin integrity is needed for cellular survival. One explanation for the importance of heterochromatin integrity is that unchecked DNA damage in heterochromatin causes chromosome structural defects and aneuploidy (Figure 4, Chapter 3) that are detrimental to the cell. As explained above, the described regulatory functions and perhaps other undiscovered functions of heterochromatin may also require safeguarding the structural integrity of heterochromatin.

Su(var)3-9, HP1, H3K9 methylation, and RNA interference (RNAi) in heterochromatin

As an epigenetically regulated structure, heterochromatin does not contain any DNA sequence consensus that defines its formation. Rather, repeated DNA sequences in heterochromatin are associated with nucleosomes containing H3K9me (dimethylation in *Schizosaccharomyces pombe* and *D. melanogaster* but trimethylation in vertebrates). It is unclear how repeated DNAs accumulate and come to associate with H3K9me-nucleosomes. Ectopic transgene insertion to establish a high density of repeated DNAs within euchromatin can ‘attract’ HP1

and H3K9 methylation (Janicki et al., 2004), suggesting that a high density of repeats is sufficient for 'heterochromatinization.' This process is likely RNAi-mediated and directed by double-strand RNAs (dsRNAs) transcribed from these repeats (Grewal and Jia, 2007; Moazed et al., 2006).

How repeated DNAs accumulate within heterochromatin through evolutionary time is not known and difficult to investigate. In lower eukaryotes, the heterochromatic regions are centromeres, telomeres, mating type loci, and rDNA, all of which perform clearly defined functions. In higher eukaryotes, heterochromatin as a whole exhibits functions described above and in Chapter 1. But why do higher eukaryotes need tens to hundreds of megabases of repeated DNA sequences to accomplish these tasks? Moreover, did heterochromatin-specific functions derive before repeated DNA accumulation, or vice versa? These may be questions untestable by conventional techniques. Nonetheless, comparative genomic and epigenomic studies of heterochromatin in closely-related species may yield illuminating information.

Investigations of heterochromatin and RNAi mechanisms in *S. pombe* help elucidate how repeated DNA sequences come to associate with H3K9me-nucleosomes and HP1. RNAs transcribed from repeated DNAs form double-stranded RNAs (dsRNAs) that are processed by dicer to produce small interfering RNAs (siRNAs). These siRNAs recruit the RITS (RNA-induced transcriptional gene silencing) complex to heterochromatic regions, where the RITS complex recruits Su(var)3-9/clr4 (Su(var)3-9 from now on), which methylates H3K9 residues and establishes heterochromatin (Grewal and Jia,

2007; Moazed et al., 2006). Intriguingly, recruitment of the RITS complex to heterochromatin also requires Su(var)3-9 binding (Noma et al., 2004), demonstrating a cooperative relationship that is essential for both Su(var)3-9 and the RITS complex. To maintain heterochromatin structure, HP1 recruits more Su(var)3-9 proteins to heterochromatin by its physical associations with both the H3K9me residue and the Su(var)3-9 protein (Nakayama et al., 2001). Both establishment and maintenance processes provide specificity for Su(var)3-9 to act as the enzymatic component for heterochromatin identity. These findings also highlight the importance of Su(var)3-9 activity.

While it establishes and maintains heterochromatic regions, the cell must also restrict heterochromatin from spreading into the flanking euchromatin; without this active confinement, heterochromatin-mediated silencing would disrupt gene expression. The euchromatin-heterochromatin junction is likely also epigenetically regulated. Chromatin immunoprecipitation-PCR (ChIP-PCR) analysis of chromatin surrounding the centromeres and the mating type locus in *S. pombe* showed inverse distribution patterns of H3K4me and H3K9me in heterochromatin and the flanking euchromatin. Enriched H3K9me and Swi6/HP1 in heterochromatin sharply decrease at the euchromatin-heterochromatin junction, while the reverse is true for H3K4me. Deletion of the IR-L and IR-R repeats, which are boundary elements that flank the mating type locus, results in heterochromatin spreading into the neighboring euchromatin (Noma et al., 2001). Multiple mechanistic models explain how the cell may modulate chromatin changes at the heterochromatin-euchromatin junction to restrict heterochromatin

spreading, and recent studies focused on two opposing scenarios. One model states that nucleosome replacement at the heterochromatin-euchromatin junction defines the boundary. The alternative model proposes that histone lysine-demethylases serve to define this boundary.

In essence, the two models describe alternative mechanisms by which the cell continually counteracts H3K4 and H3K9 methyltransferase activities from euchromatin and heterochromatin. Proponents of the nucleosome replacement model took notice of the observations in *Saccharomyces cerevisiae* and *D. melanogaster* that nucleosome turnover is consistently higher at boundary-associated DNA elements compared to the surrounding DNA regions (Dion et al., 2007; Mito et al., 2007). In support of the alternative model, mutations of lysine demethylases disrupt heterochromatin status. The homologs of the first identified lysine demethylase hLSD1 (Shi et al., 2004) are enriched in the heterochromatin boundary elements in *S. pombe* (Lan et al., 2007) and mutations disrupt heterochromatin-mediated silencing in *Drosophila* (Rudolph et al., 2007). Intriguingly, hLSD1 has been shown to demethylate both H3K4 (Shi et al., 2004) and H3K9 (Metzger et al., 2005); its specificity seems to be regulated by hLSD1's binding partners. Mutation of LSD1 in *S. pombe, Splsd1*, causes H3K9me2 spreading at the boundary elements, demonstrating its *in vivo* H3K9 demethylase activity (Lan et al., 2007). However, null mutations of *Drosophila* LSD1 (*Su(var)3-3*) decreases H3K9me2 at the boundary elements, further supporting the *in vitro* demonstration that Su(var)3-3 is a H3K4 demethylase (Rudolph et al., 2007).

These differences reveal additional complexity in lysine demethylase regulation that can impact heterochromatin status.

Investigations of heterochromatin formation mainly focus on its epigenetic regulation, because H3K9 methylation strongly correlates with heterochromatin functions. Another reason is the accepted view that H3K9 methylation is a more 'permanent' feature of heterochromatin and epigenetically silenced regions, because no demethylase had been proven to exist until 2004 (Shi et al., 2004). The demonstrations that different mechanisms can remove H3K9 methylation from chromatin revealed the plasticity of H3K9 methylation and heterochromatin.

The plasticity inherent to heterochromatin manifests not only epigenetically but is also reflected in sequence changes. Comparative sequence analysis of heterochromatic and euchromatic gene counterparts in *Arabidopsis*, *D. melanogaster* and *D. pseudoobscura* suggest dramatic structural reorganization of genes that move between euchromatin and heterochromatin during evolution. Specifically, as euchromatic genes moved into heterochromatin, they accumulated transposable elements (TEs) in their introns and flanking regions, in addition to increased A-T content in the coding sequences (Carvalho and Clark, 2005; Lippman et al., 2004; Yasuhara et al., 2005). Also, repeated DNA sequences undergo homogenization, in which variant sequences become more similar, over evolutionary time (Elder and Turner, 1995). The alpha repeats in nonhomologous chromosomes in both human and chimpanzees have been shown to undergo homogenization (Jorgensen et al., 1992), suggesting that unequal crossover and/or gene conversion occurs between similar sequences on

nonhomologous chromosomes. Unequal exchange between non-homologous chromosomes can result in dicentric chromosome formation and aneuploidy, or neocentromere formation from the alphoid repeats (Wevrick and Willard, 1989). However, homogenization can occur without reciprocal exchange, for example via gene conversion, which would not result in rearrangements and aneuploidy. These observations suggest that heterochromatin is not recombinationally 'silent', at least over evolutionary timescales, despite the absence of reciprocal recombination during meiosis. Combined with the results presented in my thesis, I propose that DNA breaks in heterochromatin and euchromatin may be processed differently to avoid problems that arise when repeats recombine. For example, both the exchange of information among repeats observed during evolution, the absence of reciprocal recombination during meiosis, and the cellular and organismal defects that result from loss of heterochromatin pathways can be accommodated by imagining that chromatin structure in heterochromatin reduces the probability of homologous recombination between repeats and increases the utilization of NHEJ and gene conversion pathways. Factors that can influence gene structural changes and repeat homogenization are DNA replication, recombination and repair, all of which are likely regulated by chromatin structure.

My thesis works point to the intriguing possibility that chromatin structural variations caused by chromatin remodeling deregulation affect DNA recombination and replication, thereby contributing to regional sequence alterations and genome reorganization. This can be a component of speciation

mechanisms and the evolution of complex-DNA genomes, in which coding sequences constitute a very small percentage of sequence while repeated DNAs constitute the majority of the genome. Further investigations into whether and how chromatin structural variations contribute to genome reorganization will greatly benefit our understanding about mechanisms that affect genome plasticity.

Future directions: H3K9methylation functions in heterochromatin stability

My thesis investigated the consequences of reduced H3K9me content on the stability of heterochromatic regions and nuclear architecture. However, this project provided little understanding about the mechanisms by which H3K9me regulates genome stability. For example, we now know that increased extrachromosomal DNA (eccDNA) formation in the *Su(var)3-9*^{null} and the RNAi mutants (Chapter 2) is likely a consequence of DNA damage in heterochromatin (Chapter 3). Yet little is known about how these defects occur, and how reduced H3K9me levels lead to increased DNA damage in heterochromatin. Here I will propose potential functions of H3K9me in maintaining genome stability and outline projects to investigate these functions.

The H3K9me-based chromatin potentially exhibits these functions in maintaining genome stability: 'protecting' DNA from damaging agents, coordinating replisome firings and replication timing, and affecting the DNA damage response (Chapter 3). These proposed functions are not mutually exclusive, and the DNA damage response can encompass processes that include chromatin decondensation around double-strand break (DSB) sites and

coordination of DNA repair factor loading (Chapter 3). Here I separate H3K9me's proposed function in the DNA damage response from its 'protection' of heterochromatin from damaging agents.

The observed DNA damage in the *Su(var)3-9* and *dcr-2* mutant cells is likely not caused by the failure of chromatin's 'protecting' ability; no DNA damaging agent was used to cause the high incidence of DNA breaks (Figure 2, Chapter 3). However, this potential function by H3K9me in general genome stability cannot be excluded. Heterochromatin has been shown to allow less access to DNases than euchromatin (Cartwright et al., 1999), presumably due to certain physical rigidity which may also reduce access by damaging agents to DNA. To investigate this problem, one can compare DNA damage frequency, by quantitative analysis of terminal deoxytidyltransferase (TUNEL) and γH2Av signals, in DAPI-bright regions of wild type vs. the *Su(var)3-9*^{null} mutant after exposing them to exogenous DNA damaging reagents. If H3K9me chromatin serves a 'protecting' function, DNA damage frequencies in wild-type DAPI-bright regions would be significantly less than that in the *Su(var)3-9*^{null} DAPI-bright regions. It is important to point out that fewer observed DNA breaks in DAPI-bright regions can also be caused by lower DNA repair efficiency in heterochromatin; time-course experiments monitoring DNA break repair, indicated by foci disappearance, can rule out this possibility.

Comparing replication timing and stalled replication forks in repeated DNAs and/or heterochromatin of wild type and the *Su(var)3-9*^{null} mutant will elucidate whether H3K9me chromatin impacts these processes. Replication

timing can be monitored via pulse-chase-pulse incorporation of iododeoxyuridine (IdU) and chlorodeoxyuridine (CldU) followed by immunofluorescence (IF) analysis as previously described (Sullivan and Karpen, 2001). Two-dimensional DNA electrophoresis followed by Southern blotting to target specific heterochromatic DNAs can be used to visualize and quantitate stalled replication forks for comparative analysis. If H3K9me chromatin regulates replication timing, heterochromatin replication, which normally occurs in late S phase, would initiate during early and mid S phase and stalled replication forks would increase in the *Su(var)3-9*^{null} mutant cells.

Response to DNA damage includes processes and components involved in damage recognition, repair, and cell cycle checkpoints. H3K9 chromatin may be involved in damage recognition and repair coordination. For example, DSBs in repeated DNAs are preferentially repaired by non-homologous end-joining (NHEJ) or single-strand annealing repair (SSAR), in which two single-strand homologues generated from opposite sides of a DSB to facilitate recombination repair (Lambert et al., 1999; Weinstock et al., 2006). H3K9 chromatin may help the cell recognize that the DSBs lie within repeated DNAs and therefore require SSAR or NHEJ instead of conventional homologous recombination (HR). One may investigate the decision-making process, to choose HR, NHEJ, or SSAR for heterochromatin repair, by comparing the dynamics of repair factor recruitment (using cytological or biochemical assays) to induced DSBs (described below) in wild type and the *Su(var)3-9*^{null} mutant cells.

Investigation of damage recognition is more difficult because no factors have been identified that specifically function in DNA damage recognition. Instead one can monitor physiological events, such as chromatin decondensation and γH2Av recruitment, both of which take place less than 30 seconds after DNA breaks occur. To do that, site-specific endonucleases are utilized to induce DSBs in heterochromatin and the dynamics of γH2Av foci formation and chromatin decondensation—using FISH probes covering the endonuclease sites and quantitate the area of FISH probe coverage before and after endonuclease induction—can be compared between wild type and the *Su(var)3-9*^{null} mutant cells. For example, endogenous sites for I-Cre endouclease within the ribosomal DNA (rDNA) transcription unit have been identified and shown to induce DSBs that can cause X-Y translocations and increased recombination rates between the sex chromosomes (Maggert and Golic, 2005). It will be very interesting to find out whether DSBs produced by I-Cre in rDNA of wild type and *Su(var)3-9*^{null} mutants are repaired with equal efficiency. This system and other similar systems can also be used to compare the dynamics and efficiency of different repair processes in heterochromatin of wild type and *Su(var)3-9*^{null} cells.

These experiments will yield extremely useful information about the functions of H3K9 chromatin in replication control, DNA damage protection, damage recognition, and coordination of different DNA repair processes. Information from these experiments will also provide a foundation for understanding the specific biological processes that H3K9me may function for maintaining the human genome.

Future directions: H3K9 methylation in human genome stability

The majority of published studies about chromatin modifications focus on its regulatory functions in transcription. Current epigenomic characterizations of different cancer types also put great emphasis on epigenetic regulation of transcription, showing dramatic chromatin alterations of oncogenic or tumor suppressor genes whose transcriptional deregulation contribute to cancer progression (Egger et al., 2004; Esteller, 2007). Well-studied examples of these genes are *p16*^{INK4a}, *p73*, *Rb*, and *BRCA1* (Esteller, 2007). My thesis works strengthened the idea that chromatin structure contributes to genome stability in addition to regulating genes that control cell growth, and that local chromatin structure can impact genome structural integrity and the DNA damage response. Specifically, I showed that hetero schromatin with reduced H3K9me levels exhibit increased damage that causes chromosome structural defects, such as translocations, deletions and duplications, events that can lead to uncontrolled cell growth and eventual tumorigenesis.

Drosophila heterochromatin, not euchromatin, resembles the mammalian genomes in their complex DNA organization. Mammalian systems may employ mechanisms similar to *Drosophila* heterochromatin to regulate the stability of repeated DNAs. Human Alu repeats and heterochromatin on human chromosome 1 (band 1q12) both contain ‘fragile’ sites, which can produce chromosomal rearrangements found in malignant cancers (Le Beau et al., 1984; Yunis and Soreng, 1984). Vulnerability in these DNA elements is also highly correlated with their chromatin composition (Kondo and Issa, 2003; Wong et al.,

2001). Understanding how H3K9me helps stabilize *Drosophila* heterochromatin would help direct efforts to elucidating how mammalian systems stabilize their genomes, especially repeated DNA elements.

Investigations of H3K9me functions in mammalian systems will pose more technical difficulties than *Drosophila* studies because all mammalian H3K9 methyltransferases identified thus far, Suv39h 1 and 2, G9a, SETB1, and RIZ1, function in transcriptional silencing in both euchromatin and heterochromatin (Kim et al., 2003; Peters et al., 2001; Schultz et al., 2002; Tachibana et al., 2002). Mouse knockouts of G9a and Suv39h1 and 2 exhibit either embryonic lethality or severe developmental defects. Suv39h1's regulatory function of developmental genes is an evolutionarily conserved function; morpholino knockdown of Suv39h1 in zebrafish larvae causes severe developmental defects (Rai et al., 2006). These results suggest that loss of function assays of H3K9me in human cells, by H3K9 methyltransferase knock-down, would not be able to rule out indirect effects from H3K9me-mediated transcriptional regulation.

Suv39h1 and 2 knock-down experiments in human cells, via siRNA treatment, are nevertheless a worthwhile approach because of two important reasons. Human tissue culture cells do not require developmental gene regulation that is essential for the mouse and zebrafish animals. Secondly, Suv39h1 and 2 knock-down is a very rapid technique to test the question whether human heterochromatin or euchromatin exhibit higher DNA damage frequencies due to H3K9me reduction. Analysis of damage in heterochromatin can make use of internal controls, comparing DSB frequencies in euchromatin,

heterochromatin with regular H3K9me content, and heterochromatin with reduced H3K9me content in siRNA-treated cells, which will facilitate quantitation. Positive results from this experiment would be very encouraging and also lay the groundwork for more carefully designed assays to characterize H3K9me functions in human genome stability and cancer.

In summary, I have shown that H3K9me in heterochromatin of *D. melanogaster* is important for genome stability, repeated DNA integrity, and nuclear architecture. Further experiments will be needed to elucidate the mechanisms involved in H3K9me-based stabilization of genomes with complex DNA organization.

Reference

Abner, C. W., and McKinnon, P. J. (2004). The DNA double-strand break response in the nervous system. DNA Repair (Amst) *3*, 1141-1147.

Abranches, R., Beven, A. F., Aragon-Alcaide, L., and Shaw, P. J. (1998). Transcription Sites Are Not Correlated with Chromosome Territories in Wheat Nuclei. J Cell Biol *143*, 5-12.

Adams, M. D., McVey, M., and Sekelsky, J. J. (2003). Drosophila BLM in double-strand break repair by synthesis-dependent strand annealing. Science *299*, 265-267.

Ahel, I., Rass, U., El-Khamisy, S. F., Katyal, S., Clements, P. M., McKinnon, P. J., Caldecott, K. W., and West, S. C. (2006). The neurodegenerative disease protein aprataxin resolves abortive DNA ligation intermediates. Nature *443*, 713-716.

Allshire, R. C. (2004). RNA interference, heterochromatin, and centromere function. Cold Spring Harb Symp Quant Biol *69*, 389-395.

Aravin, A. A., Klenov, M. S., Vagin, V. V., Bantignies, F., Cavalli, G., and Gvozdev, V. A. (2004). Dissection of a natural RNA silencing process in the Drosophila melanogaster germ line. Mol Cell Biol *24*, 6742-6750.

Aravin, A. A., Lagos-Quintana, M., Yalcin, A., Zavolan, M., Marks, D., Snyder, B., Gaasterland, T., Meyer, J., and Tuschl, T. (2003). The Small RNA Profile during Drosophila melanogaster Development. Developmental Cell *5*, 337.

Astrom, S. U., Cline, T. W., and Rine, J. (2003). The Drosophila melanogaster sir2+ gene is nonessential and has only minor effects on position-effect variegation. Genetics *163*, 931-937.

Austin, R. J., Orr-Weaver, T. L., and Bell, S. P. (1999). Drosophila ORC specifically binds to ACE3, an origin of DNA replication control element. Genes Dev *13*, 2639-2649.

Belyaeva, E. S., Zhimulev, I. F., Volkova, E. I., Alekseyenko, A. A., Moshkin, Y. M., and Koryakov, D. E. (1998). Su(UR)ES: a gene suppressing DNA underreplication in intercalary and pericentric heterochromatin of Drosophila melanogaster polytene chromosomes. Proc Natl Acad Sci U S A *95*, 7532-7537.

Bernard, P., Maure, J. F., Partridge, J. F., Genier, S., Javerzat, J. P., and Allshire, R. C. (2001). Requirement of heterochromatin for cohesion at centromeres. Science *294*, 2539-2542.

Bier, E. (2005). Drosophila, the golden bug, emerges as a tool for human genetics. Nature Reviews Genetics *6*, 9-23.

Bilen, J., and Bonini, N. M. (2005). Drosophila as a model for human neurodegenerative disease Annual Review of Genetics *39*, 153-171.

Blander, G., and Guarente, L. (2004). The Sir2 family of protein deacetylases. Annu Rev Biochem *73*, 417-435.

Brodsky, M. H., Sekelsky, J. J., Tsang, G., Hawley, R. S., and Rubin, G. M. (2000). mus304 encodes a novel DNA damage checkpoint protein required during Drosophila development. Genes Dev *14*, 666-678.

Brodsky, M. H., Weinert, B. T., Tsang, G., Rong, Y. S., McGinnis, N. M., Golic, K. G., Rio, D. C., and Rubin, G. M. (2004). Drosophila melanogaster MNK/Chk2 and p53 regulate multiple DNA repair and apoptotic pathways following DNA damage. Mol Cell Biol *24*, 1219-1231.

Brown, K. E., Baxter, J., Graf, D., Merkenschlager, M., and Fisher, A. G. (1999). Dynamic repositioning of genes in the nucleus of lymphocytes preparing for cell division. Mol Cell *3*, 207-217.

Cam, H. P., Sugiyama, T., Chen, E. S., Chen, X., FitzGerald, P. C., and Grewal, S. I. (2005). Comprehensive analysis of heterochromatin- and RNAi-mediated epigenetic control of the fission yeast genome. Nat Genet *37*, 809-819.

Carmo-Fonseca, M. (2002). New clues to the function of the Cajal body. EMBO Rep *3*, 726-727.

Cartwright, I. L., Cryderman, D. E., Gilmour, D. S., Pile, L. A., Wallrath, L. L., Weber, J. A., and Elgin, S. C. (1999). Analysis of Drosophila chromatin structure in vivo. Methods Enzymol *304*, 462-496.

Carvalho, A. B., and Clark, A. G. (2005). Y chromosome of D. pseudoobscura is not homologous to the ancestral Drosophila Y. Science *307*, 108-110.

Cohen, S., Yacobi, K., and Segal, D. (2003). Extrachromosomal circular DNA of tandemly repeated genomic sequences in Drosophila. Genome Res *13*, 1133-1145.

Cohen, Z., Bacharach, E., and Lavi, S. (2006). Mouse major satellite DNA is prone to eccDNA formation via DNA Ligase IV-dependent pathway. Oncogene.

Cook, H. A., Koppetsch, B. S., Wu, J., and Theurkauf, W. E. (2004). The Drosophila SDE3 homolog armitage is required for oskar mRNA silencing and embryonic axis specification. Cell *116*, 817-829.

Cremer, T., and Cremer, C. (2001). CHROMOSOME TERRITORIES, NUCLEAR ARCHITECTURE AND GENE REGULATION IN MAMMALIAN CELLS. Nature Reviews Genetics *2*, 292.

D. Gilliland, W., M. Wayson, S., and Hawley, R. S. (2005). The Meiotic Defects of Mutants in the Drosophila mps1 Gene Reveal A Critical Role of Mps1 in the Segregation of Achiasmate Homologs. Current Biology *15*, 672-677.

de Lange, T. (2005). Shelterin: the protein complex that shapes and safeguards human telomeres. Genes Dev *19*, 2100-2110.

Debatisse, M., Coquelle, A., Toledo, F., and Buttin, G. (1998). Gene amplification mechanisms: the role of fragile sites. Recent Results Cancer Res *154*, 216-226.

Deckbar, D., Birraux, J., Krempler, A., Tchouandong, L., Beucher, A., Walker, S., Stiff, T., Jeggo, P., and Lobrich, M. (2007). Chromosome breakage after G2 checkpoint release. J Cell Biol *176*, 749-755.

Dernburg, A. F., Broman, K. W., Fung, J. C., Marshall, W. F., Philips, J., Agard, D. A., and Sedat, J. W. (1996a). Perturbation of nuclear architecture by long-distance chromosome interactions. Cell *85*, 745-759.

Dernburg, A. F., Sedat, J. W., and Hawley, R. S. (1996b). Direct evidence of a role for heterochromatin in meiotic chromosome segregation. Cell *86*, 135-146.

Dion, M. F., Kaplan, T., Kim, M., Buratowski, S., Friedman, N., and Rando, O. J. (2007). Dynamics of Replication-Independent Histone Turnover in Budding Yeast. Science *315*, 1405-1408.

Donaldson, K. M., Lui, A., and Karpen, G. H. (2002). Modifiers of terminal deficiency-associated position effect variegation in Drosophila. Genetics *160*, 995-1009.

Dorsett, D., Eissenberg, J. C., Misulovin, Z., Martens, A., Redding, B., and McKim, K. (2005). Effects of sister chromatid cohesion proteins on cut gene expression during wing development in Drosophila. Development *132*, 4743-4753.

Egger, G., Liang, G., Aparicio, A., and Jones, P. A. (2004). Epigenetics in human disease and prospects for epigenetic therapy. Nature *429*, 457-463.

Elder, J. F., Jr., and Turner, B. J. (1995). Concerted evolution of repetitive DNA sequences in eukaryotes. Q Rev Biol *70*, 297-320.

Esteller, M. (2007). Cancer epigenomics: DNA methylomes and histone-modification maps. Nat Rev Genet *8*, 286-298.

Flores-Rozas, H., and Kolodner, R. D. (2000). Links between replication, recombination and genome instability in eukaryotes. Trends Biochem Sci *25*, 196-200.

Francastel, C., Schubeler, D., Martin, D. I., and Groudine, M. (2000). Nuclear compartmentalization and gene activity. Nat Rev Mol Cell Biol *1*, 137-143.

Fritsch, O., Benvenuto, G., Bowler, C., Molinier, J., and Hohn, B. (2004). The INO80 protein controls homologous recombination in Arabidopsis thaliana. Mol Cell *16*, 479-485.

Gillespie, D. E., and Berg, C. A. (1995). Homeless is required for RNA localization in Drosophila oogenesis and encodes a new member of the DE-H family of RNA-dependent ATPases. Genes Dev *9*, 2495-2508.

Gindhart-Jr, J. G., and Kaufman, T. C. (1995). Identification of Polycomb and trithorax Group Responsive Elements in the Regulatory Region of the Drosophila Homeotic Gene Sex combs reduced. Genetics *139*, 797-814.

Glaser, R. L., Karpen, G. H., and Spradling, A. C. (1992). Replication forks are not found in a Drosophila minichromosome demonstrating a gradient of polytenization. Chromosoma *102*, 15-19.

Gonzalez-Reyes, A., Elliott, H., and St Johnston, D. (1997). Oocyte determination and the origin of polarity in Drosophila: the role of the spindle genes. Development *124*, 4927-4937.

Grewal, S. I., and Jia, S. (2007). Heterochromatin revisited. Nat Rev Genet *8*, 35-46.

Grewal, S. I., and Moazed, D. (2003). Heterochromatin and epigenetic control of gene expression. Science *301*, 798-802.

Grigliatti, T. (1991). Position-effect variegation--an assay for nonhistone chromosomal proteins and chromatin assembly and modifying factors. Methods Cell Biol *35*, 587-627.

Hadjiolova, K. V., Hadjiolov, A. A., and Bachellerie, J. P. (1995). Actinomycin D stimulates the transcription of rRNA minigenes transfected into mouse cells. Implications for the in vivo hypersensitivity of rRNA gene transcription. Eur J Biochem *228*, 605-615.

Hari, K. L., Cook, K. R., and Karpen, G. H. (2001a). The Drosophila *Su(var)2-10* Locus Encodes A Member of the PIAS Protein Family and Regulates Chromosome Structure and Function. Genes and Development *15*, 1334-1348.

Hari, K. L., Cook, K. R., and Karpen, G. H. (2001b). The Drosophila Su(var)2-10 locus regulates chromosome structure and function and encodes a member of the PIAS protein family. Genes Dev *15*, 1334-1348.

Hari, K. L., Santerre, A., Sekelsky, J. J., McKim, K. S., Boyd, J. B., and Hawley, R. S. (1995). The mei-41 gene of D. melanogaster is a structural and functional homolog of the human ataxia telangiectasia gene. Cell *82*, 815-821.

Hawley, R. S., and Marcus, C. H. (1989). Recombinational controls of rDNA redundancy in Drosophila. Annu Rev Genet *23*, 87-120.

Heitz, E. (1928). Das heterochromatin der moose. I Jb wiss Bot *69*, 762-818.

Henson, J. D., Neumann, A. A., Yeager, T. R., and Reddel, R. R. (2002). Alternative lengthening of telomeres in mammalian cells. Oncogene *21*, 598-610.

Hernandez-Verdun, D. (2006). Nucleolus: from structure to dynamics. Histochem Cell Biol *125*, 127-137.

Hirt, B. (1967). Selective extraction of polyoma DNA from infected mouse cell cultures. J Mol Biol *26*, 365-369.

Hochstrasser, M., Mathog, D., Gruenbaum, Y., Saumweber, H., and Sedat, J. W. (1986). Spatial organization of chromosomes in the salivary gland nuclei of Drosophila melanogaster. J Cell Biol *102*, 112-123.

Hodgson, J. W., Cheng, N. N., Sinclair, D. A., Kyba, M., Randsholt, N. B., and Brock, H. W. (1997). The polyhomeotic locus of Drosophila melanogaster is transcriptionally and post-transcriptionally regulated during embryogenesis. Mech Dev *66*, 69-81.

Ivessa, A. S., Zhou, J. Q., and Zakian, V. A. (2000). The Saccharomyces Pif1p DNA helicase and the highly related Rrm3p have opposite effects on replication fork progression in ribosomal DNA. Cell *100*, 479-489.

Jackson, P. K. (2001). A new RING for SUMO: wrestling transcriptional responses into nuclear bodies with PIAS family E3 SUMO ligases. Genes Dev *15*, 3053-3058.

Jaklevic, B. R., and Su, T. T. (2004). Relative contribution of DNA repair, cell cycle checkpoints, and cell death to survival after DNA damage in Drosophila larvae. Curr Biol *14*, 23-32.

Janicki, S. M., Tsukamoto, T., Salghetti, S. E., Tansey, W. P., Sachidanandam, R., Prasanth, K. V., Ried, T., Shav-Tal, Y., Bertrand, E., Singer, R. H., and Spector, D. L. (2004). From silencing to gene expression: real-time analysis in single cells. Cell *116*, 683-698.

Jenuwein, T., and Allis, C. D. (2001). Translating the histone code. Science *293*, 1074-1080.

Jia, S., Yamada, T., and Grewal, S. I. (2004). Heterochromatin regulates cell type-specific long-range chromatin interactions essential for directed recombination. Cell *119*, 469-480.

John, B. (1988). The biology of heterochromatin, In Heterochromatin: Molecular and Structural Aspects, R. S. Verma, ed. (Cambridge: Cambridge University Press), pp. 1-147.

Jorgensen, A. L., Laursen, H. B., Jones, C., and Bak, A. L. (1992). Evolutionarily Different Alphoid Repeat DNA on Homologous Chromosomes in Human and Chimpanzee. PNAS *89*, 3310-3314.

Kaeberlein, M., McVey, M., and Guarente, L. (1999). The SIR2/3/4 complex and SIR2 alone promote longevity in Saccharomyces cerevisiae by two different mechanisms. Genes Dev *13*, 2570-2580.

Karagiannis, T. C., and El-Osta, A. (2006). Chromatin modifications and DNA double-strand breaks: the current state of play. Leukemia *21*, 195-200.

Karpen, G. H., Le, M. H., and Le, H. (1996). Centric heterochromatin and the efficiency of achiasmate disjunction in Drosophila female meiosis. Science *273*, 118-122.

Karpen, G. H., Schaefer, J. E., and Laird, C. D. (1988). A Drosophila rRNA gene located in euchromatin is active in transcription and nucleolus formation. Genes Dev *2*, 1745-1763.

Keogh, M.-C., Kim, J.-A., Downey, M., Fillingham, J., Chowdhury, D., Harrison, J. C., Onishi, M., Datta, N., Galicia, S., Emili, A.*, et al.* (2006). A phosphatase complex that dephosphorylates [gamma]H2AX regulates DNA damage checkpoint recovery. Nature *439*, 497-501.

Kim, K.-C., Geng, L., and Huang, S. (2003). Inactivation of a Histone Methyltransferase by Mutations in Human Cancers. Cancer Res *63*, 7619-7623.

Klattenhoff, C., Bratu, D. P., McGinnis-Schultz, N., Koppetsch, B. S., Cook, H. A., and Theurkauf, W. E. (2007). Drosophila rasiRNA pathway mutations disrupt embryonic axis specification through activation of an ATR/Chk2 DNA damage response. Dev Cell *12*, 45-55.

Kobayashi, T., and Ganley, A. R. (2005). Recombination regulation by transcription-induced cohesin dissociation in rDNA repeats. Science *309*, 1581-1584.

Kolomietz, E., Meyn, M. S., Pandita, A., and Squire, J. A. (2002). The role of Alu repeat clusters as mediators of recurrent chromosomal aberrations in tumors. Genes Chromosomes Cancer *35*, 97-112.

Kondo, Y., and Issa, J.-P. J. (2003). Enrichment for Histone H3 Lysine 9 Methylation at Alu Repeats in Human Cells. J Biol Chem *278*, 27658-27662.

Kruhlak, M. J., Celeste, A., Dellaire, G., Fernandez-Capetillo, O., Muller, W. G., McNally, J. G., Bazett-Jones, D. P., and Nussenzweig, A. (2006). Changes in chromatin structure and mobility in living cells at sites of DNA double-strand breaks. J Cell Biol *172*, 823-834.

Kuschak, T. I., Kuschak, B. C., Smith, G. M., Wright, J. A., and Mai, S. (2001). Isolation of extrachromosomal elements by histone immunoprecipitation. Biotechniques *30*, 1064-1068, 1070-1062.

Lambert, S., Saintigny, Y., Delacote, F., Amiot, F., Chaput, B., Lecomte, M., Huck, S., Bertrand, P., and Lopez, B. S. (1999). Analysis of intrachromosomal homologous recombination in mammalian cell, using tandem repeat sequences. Mutat Res *433*, 159-168.

Lamond, A. I., and Spector, D. L. (2003). Nuclear speckles: a model for nuclear organelles. Nat Rev Mol Cell Biol *4*, 605-612.

Lan, F., Zaratiegui, M., Villen, J., Vaughn, M. W., Verdel, A., Huarte, M., Shi, Y., Gygi, S. P., Moazed, D., Martienssen, R. A., and Shi, Y. (2007). S. pombe

LSD1 Homologs Regulate Heterochromatin Propagation and Euchromatic Gene Transcription. Molecular Cell *26*, 89-101.

Lander, E. S., Linton, L. M., Birren, B., Nusbaum, C., Zody, M. C., Baldwin, J., Devon, K., Dewar, K., Doyle, M., FitzHugh, W.*, et al.* (2001). Initial sequencing and analysis of the human genome. Nature *409*, 860-921.

Larocque, J. R., Jaklevic, B. R., Su, T. T., and Sekelsky, J. (2006). Drosophila ATR in double-strand break repair. Genetics.

Le Beau, M. M., Westbrook, C. A., Diaz, M. O., and Rowley, J. D. (1984). Evidence for two distinct c-src loci on human chromosomes 1 and 20. Nature *312*, 70-71.

Lee, Y. S., Nakahara, K., Pham, J. W., Kim, K., He, Z., Sontheimer, E. J., and Carthew, R. W. (2004). Distinct Roles for Drosophila Dicer-1 and Dicer-2 in the siRNA/miRNA Silencing Pathways. Cell *117*, 69.

Lin, H., and Spradling, A. C. (1997). A novel group of pumilio mutations affects the asymmetric division of germline stem cells in the Drosophila ovary. Development *124*, 2463-2476.

Lin, Y. H., and Keil, R. L. (1991). Mutations affecting RNA polymerase I-stimulated exchange and rDNA recombination in yeast. Genetics *127*, 31-38.

Lippman, Z., Gendrel, A.-V., Black, M., Vaughn, M. W., Dedhia, N., Richard McCombie, W., Lavine, K., Mittal, V., May, B., Kasschau, K. D.*, et al.* (2004). Role of transposable elements in heterochromatin and epigenetic control. Nature *430*, 471-476.

Lodish, H., Berk, A., and SL, Z. (2004). Molecular Cell Biology, 4th edn (New York: WH Freeman).

Long, E. O., and Dawid, I. B. (1980). Repeated genes in eukaryotes. Annu Rev Biochem *49*, 727-764.

Losada, A., Hirano, M., and Hirano, T. (1998). Identification of Xenopus SMC protein complexes required for sister chromatid cohesion. Genes Dev *12*, 1986-1997.

Maggert, K. A., and Golic, K. G. (2005). Highly efficient sex chromosome interchanges produced by I-CreI expression in Drosophila. Genetics *171*, 1103-1114.

Martin, C., and Zhang, Y. (2005). The diverse functions of histone lysine methylation. Nat Rev Mol Cell Biol *6*, 838-849.

McKee, B. D., and Karpen, G. H. (1990). Drosophila ribosomal RNA genes function as an X-Y pairing site during male meiosis. Cell *61*, 61-72.

McKim, K. S., and Hayashi-Hagihara, A. (1998). mei-W68 in Drosophila melanogaster encodes a Spo11 homolog: evidence that the mechanism

for initiating meiotic recombination is conserved. Genes Dev *12*, 2932-2942.

Mehrotra, S., and McKim, K. S. (2006). Temporal analysis of meiotic DNA double-strand break formation and repair in Drosophila females. PLoS Genet *2*, e200.

Metzger, E., Wissmann, M., Yin, N., Muller, J. M., Schneider, R., Peters, A. H., Gunther, T., Buettner, R., and Schule, R. (2005). LSD1 demethylates repressive histone marks to promote androgen-receptor-dependent transcription. Nature *437*, 436-439.

Mirkin, S. M. (2006). DNA structures, repeat expansions and human hereditary disorders. Current Opinion in Structural Biology *16*, 351-358.

Mis, J., Ner, S., and Grigliatti, T. (2006). Identification of three histone methyltransferases in Drosophila dG9a is a suppressor of PEV and is required for gene silencing. Molecular Genetics and Genomics, 1.

Mitelman, F., Johansson, B., and Mertens, F. (2007). The impact of translocations and gene fusions on cancer causation. Nat Rev Cancer *7*, 233-245.

Mito, Y., Henikoff, J. G., and Henikoff, S. (2007). Histone Replacement Marks the Boundaries of cis-Regulatory Domains. Science *315*, 1408-1411.

Moazed, D., Buhler, M., Buker, S. M., Colmenares, S. U., Gerace, E. L., Gerber, S. A., Hong, E. J., Motamedi, M. R., Verdel, A., Villen, J., and Gygi, S. P. (2006). Studies on the Mechanism of RNAi-dependent Heterochromatin Assembly. Cold Spring Harb Symp Quant Biol *71*, 461-471.

Mora, L., Sanchez, I., Garcia, M., and Ponsa, M. (2006). Chromosome territory positioning of conserved homologous chromosomes in different primate species. Chromosoma *115*, 367-375.

Morrison, A. J., Highland, J., Krogan, N. J., Arbel-Eden, A., Greenblatt, J. F., Haber, J. E., and Shen, X. (2004). INO80 and gamma-H2AX interaction links ATP-dependent chromatin remodeling to DNA damage repair. Cell *119*, 767-775.

Muller, H. J. (1930). Types of visible variations induced by X-rays in Drosophila. J Genet *22*, 299-334.

Nakayama, J., Rice, J. C., Strahl, B. D., Allis, C. D., and Grewal, S. I. (2001). Role of histone H3 lysine 9 methylation in epigenetic control of heterochromatin assembly. Science *292*, 110-113.

Nielsen, S. J., Schneider, R., Bauer, U. M., Bannister, A. J., Morrison, A., O'Carroll, D., Firestein, R., Cleary, M., Jenuwein, T., Herrera, R. E., and Kouzarides, T. (2001). Rb targets histone H3 methylation and HP1 to promoters. Nature *412*, 561-565.

Noma, K., Sugiyama, T., Cam, H., Verdel, A., Zofall, M., Jia, S., Moazed, D., and Grewal, S. I. (2004). RITS acts in cis to promote RNA interference-mediated transcriptional and post-transcriptional silencing. Nat Genet *36*, 1174-1180.

Noma, K.-i., Allis, C. D., and Grewal, S. I. S. (2001). Transitions in Distinct Histone H3 Methylation Patterns at the Heterochromatin Domain Boundaries. Science *293*, 1150-1155.

Nonaka, N., Kitajima, T., Yokobayashi, S., Xiao, G., Yamamoto, M., Grewal, S. I. S., and Watanabe, Y. (2002). Recruitment of cohesin to heterochromatic regions by Swi6/HP1 in fission yeast. Nat Cell Biol *4*, 89-93.

Oegema, K., Desai, A., Rybina, S., Kirkham, M., and Hyman, A. A. (2001). Functional Analysis of Kinetochore Assembly in Caenorhabditis elegans. J Cell Biol *153*, 1209-1226.

Osipovich, O., Milley, R., Meade, A., Tachibana, M., Shinkai, Y., Krangel, M. S., and Oltz, E. M. (2004). Targeted inhibition of V(D)J recombination by a histone methyltransferase. Nat Immunol *5*, 309-316.

Pak, D. T. S., Pflumm, M., Chesnokov, I., Huang, D. W., Kellum, R., Marr, J., Romanowski, P., and Botchan, M. R. (1997). Association of the Origin Recognition Complex with Heterochromatin and HP1 in Higher Eukaryotes. Cell *91*, 311-323.

Pal-Bhadra, M., Leibovitch, B. A., Gandhi, S. G., Rao, M., Bhadra, U., Birchler, J. A., and Elgin, S. C. (2004). Heterochromatic silencing and HP1 localization in Drosophila are dependent on the RNAi machinery. Science *303*, 669-672.

Parada, L., and Misteli, T. (2002). Chromosome positioning in the interphase nucleus. Trends Cell Biol *12*, 425-432.

Parkes, T. L., Elia, A. J., Dickinson, D., Hilliker, A. J., Phillips, J. P., and Boulianne, G. L. (1998). Extension of Drosophila lifespan by overexpression of human SOD1 in motorneurons. Nat Genet *19*, 171-174.

Pearson, C. E., Edamura, K. N., and Cleary, J. D. (2005). Repeat Instability: Mechanisms of dynamic mutations. Nature Reviews Genetics *6*, 729-742.

Peng, J. C., and Karpen, G. H. (2007). H3K9 methylation and RNA interference regulate nucleolar organization and repeated DNA stability. Nat Cell Biol *9*, 25-35.

Peters, A. H., O'Carroll, D., Scherthan, H., Mechtler, K., Sauer, S., Schofer, C., Weipoltshammer, K., Pagani, M., Lachner, M., Kohlmaier, A*., et al.* (2001). Loss of the Suv39h histone methyltransferases impairs mammalian heterochromatin and genome stability. Cell *107*, 323-337.

Peters, A. H. F. M., Kubicek, S., Mechtler, K., O'Sullivan, R. J., Derijck, A. A. H. A., Perez-Burgos, L., Kohlmaier, A., Opravil, S., Tachibana, M., and

Shinkai, Y. (2003). Partitioning and Plasticity of Repressive Histone Methylation States in Mammalian Chromatin. Molecular Cell *12*, 1577.

Phair, R. D., and Misteli, T. (2000). High mobility of proteins in the mammalian cell nucleus. Nature *404*, 604-609.

Pont, G., Degroote, F., and Picard, G. (1987). Some extrachromosomal circular DNAs from Drosophila embryos are homologous to tandemly repeated genes. J Mol Biol *195*, 447-451.

Rai, K., Nadauld, L. D., Chidester, S., Manos, E. J., James, S. R., Karpf, A. R., Cairns, B. R., and Jones, D. A. (2006). Zebra Fish Dnmt1 and Suv39h1 Regulate Organ-Specific Terminal Differentiation during Development. Mol Cell Biol *26*, 7077-7085.

Reuter, G., and Spierer, P. (1992). Position effect variegation and chromatin proteins. Bioessays *14*, 605-612.

Reuter, G., Werner, W., and Hoffmann, H. J. (1982). Mutants affecting position-effect heterochromatinization in Drosophila melanogaster. Chromosoma *85*, 539-551.

Romeijn, R., and Ferro, W. (2004). ligase4 mutations.

Royou, A., Macias, H., and Sullivan, W. (2005). The Drosophila Grp/Chk1 DNA Damage Checkpoint Controls Entry into Anaphase. Current Biology *15*, 334-339.

Rudolph, T., Yonezawa, M., Lein, S., Heidrich, K., Kubicek, S., Schafer, C., Phalke, S., Walther, M., Schmidt, A., Jenuwein, T., and Reuter, G. (2007). Heterochromatin Formation in Drosophila Is Initiated through Active Removal of H3K4 Methylation by the LSD1 Homolog SU(VAR)3-3. Molecular Cell *26*, 103-115.

Rupa, D. S., Hasegawa, L., and Eastmond, D. A. (1995). Detection of chromosomal breakage in the 1cen-1q12 region of interphase human lymphocytes using multicolor fluorescence in situ hybridization with tandem DNA probes. Cancer Res *55*, 640-645.

Santoro, R., Li, J., and Grummt, I. (2002). The nucleolar remodeling complex NoRC mediates heterochromatin formation and silencing of ribosomal gene transcription. Nat Genet *32*, 393-396.

Schotta, G., Ebert, A., Dorn, R., and Reuter, G. (2003). Position-effect variegation and the genetic dissection of chromatin regulation in Drosophila. Semin Cell Dev Biol *14*, 67-75.

Schotta, G., Ebert, A., Krauss, V., Fischer, A., Hoffmann, J., Rea, S., Jenuwein, T., Dorn, R., and Reuter, G. (2002). Central role of Drosophila SU(VAR)3-9 in histone H3-K9 methylation and heterochromatic gene silencing. Embo J *21*, 1121-1131.

Schotta, G., Lachner, M., Sarma, K., Ebert, A., Sengupta, R., Reuter, G., Reinberg, D., and Jenuwein, T. (2004). A silencing pathway to induce H3-K9 and H4-K20 trimethylation at constitutive heterochromatin. Genes Dev *18*, 1251-1262.

Schultz, D. C., Ayyanathan, K., Negorev, D., Maul, G. G., and Rauscher, F. J., III (2002). SETDB1: a novel KAP-1-associated histone H3, lysine 9-specific methyltransferase that contributes to HP1-mediated silencing of euchromatic genes by KRAB zinc-finger proteins. Genes Dev *16*, 919-932.

Shermoen, A. W., and Kiefer, B. I. (1975). Regulation in rDNA-deficient Drosophila melanogaster. Cell *4*, 275-280.

Shi, Y., Lan, F., Matson, C., Mulligan, P., Whetstine, J. R., Cole, P. A., Casero, R. A., and Shi, Y. (2004). Histone demethylation mediated by the nuclear amine oxidase homolog LSD1. Cell *119*, 941-953.

Song, Y. H. (2005). Drosophila melanogaster: a model for the study of DNA damage checkpoint response. Mol Cells *19*, 167-179.

Spradling, A., and Orr-Weaver, T. (1987). Regulation of DNA replication during Drosophila development. Annu Rev Genet *21*, 373-403.

Stern, C. (1936). Somatic Crossing over and Segregation in Drosophila Melanogaster. Genetics *21*, 625-730.

Subba Rao, K. (2007). Mechanisms of disease: DNA repair defects and neurological disease. Nat Clin Pract Neurol *3*, 162-172.

Sullivan, B., and Karpen, G. (2001). Centromere identity in Drosophila is not determined in vivo by replication timing. J Cell Biol *154*, 683-690.

Sullivan, B. A., and Karpen, G. H. (2004). Centromeric chromatin exhibits a histone modification pattern that is distinct from both euchromatin and heterochromatin. Nat Struct Mol Biol *11*, 1076-1083.

Tachibana, M., Sugimoto, K., Nozaki, M., Ueda, J., Ohta, T., Ohki, M., Fukuda, M., Takeda, N., Niida, H., Kato, H., and Shinkai, Y. (2002). G9a histone methyltransferase plays a dominant role in euchromatic histone H3 lysine 9 methylation and is essential for early embryogenesis. Genes Dev *16*, 1779-1791.

Tanabe, H., Muller, S., Neusser, M., von Hase, J., Calcagno, E., Cremer, M., Solovei, I., Cremer, C., and Cremer, T. (2002). Evolutionary conservation of chromosome territory arrangements in cell nuclei from higher primates. PNAS *99*, 4424-4429.

Tearle, R. G., and Nusslein-Volhard, C. (1987). Tubingen mutants and stock list, Vol 66).

Theurkauf, W. E., Klattenhoff, C., Bratu, D. P., McGinnis-Schultz, N., Koppetsch, B. S., and Cook, H. A. (2006). rasiRNAs, DNA Damage, and Embryonic

Axis Specification. Cold Spring Harbor Symposia on Quantitative Biology *71*, 171-180.

Tollervey, D., Lehtonen, H., Jansen, R., Kern, H., and Hurt, E. C. (1993). Temperature-sensitive mutations demonstrate roles for yeast fibrillarin in pre-rRNA processing, pre-rRNA methylation, and ribosome assembly. Cell *72*, 443.

Tomari, Y., Du, T., Haley, B., Schwarz, D. S., Bennett, R., Cook, H. A., Koppetsch, B. S., Theurkauf, W. E., and Zamore, P. D. (2004). RISC assembly defects in the Drosophila RNAi mutant armitage. Cell *116*, 831-841.

Tsukuda, T., Fleming, A. B., Nickoloff, J. A., and Osley, M. A. (2005). Chromatin remodelling at a DNA double-strand break site in Saccharomyces cerevisiae. Nature *438*, 379-383.

Unal, E., Arbel-Eden, A., Sattler, U., Shroff, R., Lichten, M., Haber, J. E., and Koshland, D. (2004). DNA damage response pathway uses histone modification to assemble a double-strand break-specific cohesin domain. Mol Cell *16*, 991-1002.

Vagin, V. V., Sigova, A., Li, C., Seitz, H., Gvozdev, V., and Zamore, P. D. (2006). A distinct small RNA pathway silences selfish genetic elements in the germline. Science *313*, 320-324.

Vakoc, C. R., Mandat, S. A., Olenchock, B. A., and Blobel, G. A. (2005). Histone H3 lysine 9 methylation and HP1gamma are associated with transcription elongation through mammalian chromatin. Mol Cell *19*, 381-391.

van Attikum, H., Fritsch, O., Hohn, B., and Gasser, S. M. (2004). Recruitment of the INO80 complex by H2A phosphorylation links ATP-dependent chromatin remodeling with DNA double-strand break repair. Cell *119*, 777-788.

van Attikum, H., and Gasser, S. M. (2005). The histone code at DNA breaks: a guide to repair? Nat Rev Mol Cell Biol *6*, 757-765.

Wallace, J. A., and Orr-Weaver, T. L. (2005). Replication of heterochromatin: insights into mechanisms of epigenetic inheritance. Chromosoma *114*, 389-402.

Weinstock, D. M., Richardson, C. A., Elliott, B., and Jasin, M. (2006). Modeling oncogenic translocations: distinct roles for double-strand break repair pathways in translocation formation in mammalian cells. DNA Repair (Amst) *5*, 1065-1074.

Westphal, T., and Reuter, G. (2002). Recombinogenic effects of suppressors of position-effect variegation in Drosophila. Genetics *160*, 609-621.

Wevrick, R., and Willard, H. F. (1989). Long-Range Organization of Tandem Arrays of alpha Satellite DNA at the Centromeres of Human

Chromosomes: High-Frequency Array-Length Polymorphism and Meiotic Stability. PNAS *86*, 9394-9398.

Wilson, J. E., Connell, J. E., Schlenker, J. D., and Macdonald, P. M. (1996). Novel genetic screen for genes involved in posterior body patterning in Drosophila. Dev Genet *19*, 199-209.

Wong, N., Lam, W.-C., Lai, P. B.-S., Pang, E., Lau, W.-Y., and Johnson, P. J. (2001). Hypomethylation of Chromosome 1 Heterochromatin DNA Correlates with q-Arm Copy Gain in Human Hepatocellular Carcinoma. Am J Pathol *159*, 465-471.

Xu, J., and Du, W. (2003). Drosophila chk2 plays an important role in a mitotic checkpoint in syncytial embryos. FEBS Letters *545*, 209-212.

Xu, J., Xin, S., and Du, W. (2001). Drosophila Chk2 is required for DNA damage-mediated cell cycle arrest and apoptosis. FEBS Lett *508*, 394-398.

Xu, K., Bogert, B. A., Li, W., Su, K., Lee, A., and Gao, F.-B. (2004). The fragile X-related Gene Affects the Crawling Behavior of Drosophila Larvae by Regulating the mRNA Level of the DEG/ENaC Protein Pickpocket1. Current Biology *14*, 1025-1034.

Yasuhara, J. C., DeCrease, C. H., and Wakimoto, B. T. (2005). Evolution of heterochromatic genes of Drosophila. PNAS *102*, 10958-10963.

Yasuhara, J. C., and Wakimoto, B. T. (2006). Oxymoron no more: the expanding world of heterochromatic genes. Trends in Genetics *22*, 330-338.

Ye, J., and Eickbush, T. H. (2006). Chromatin Structure and Transcription of the R1- and R2-Inserted rRNA Genes of Drosophila melanogaster. Mol Cell Biol *26*, 8781-8790.

Yunis, J. J., and Soreng, A. L. (1984). Constitutive fragile sites and cancer. Science *226*, 1199-1204.

Zachos, G., Black, E. J., Walker, M., Scott, M. T., Vagnarelli, P., Earnshaw, W. C., and Gillespie, D. A. (2007). Chk1 is required for spindle checkpoint function. Dev Cell *12*, 247-260.